Study on Microenvironment Mediated Chemoresistance in Chronic Myeloid Leukemia

A thesis submitted in partial fulfilment of the requirements of the degree of

Doctor of Philosophy

of the

Indian Institute of Technology Guwahati

by

Atul Kumar

(11610603)

Supervisor:

Dr. Bithiah Grace Jaganathan

Department of Biosciences and Bioengineering

Indian Institute of Technology Guwahati

Guwahati-781039, Assam, India

October 2016

Department of Biosciences and Bioengineering
Indian Institute of Technology Guwahati
Guwahati-781039, Assam, India

Declaration

I hereby declare that the contents of the research work described in the thesis entitled "**Study of Microenvironment Mediated Chemoresistance in Chronic Myeloid Leukemia"** is a presentation of my original research work carried out in the Department of Biosciences and Bioengineering, Indian Institute of Technology Guwahati, India under the supervision of Dr. Bithiah Grace Jaganathan.

All contributions from others in terms of techniques, quotations or any other materials are adequately cited and referenced to the original sources. All collaborative work, discussions and help during the experiments are duly acknowledged.

Date:

Atul Kumar

Roll. No: 11610603

Department of Biosciences and Bioengineering
Indian Institute of Technology Guwahati
Guwahati-781039, Assam, India

Certificate

This is to certify that the research work described in the thesis entitled "**Study of Microenvironment Mediated Chemoresistance in Chronic Myeloid Leukemia"** by **Atul Kumar** (Roll no: 11610603) submitted to Indian Institute of Technology Guwahati, Guwahati, India for the award of the degree of **Doctor of Philosophy** is a original record of research work carried under my supervision in the Department of Biosciences and Bioengineering, Indian Institute of Technology Guwahati, India.

The present thesis or any part thereof has not been submitted elsewhere for the award of any other degree or diploma.

Date:

Dr. Bithiah Grace Jaganathan
Thesis Supervisor

TABLE OF CONTENTS

ABBREVIATIONS

ABL	Ableson leukemia virus
ADIPOQ	Adiponectin
ALCAM	Activated leukocyte cell adhesion molecule
ALL	Acute Lymphoid Leukemia
AML	Acute Myeloid Leukemia
AP	Accelerated phase
Ara-C	Cytosine arabinoside, Cytarabine
ATP	Adenosine Triphosphate
BAD	Bcl-2-associated death promoter
BCR	Breakpoint cluster region
BM	Bone Marrow
BMP	Bone morphogenetic protein
BP	Blast phase
BSP	Bone sialoprotein
CAR	CXCL12-abundant reticular
CD	Cluster of Differentiation
cIAP	Cellular inhibitor of apoptosis
CLL	Chronic Lymphoid Leukemia
CLP	Common lymphoid progenitor
CML	Chronic myeloid leukemia
CMP	Common myeloid progenitor
CM	Conditioned media
CP	Chronic phase
CR	Cytogenetic response
CRKL	Crk-like protein
CXCL12	C-X-C Motif Chemokine Ligand 12
CXCR4	C-X-C chemokine receptor-4
CYB	Cytochalasin B
CYD	Cytochalasin D

DKK1	Dickkopf homolog 1
DMEM	Dulbecco's Modified Eagle's Medium
DNA	Deoxyribonucleic Acid
DS	Dasatanib
ECM	Extra cellular matrix
EGF	Epidermal growth factor
ELISA	Enzyme linked immunosorbent assay
ERK	Extracellular signal–regulated kinase
Fak	Focal-Adhesion kinase
FDA	Food and Drug Administration
FGF	fibroblast growth factor
FISH	Fluorescence in-situ Hybridization
FLT3	Fms Related Tyrosine Kinase 3
GAB2	GRB2-associated binding protein 2
GAP	GTPase-activating protein
G-CSF	Granulocyte-colony stimulating factor
GDF3	Growth differentiation factor-3
GFP	Green fluorescent protein
GM-CSF	Granulocyte-macrophage colony-stimulating factor
GEF	Guanine nucleotide exchange factor
GRB2	Growth factor receptor-bound protein 2
HCT	Hematopoietic cell transplantation
HGF	Hepatocyte growth factor
HLA	Human leukocyte antigen
HR	Hematologic response
HSC	Hematopoietic Stem cells
IDO	Indolamine 2,3dioxygenase
IM	ImatinibMesylate
IL-6	Interleukin-6
IL-8	Interleukin-8
IFN	Interferon

rIFN	recombinant Interferon
IκB	Inhibitor of kappa B
IRIS	International Randomized Study of Interferon and STI571
JAK	Janus Kinase
JNK	c-Jun N-terminal kinases
KD	kilodalton
KTLS	c-Kit+ Thy-1.1lo Lin-/lo Sca-1+
lin-	Lineage negative
LTR	Long-term reconstitution
LSC	Leukemic Stem cells
LSK	Lineage negative , c-kit positive and sca-1 positive
LT-HSC	Long-term Hematopoietic Stem cells
MAPK	Mitogen-activated protein kinase
M-CSF	Macrophage colony-stimulating factor
MM	Multiple Myeloma
MPP	Multipotent progenitor
MR	Molecular response
MSC	Mesenchymal Stem/Stromal cells
N-cad	N-cadherin
NFκB	Nuclear Factor Kappa B
NI	Nilotinib
NK	Natural Killer
NO	Nitric oxide
PB	Peripheral blood
PDGF	Platelet-derived growth factor
PDGFR	Platlet derived growth factor receptor
PI3K	Phosphatidylinositol 3-kinase
PGE2	Prostaglandin E2
PlGF	Placental growth factor
RHOA	Ras Homology protein A
RNA	Ribonucleic Acid

RPMI	Roswell Park Memorial Institute medium
Sca-1	Stem cells antigen-1
SDF	Stem cell derived factor
SFFV	Spleen focus-forming virus
SH	Src Homology
SMAD	Mothers against decapentaplegic homolog
SOS	son of sevenless
S/T	Serine/threonine
ST-HSC	Short-term Hematopoietic Stem cells
STAT	Signal transducer and activator of transcription
TGF	transforming growth factor
TKI	Tyrosine kinase inhibitor
TNF-α	Tumor necrosis factor-α
TPO	Thrombopoietin
VCAM	Vascular cell adhesion molecule
VEGF	Vascular endothelial growth factor
VLA	Very Late Antigen
QPCR	Quantitative reverse-transcription PCR
WPRE	Woodchuck hepatitis virus posttranscriptional regulatory element

ABSTRACT

Chronic Myeloid Leukemia (CML) is a myeloproliferative disorder in which the leukemic stem cells (LSC) give rise to abnormally high number of myeloid cells. CML is initiated by BCR-ABL fusion (9;22)(q34;q11) which is the result of reciprocal translocation between chromosome 9 and chromosome 22. *BCR-ABL* fusion gene codes for *BCR-ABL* fusion protein which is a constitutively active tyrosine kinase. Tyrosine kinase inhibitors (TKIs) such as Imatinib mesylate (IM) is the mainline drug used for the treatment of CML. CML responds to IM treatment efficiently, especially in the chronic phase. However, in several patients, CML relapses even after few years of remission, mainly upon discontinuation of IM intake. Mutations in the BCR-ABL kinase domain have been reported to be the main cause of IM resistance. However, persistent leukemic cells in the BM inspite of IM treatment play a major role in causing relapse in CML patients. BM stromal microenvironment has been implicated to be the major cause of this persistence, where mesenchymal stromal cells (MSC) and their derivatives provide chemoprotection to CML cells through secreted factors as well as direct cell-cell contact.

In the present work, we studied the major signaling pathways involved in stroma mediated chemoprotection of CML cells. MAPK pathways (ERK, P38), NFkB, STAT pathways (STAT3/5), BMP signaling pathway through SMAD, CXCL12-CXCR-4 signaling axis, actin cytoskeleton and RhoA GTPase were examined for their role in CML-stromal interactions and CML chemoprotection. We found that actin cytoskeleton, RhoA GTPase and BMP-SMAD signaling plays an important role in establishing direct cell-cell interaction between CML and stromal cells. ERK-MAPK and BMP-SMAD signaling were found to be activated by stromal interactions in spite of IM treatment. This effect could be abrogated by use of small molecule inhibitors for ERK-MAPK and BMP-SMAD signaling as well as actin cytoskeleton disruptions in combination with IM. Moreover, it was observed that as a result of stroma mediated chemoprotection, CML cell line K562 cells could persist long-term in the presence of IM when attached to stromal cells. These persistent K562 cells acquired stroma-dependent chemoresistance which was mediated by the above mentioned signaling pathways. Interestingly, we found that after 8-12 weeks in stromal co-culture system, these K562 cells could be maintained in stroma

independent suspension culture in the presence of IM, thus having acquiredstroma independent chemoresistance which resembles a relapse status in the patient. The resulting chemoresistant cells showed activation of BCR-ABL independent signaling pathways and the cells could be induced to undergo apoptosis by use of small molecule inhibitors along with IM treatment.

In conclusion, the present study showed that a reciprocal interaction exists between the CML cells and the stromal cells in their microenvironment. The stromal cells, modified by the leukemic cells, chemoprotected CML cells from IM induced cell death, which further developed into stroma independent chemoresistance which can be effectively targeted by inhibiting oncogene-independent signaling pathways.

1.0 SCIENTIFIC BACKGROUND

1.1 Hematopoiesis and Leukemia

Hematopoietic stem cells (HSC) present in the bone marrow (BM) give rise to all the different types of blood cells. HSC maintain their own population by self renewal and give rise to mature blood cells through differentiation. During differentiation, the long-term HSC (LT-HSC) in the BM give rise to short-term HSC (ST-HSC) which further produce the multipotent progenitor (MPP) cells. MPP cells differentiate into common myeloid progenitor (CMP) or common lymphoid progenitor (CLP) cells. CMP give rise to mature myeloid cells i.e. granulocytes, monocytes, erythrocytes and megakaryocytes whereas CLP give rise to mature cells of lymphoid lineage i.e. B-cells, T-cells and Natural Killer (NK) cells (Passegue et al., 2003) (Figure 1.1).

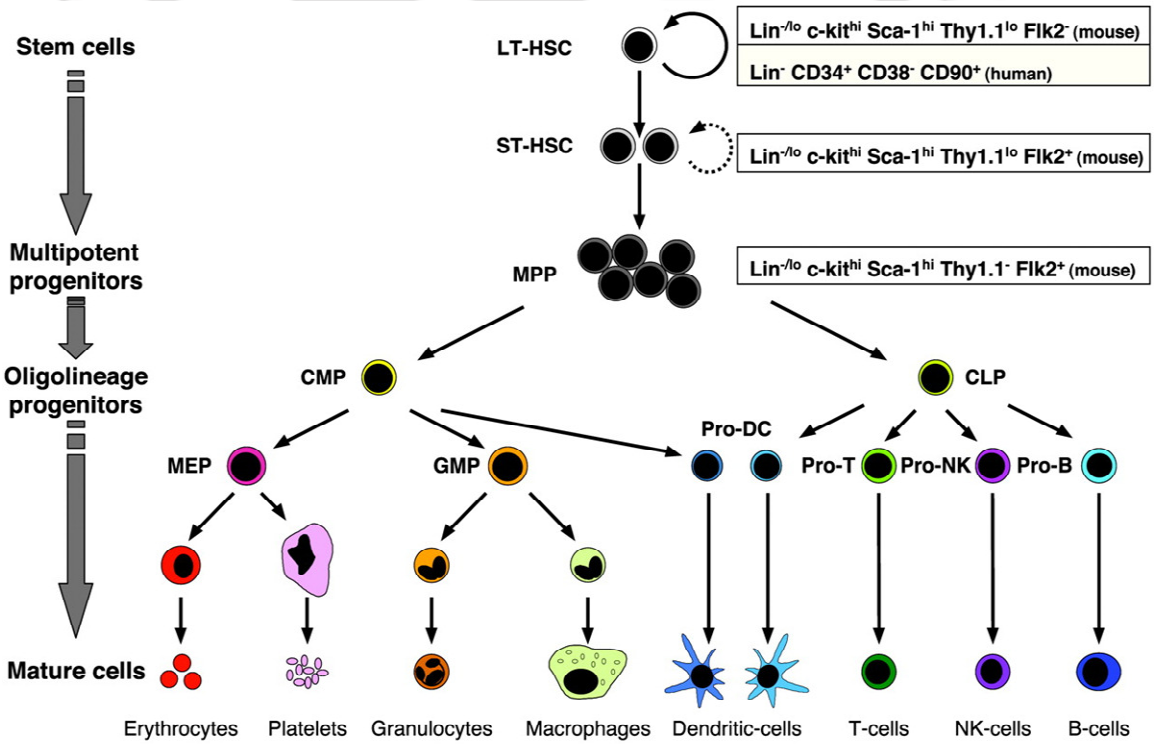

Figure 1.1: *HSC and hematopoietic hierarchy. From: (Passegue et al., 2003)*

Leukemia is a disease of the hematopoietic cells. Leukemia is initiated by mutations in the HSC or their progenitor cells giving rise to the leukemic stem cells (LSC). LSC are long term dormant cancer cells which differentiate into non-functional leukemic blast cells. These blast cells carry leukemic mutations, have proliferative advantage over the normal progenitor cells and also lack response to apoptotic signaling. Leukemic blast cells do not differentiate into mature functional blood cells. Hence, BM is crowded with non-functional immature blast cells, which leads to BM failure.

1.2 Chronic myeloid leukemia

Chronic myeloid leukemia (CML) is a myelo-proliferative disorder resulting in abnormally high number of myeloid cells in the BM (Druker et al., 2006). CML is initiated by reciprocal translocation t(9;22)(q34;q11) between chromosome 9 and chromosome 22 in HSC, resulting in a shorter chromosome 22 which is referred to as Philadelphia (Ph) chromosome (Figure 1.2). This translocation leads to the fusion of breakpoint cluster region (*BCR*) and Abelson leukemia virus (*ABL*) genes on chromosomes 22 and 9 respectively, resulting in formation of *BCR-ABL* fusion gene on chromosome 22 (Sawyers, 1999). *ABL* is a proto-oncogene located on chromosome 9 which codes for ABL tyrosine kinase protein. However in the CML cells, the *BCR-ABL* gene codes for constitutively active BCR-ABL tyrosine kinase protein (Sawyers, 1999).

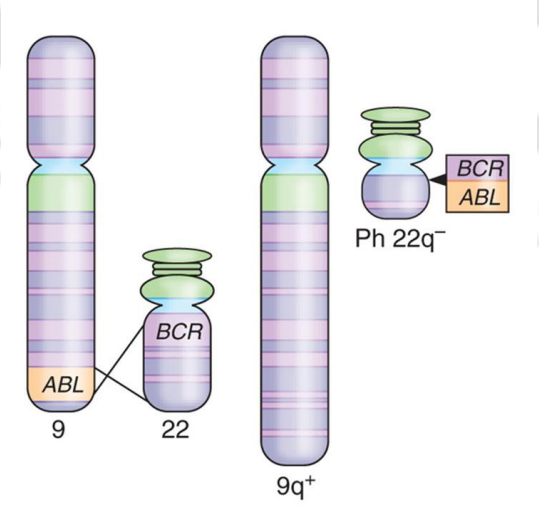

Figure 1.2: *Formation of BCR-ABL fusion gene as a result of reciprocal translocation between chromosome 9 and 22. From: (Lydon, 2009)*

CML disease progression in the patients can be divided into three phases. The first phase is the chronic phase (CP), in which the *BCR-ABL* positive HSC give rise to myeloid progenitor cells which can give rise to functionally mature myeloid cells (Figure 1.3). However, the number of mature myeloid cells is higher than normal. In CP-CML, the percentage of blast cells is less than 10% of the total cells in the BM. Most CML patients are diagnosed in the chronic phase as a result of blood tests for related or unrelated symptoms. Most CP-CML patients respond well to treatment and have higher survival rates. In the accelerated phase (AP), because of additional mutations the percentage of blast cells increases and is between 10-20% of the total cells. The patients have increased granulocyte count as well as increased or decreased platelet count. In the blast phase (BP), the percentage of blast cells is higher than 20% of the total cells. The patients in BP have symptoms like acute leukemia such as enlarged spleen, bleeding, bone pain and fever. In BP, the leukemic cells also spread to other organs. BP-CML patients respond poorly to therapy and have very low survival rates (Vardiman et al., 2002).

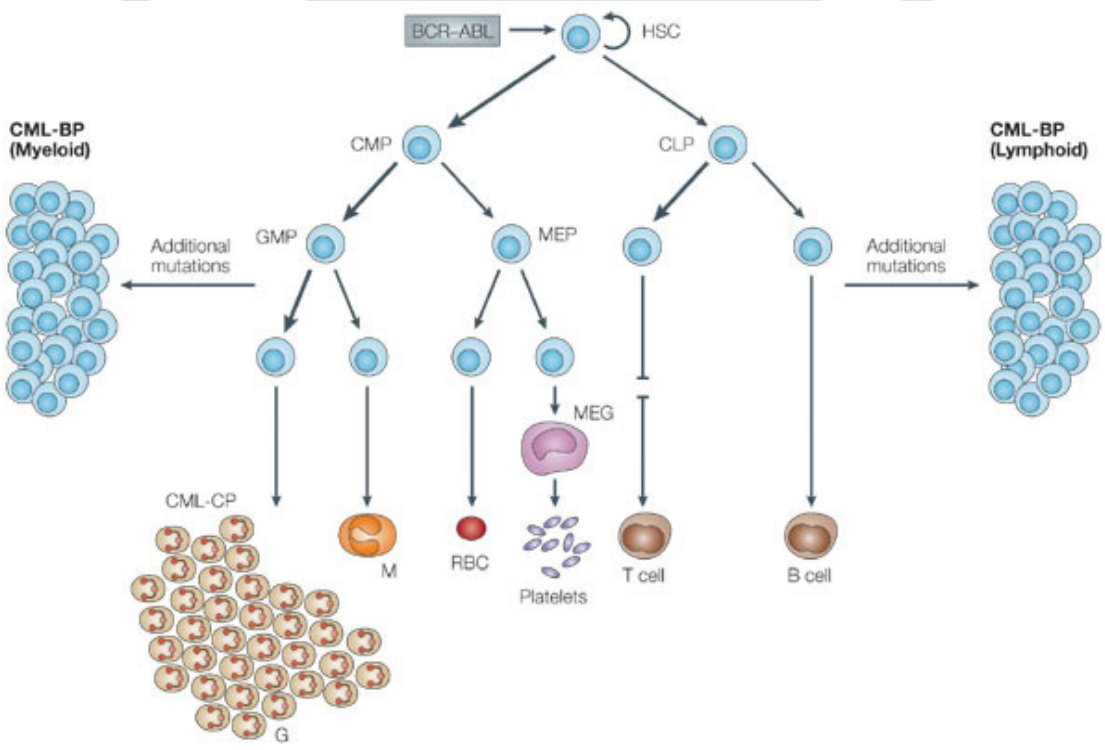

Figure 1.3: *Hierarchy of CML stem cells and different phases of CML (Ren 2005).*

CML is diagnosed by detecting the presence of Ph chromosome and BCR-ABL fusion gene in the peripheral blood (PB) and BM samples of the patient. The phase of the disease at diagnosis is confirmed by checking percentage of blast and myeloid cells in the BM and PB. The WHO criteria for CML accelerated and blast phase are as follows (Vardiman et al., 2002):

CML, accelerated phase

If one or more of the following is present:

- Blasts 10% to 19% of peripheral blood white cells or bone marrow cells
- Peripheral blood basophils at least 20%
- Persistent thrombocytopenia (< $100x10^9$/L) unrelated to therapy, or persistent thrombocytosis (> $1000x10^9$/L) unresponsive to therapy
- Increasing spleen size and increasing WBC count unresponsive to therapy
- Cytogenetic evidence of clonal evolution (the appearance of an additional genetic abnormality that was not present in the initial specimen at the time of diagnosis of chronic phase CML)

CML, blast phase

If one or more of following is present:

- Blasts 20% or more of peripheral blood white cells or bone marrow cells
- Extramedullary blast proliferation
- Large foci or clusters of blasts in bone marrow biopsy

1.2.1 BCR and ABL proteins

1.2.1.1 ABL protein

ABL is a 145 kilo dalton (kd) non-receptor tyrosine kinase protein which is involved in signaling pathways related to cell proliferation, survival and cytoskeletal modifications (Pendergast, 2002).Tyrosine kinases catalyze the transfer of the terminal phosphate group form Adenosine Triphosphate (ATP) to a tyrosine amino acid in the target protein. ABL tyrosine kinase consists of three Src Homology (SH) domains. SH1 domain has the tyrosine kinase catalytic activity responsible for tyrosine phosphorylation. SH2 domain increases the kinase efficiency by binding to the tyrosine phosphorylated proteins, which enables the kinase domain to phosphorylate at multiple phosphorylation sites in the target proteins (Duyster et al., 1995; Mayer et al., 1995). SH3 domain binds to proline rich

peptides in the target proteins. SH3 domain also regulates the tyrosine kinase activity by interacting with SH2 liker region and keeping the protein in inactive form (Barila and Superti-Furga, 1998).Tyrosine kinase activity is also negatively regulated by a myristoyl group present at the N-terminus, which interacts with the SH3 domain resulting in conformational changes in the kinase domain (Nagar et al., 2003). Towards the COOH-terminus, ABL protein has proline rich sequences which bind to adapter proteins such as CRKL (Ren et al., 1994).The COOH-terminus region also consists of binding regions for G and F actin (Van Etten et al., 1994) and RNA Polymerase C-terminal domain (Baskaran et al., 1997). ABL protein localizes in cytoplasm where it can associate to actin cytoskeleton via C-terminus domain (Van Etten et al., 1994), as well as in nucleus. In hematopoietic cells line HL60 and KG-1, ABL protein localized more in the cytoplasm (Wetzler et al., 1993).

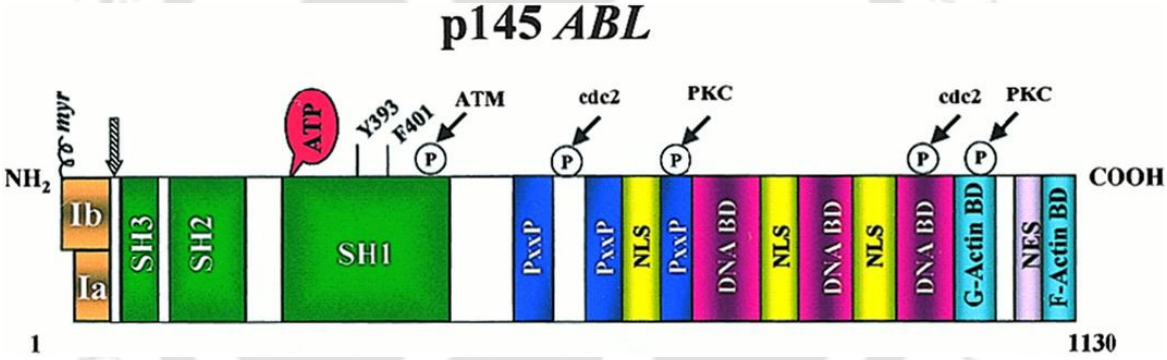

Figure 1.4: *ABL protein domains. From (Deininger et al., 2000).*

1.2.1.2 BCR protein

The *BCR* gene can code for two proteins with molecular weight 130 kd and 160 kd. In the first exon, *BCR* has a serine/threonine (S/T) kinase domain and SH2 binding domain (Laurent et al., 2001) (Figure 1.5).The SH2-binding domain can bind adaptor protein GRB2 (Pendergast et al., 1993) which is involved in RAS signal transduction pathway. It can also bind to the ABL SH2 domain in the BCR-ABL protein resulting in phosphorylation at Y177 (Muller et al., 1992; Pendergast et al., 1991). The first exon also has an oligomerisation domain which is essential for dimerisation or oligomerisation of the fusion BCR-ABL protein and crucial for interaction between BCR and BCR-ABL (Mcwhirter et al., 1993). The BCR protein also consists of Guanine nucleotide exchange

factor (GEF) domain between exons 3-10 which might play a role in the activation of G-protein associated signal transduction. Towards the COOH-terminus, BCR protein consists of GTPase-activating protein (GAP) homologous sequence which also regulates the GTPase activity of the G-proteins (Diekmann et al., 1991).

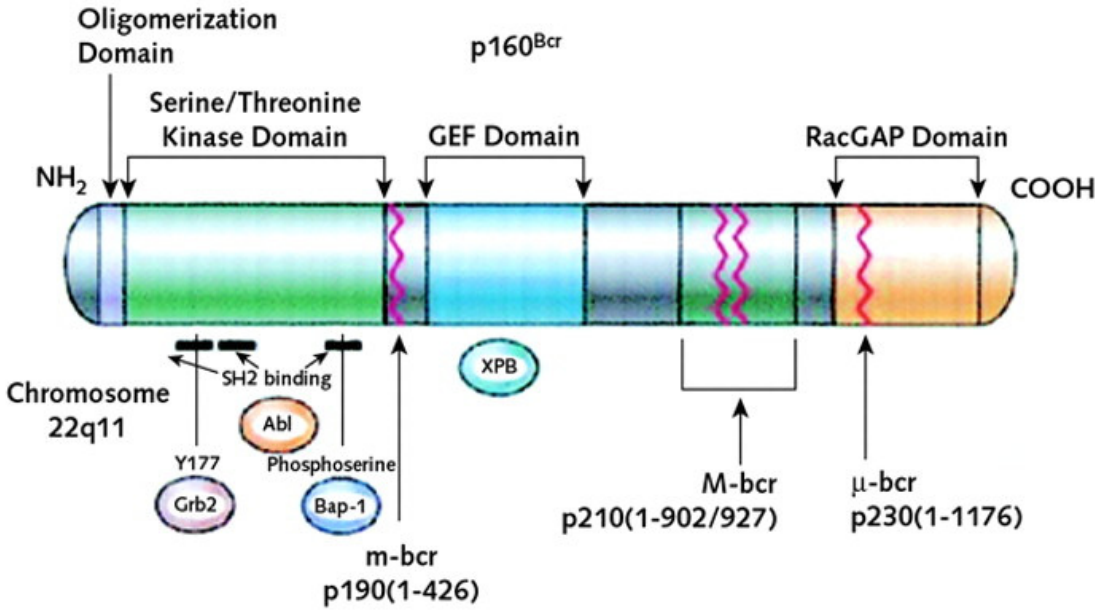

Figure1.5: *BCR protein domains. From (Kurzrock et al., 2003).*

1.2.2 BCR-ABL fusion protein

CML is characterized by the presence of *BCR-ABL* fusion gene. *BCR* gene is located on chromosome 22 and *ABL* gene is located on chromosome 9. The reciprocal translocation, between chromosome 9 and 22 results in *BCR-ABL* fusion gene. This translocation however is favored in CD34+ hematopoietic cells because of the close proximity between *ABL* and *BCR* genes during S and G2 phases of the cell cycle (Lukasova et al., 1997; Neves et al., 1999).

BCR gene generally codes for 4.5 kb or 6.7 kb mRNA transcripts. *ABL* gene codes for 6.0 kb or 7.0 kb mRNA transcripts. In the event of translocation, the break can occur in *ABL* gene downstream of exon 1a, between exon 1b and 1a or upstream of exon 1b. In *BCR* gene, there are three break point cluster regions mbcr, M-bcr and μ-bcr. In most CML

cases, break occurs at M-bcr region giving rise to 210 kd BCR-ABL protein. In case of break at m-bcr region the fusion gene codes for 190 kd protein and if the break occurs at µ-bcr, 230 kd protein is coded by the *BCR-ABL* gene (Figure 1.6) (Quintas-Cardama and Cortes, 2009).

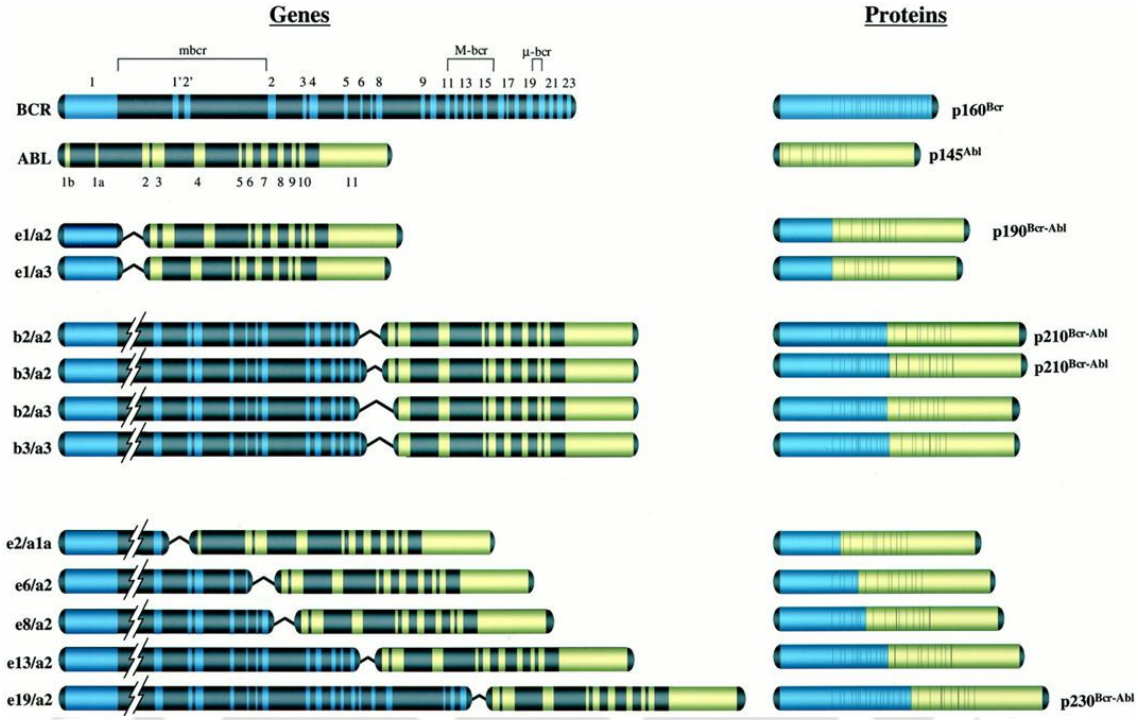

Figure 1.6: *BCR-ABL fusion products and corresponding protein size. From : (Laurent et al., 2001).*

The BCR-ABL protein is a constitutively active tyrosine kinase. BCR-ABL tyrosine kinase activity is essential for tumorogenesis. The tyrosine kinase activity of ABL kinase is inhibited by conformational regulations as a result of interactions between N-terminal myristoyl group and the kinase domain; SH2 domain and kinase domain; and SH2 linker and SH3 domain (Maru, 2012). In case of BCR-ABL protein, as a result of break in the *ABL* gene the myristoyl group on the ABL protein is absent. Also, interaction between SH3 domain and SH2 linker is also loosened because of changes in the protein conformation as a result of which SH2 domain is released. SH2 domain of the *ABL* coded region in BCR-ABL can bind to SH2 binding domain of *BCR* coded region of the fusion protein as well as other proteins resulting in their phosphorylation. The amino-terminal

coiled coil (CC) oligomerisation domain in the *BCR* coded domain helps in the dimerisation or oligomerisation of BCR-ABL protein which is essential for deregulation of BCR-ABL tyrosine kinase activity (Muller et al., 1992).

1.2.3 BCR-ABL Signaling

As a result of loss of auto-inhibitory regulations, BCR-ABL is constitutively active. The CC oligomerization domain in the BCR region promotes dimerization/tetrameriztaion of BCR-ABL resulting in trans-autophosphorylation and activation of target tyrosine sites. BCR-ABL can autophosphorylate at Y177 in the S/T kinase domain of the *BCR* coded region. Phosphorylation at Y177 was reported to be essential for leukemogenesis (Zhang et al., 2001). Phosphorylated Y177 in the S/T kinase domain binds with high affinity to the SH2 domain of GRB2. Adaptor protein GRB2 binds to son of sevenless (SOS) which is a guanine-nucleotide exchanger of RAS. GRB2 binds to SOS through its SH3 domain and activates RAS-MAPK signaling (Puil et al., 1994; Sattler et al., 2002). BCR-ABL was reported to activate JNK-MAPK pathway also through RAS activation (Raitano et al., 1995). GRB2 binds to GRB2-associated binding protein 2 (GAB2) as well through its SH3 domain. As a result of this binding, GAB2 can result in constitutive activation of phosphatidylinositol 3-kinase (PI3K)/AKT signaling pathway (Skorski et al., 1995).PI3K/AKT pathway can also be activated by adaptor protein CRKL, which binds to proline rich region in the ABL coded portion of BCR-ABL through its SH3 domain (Kolibaba et al., 1999). ERK-MAPK signaling is activated by GAB2 through SHP-2 or by RAS signaling (Sattler et al., 2002) (Figure 1.7). RAS-MAPK-ERK pathway was reported to be constitutively active in BP-CML cells and CD34+ hematopoietic cells from CML patients (Notari et al., 2006).

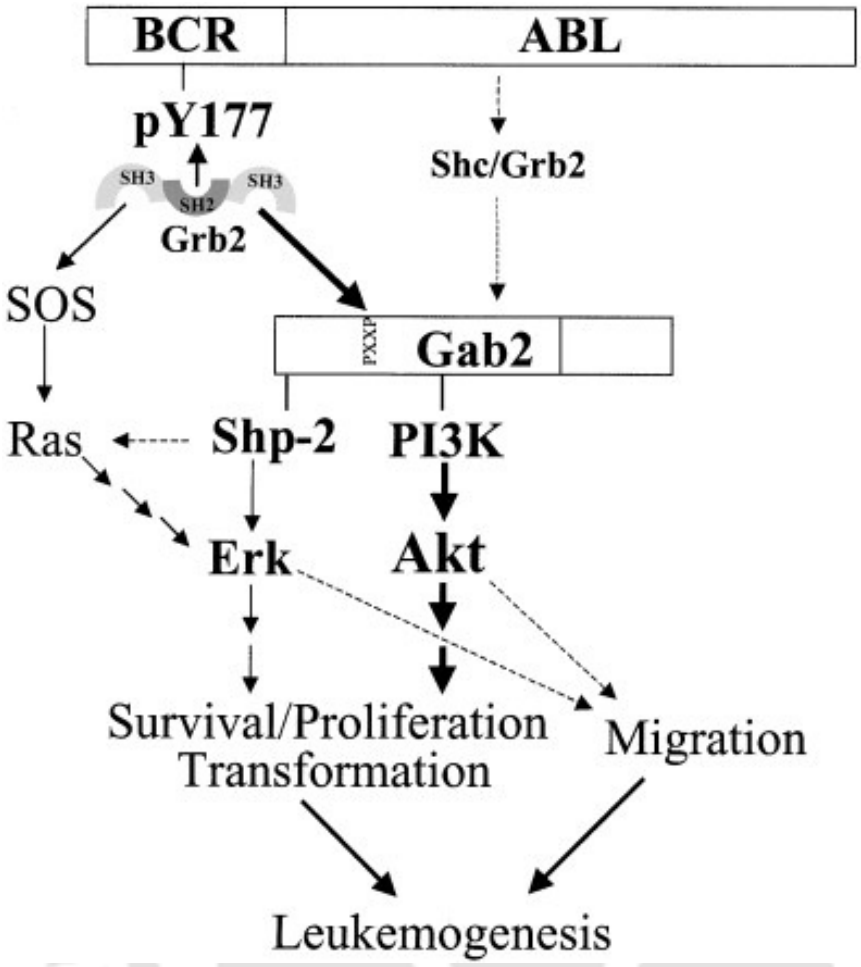

Figure 1.7: *Activation of ERK MAPK and PI3K/AKT signaling by BCR-ABL. From (Sattler et al., 2002)*

BCR-ABL activity affects transcription factors as well. Signal transducer and activator of transcription 5 (STAT5) is constitutively active in CML cells. STAT5 activation is involved in proliferation of CML cells and activation of anti-apoptotic signaling in CML cells (Carlesso et al., 1995, 1996; Frank and Varticovski, 1996). Activation of STAT5 leads to growth factor independence in CML cells. Unlike normal hematopoietic cells in which growth factors such as interleukin-3 (IL-3) or granulocyte colony forming factor (GCSF) activate STAT5 through JAK activation, BCR-ABL can directly phosphorylate STAT5 (Hantschel et al., 2012; Ilaria and VanEtten, 1996) (Figure 1.8). BCR-ABL can also activate STAT5 by acting upstream and leading to JAK phosphorylation (Chai et al., 1997; Shuai et al., 1996) or by autocrine production of IL-3 and GCSF by CML cells (Jiang et al., 1999).

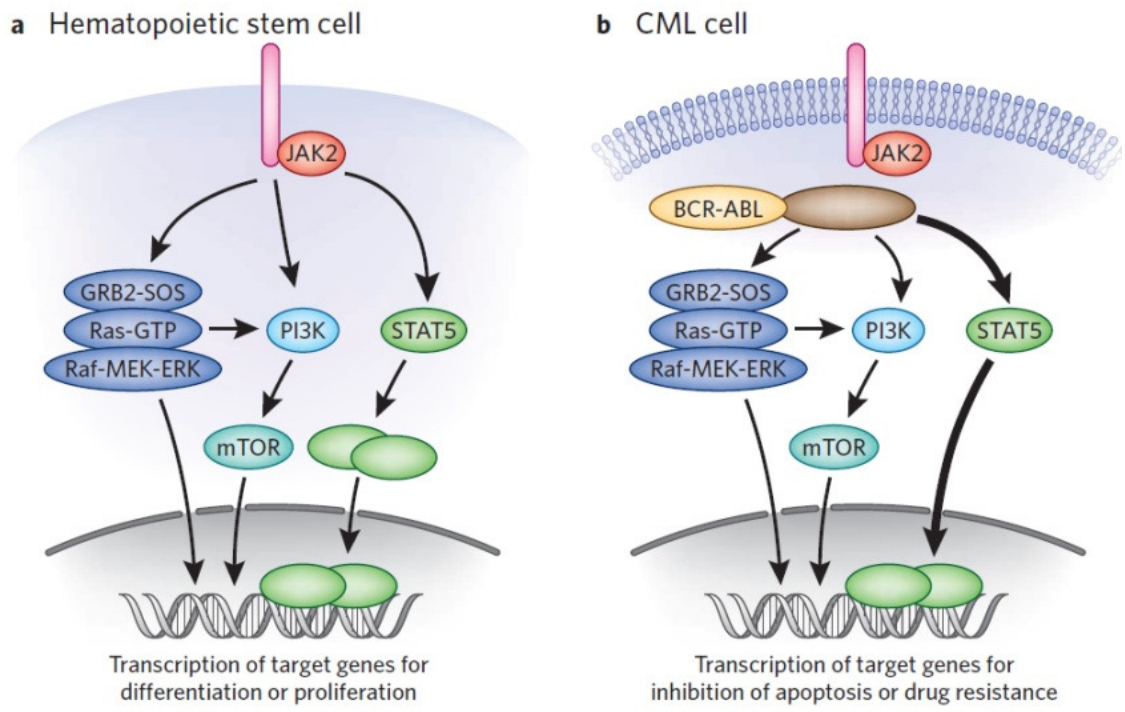

Figure 1.8: *Comparison of STAT5 activation in normal HSC and CML cells. From: (Fabbro, 2012)*

BCR-ABL tyrosine kinase also influences adhesion properties of CML cells. BCR-ABL can phosphorylate focal-adhesion kinase (Fak) (Gotoh et al., 1995; Salgia et al., 1995a). BCR-ABL expression increases the adhesion of CML cells to fibronectin coated surface through increased α5β1 expression (Kramer et al., 1999). BCR-ABL also interacts with paxillin through adaptor protein CRKL leading to increased adhesion to fibronectin (Salgia et al., 1995b; Uemura et al., 1999)

BCR-ABL directly activates JAK2 in an IL-3 independent mechanism. JAK2 forms complex with SH2 domain located near the C-terminal region of ABL (Xie et al., 2001). JAK2 activates PI3K signaling pathway which increases c-Myc expression. C-Myc transcription factor increases survivin expression through promoter region binding (Fang et al., 2009). Several Bcl-2 family apoptosis modulators are also upregulated in CML cells. PI3K/AKT signaling by BCR-ABL increases expression of BCL-XL (Tang et al., 2000). AKT also phosphorylates BAD which protects CML cells from apoptosis (Neshat et al., 2000). BCR-ABL also activates expression of anti-apoptotic gene BCL-XL by STAT5 activation (Gesbert and Griffin, 2000).

1.2.4 Treatment of CML

CML was first reported in 1865 as a disease with accumulation of white blood cells (Figure 1.9). However, in 1960 the presence of Ph chromosome was reported in CML cells (Nowell and Hungerford, 1960). In 1973, translocation t(9;22)(q34;q11) was detected as the cause for formation of Ph chromosome (Rowley, 1973). Later, the translocation t(9;22)(q34;q11) was reported to cause the generation of BCR-ABL gene (Groffen et al., 1984; Heisterkamp et al., 1983).ABL tyrosine kinase activity was discovered in 1980 and later BCR-ABL was also shown to be a tyrosine kinase (Konopka et al., 1984). In 1990, *BCR-ABL* gene was reported to be capable of initiating CML in mice (Daley et al., 1990). In the mean time, tyrosine kinase inhibitors were developed against platelet derived growth factor receptor (PDGFR), Kit and ABL tyrosine kinases. In 1998 tyrosine kinase inhibitor, Imatinib mesylate (IM, ST1-571 or Gleevec) was first tested in CML patients. IM was found to be a very effective therapy for CML and in 2001 it was approved by FDA for CML therapy (Hunter, 2007).

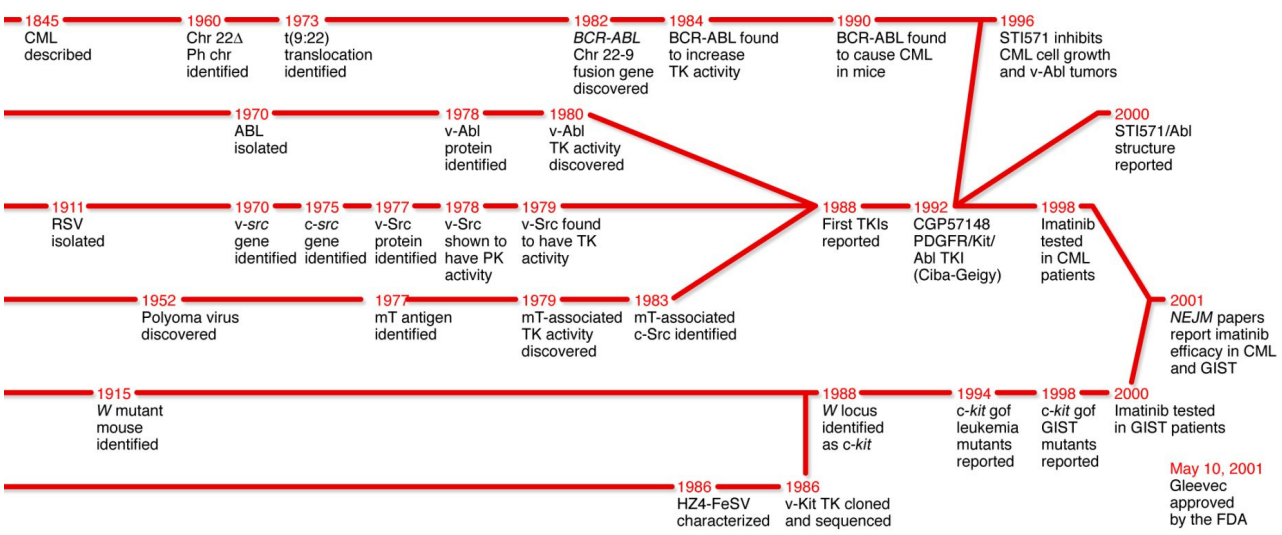

Figure 1.9: *A timeline of research on of CML and associated findings which led to the discovery of IM as an effective drug for CML therapy. From :(Hunter, 2007)*

Before the discovery of tyrosine kinase inhibitors (TKIs) such as IM, different treatment strategies were utilized for CML. Till today, allogenic hematopoietic cell transplantation (HCT) is the only curative therapy for CML. However, because of high risks associated with mismatch and a very low probability of a human leukocyte antigen (HLA) matched

donor, use of transplant in CML is very limited. Cytotoxic drugs such as busulfan and hydroxyurea were used earlier which could lower the high white blood count and clinical manifestations of the disease. However, these drugs were not effective in controlling the progression of CML into blast phase. Later, recombinant interferon-α (rIFN-α) increased the survival of CML patients leading to a complete hematologic response (HR) in many patients but only a few patients (13 to 27%) achieved complete cytogenetic response (CR). In addition, rIFN-α had several adverse effects because of which many patients (up to 20%) could not continue this therapy. Combination of IFN- α and cytosine arabinoside (ara-C) had significantly higher survival rates but the combination had increased toxicity compared to IFN- α alone. Despite the limitations, HCT and rIFN-α therapy were the main strategies for CML treatment before the advent of TKIs (An et al., 2010; Salesse and Verfaillie, 2002).

1.2.5 Mechanism of IM and chemoresistance

TKIs inhibit the tyrosine kinase activity in CML cells, which is necessary for leukemogenesis. IM was the first TKI to be developed and used in CML patients. Tyrosine kinases transfer the terminal phosphate group form ATP to the substrate. IM is a 2-phenylamino pyridine based competitive inhibitor for ATP (Figure 1.10). IM binds to the ATP binding site in the catalytic domain of BCR-ABL tyrosine kinase and thus blocks the ATP binding (Schindler et al 2000). IM binds to the catalytically inactive conformation of ABL kinase and stabilizes it. In this inactive conformation, a sequence of amino acids Asp-Phe-Gly (DFG) is flipped out of its normal position. This DFG out confirmation is not observed in crystal structures of ABL kinase which is not bound to the inhibitor. Moreover, the nucleotide binding P-loop which interacts with the phosphate group of ATP folds over IM and thus stabilizes IM bound form of the ABL kinase (Weisberg et al., 2007). Apart from ABL and BCR-ABL, IM also inhibits the activity of the PDGFR, Arg kinase and c-kit. However, IM does not inhibit the Src family kinases (Druker et al., 1996).

Successful phase I and phase II trials of IM were conducted in CML patients who were resistant or intolerant to rIFN-α treatment. Later phase II trials were conducted in advanced CML patients using 600mg/day dose of IM. After successful randomized phase

III trials [International Randomized Study of Interferon and STI571 (IRIS)] in 1106 patients unresponsive to the combination of IFN-α and ara-C, IM was approved by Food and Drug Administration (FDA) as first line treatment strategy for CP-CML patients (O'Brien et al., 2003). Inhibition of tyrosine kinase activity of BCR-ABL by TKIs specifically reduced the proliferation of CML cells and restored the growth factor dependent proliferation and differentiation of BCR/ABL+ cells lines (Druker et al., 1996; Kantarjian et al., 2007). IM also inhibited the growth of CML myeloid colony forming cells but not the growth of normal colonies. Long-term culture of BM cells with IM inhibited the growth of CML progenitors (Salesse and Verfaillie, 2002). For CML patients, IM is administered orally at a daily dose of 400mg. Efficacy of higher IM dosages between 400 to 800mg per day were compared with 400mg dose, however no striking differences were reported to rationalize the usage of higher dose of IM (An et al., 2010). IM has low toxicity towards normal cells and a dose escalation phase I trial did not reveal IM toxicity even at high concentration which were tested and thus making IM a more effective and safer drug for CML compared to other alternatives which had been tried earlier (Salesse and Verfaillie, 2002).

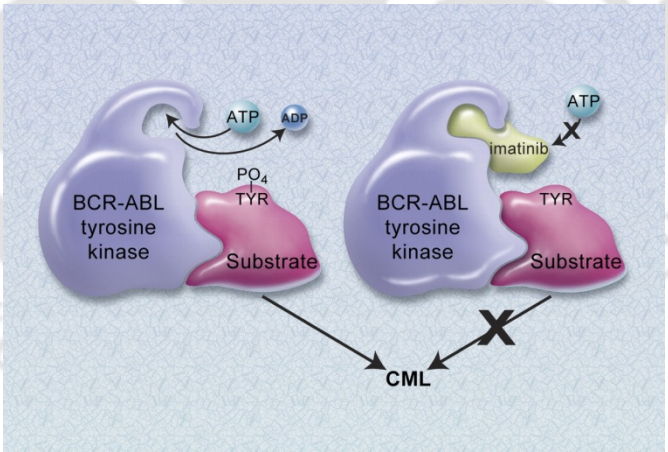

Figure 1.10: *Mechanism of BCR-ABL inhibition by IM. From: (Druker, 2008)*

Response to IM treatment is monitored by hematologic response (HR), cytogenetic response (CR) and molecular response (MR). HR is measured by checking the blood counts in the PB. CR corresponds to the percentage of BM cells positive for Ph chromosome which can be measured by Fluorescence in-situ Hybridization (FISH). MR

is checked by Quantitative reverse-transcription PCR (QPCR) by measuring the reduction in BCR-ABL mRNA compared to a standard baseline or International Scale. Definitions of HR, CR and MR in response to Imatinib Mesylate (IM) therapy as per European Leukemia Net are summarized in the table below (Baccarani et al., 2009):

Response by Type	**Definitions**
Hematologic	
Complete Hematologic Response	White Blood Cells < 10×10^9/L
	Basophils < 5%
	No myelocytes, promyelocytes, myeloblasts in the differential
	Platelet count < 450×10^9/L
	Spleen nonpalpable
Cytogenetic	
Complete Cytogenetic Response	No Ph+ metaphases
Partial Cytogenetic Response	1% to 35% Ph+ metaphases
Minor Cytogenetic Response	36% to 65% Ph+ metaphases
Minimal Cytogenetic Response	66% to 95% Ph+ metaphases
No Cytogenetic Response	> 95% Ph+ metaphases
Molecular	
Complete Molecular Response	Undetectable *BCR-ABL* mRNA transcripts by real time quantitative and/or nested PCR in two consecutive blood samples of adequate quality (sensitivity > 10^4)
Major Molecular Response	Ratio of *BCR-ABL* to *ABL* (or other housekeeping genes) ≤ 0.1% on the international scale

Table 1.1. *Response to IM treatment (Baccarani et al., 2009)*

Since the discovery of TKIs and the successful phase III IRIS trial, in which efficacy of IFN-α and ara-C combination was compared with IM, IM was adopted as the main drug against CML. CML patients, especially in chronic phase responded very well to IM. 95.3 % of the 1106 patients in the clinical trial achieved CHR, and major cytogenic response was reported in 85.2% patients (O'Brien et al., 2003). However, several patients are resistant to IM treatment which is generally referred as primary resistance. On the other hand, some patients develop IM resistant post treatment which is referred as secondary or

acquired resistance (An et al., 2010). Failure to respond to IM therapy is defined by European Leukemia Net as follows:

Evaluation period	**Suboptimal response**	**Failure to respond to imatinib**
3 months	Absence of cytogenetic response (CgR)	Incomplete hematological response (HR)
6 months	CgR but less than partial CgR	Absence of CgR
12 months	Partial CgR (presence of 1-35% Ph+ cells)	CgR but less than partial CgR
18 months	Molecular response (MR) but less than major MR (ratio of BCR-ABL/ABL<0.1%, corresponding to a ≥ 3 log reduction in BCR-ABL transcripts)	CgR but less than complete CgR
Any time during treatment	Major MR loss; mutations still sensitive to imatinib	Complete HR loss; complete CgR loss; low sensitivity of mutation to imatinib; presence of chromosome abnormalities.

Table 1.2: *Failure in response in IM treatment. (Baccarani et al., 2009; Bitencourt et al., 2011)*

Mutations in the BCR-ABL gene, which reduce the binding ability of IM to BCR-ABL was reported to help in the development of resistance to IM treatment (Gambacorti-Passerini et al., 2003). Thr315Ile mutation in the BCR-ABL kinase domain was the first mutation which was reported after a study of 9 IM resistant patients. 6 out of 9 patients were positive for this point mutation and BCR-ABL gene amplification was the reason of IM resistance in other 3 patients (Gorre et al., 2001). Since then several BCR-ABL mutations have been identified, however the most common mutations found in IM resistant patients are Leu 248Val, Gly250Ala, Gly250Glu, Tyr253His, Tyr253Phe, Glu255Lys, Glu255Val, Thr315Ile, Phe317Leu, Met 351Thr, Glu355Gly, His396Arg, Phe359Val. BCR-ABL mutations such as Thr315Ile, Phe317Leu may directly inhibit IM binding as a result of changes in the amino acid side chains responsible for hydrogen

bond formation and lipophilic interactions required for effective IM binding or by causing steric hindrance which reduces IM binding (Weisberg et al., 2007).

1.3 Bone marrow microenvironment

BM is the major site for hematopoiesis where HSC reside and differentiate into mature blood cells. The main function of BM as an organ is to maintain a constant number of differentiated hematopoietic cells of different kinds in the body. The human bone marrow produces approximately 500 billion cells every day (Fliedner et al., 2002). BM consists majorly of the cells of hematopoietic and mesenchymal lineage. Hematopoietic cells in the bone marrow are the HSC, hematopoietic progenitor cells and plasma cells. Mesenchymal Stem Cells (MSC) and its derivatives osteoblasts and adipoblasts along with HSC derived macrophages are the major components of the stromal cells present in the BM. The HSC and its stromal counterparts interact with each other through secreted factors, cell surface adhesion molecules and extra cellular matrix (ECM) components. These interactions play an important role in the regulation of HSC self renewal and differentiation into mature cells.

MSC are multipotent cells which can self renew and differentiate into cells of mesodermal lineage. MSC have been isolated form bone marrow, adipose tissue, cord blood, ocular tissues, cerebral cortex, dental pulp, skeletal muscle (Hass et al., 2011). MSC were first isolated from BM by Friedenstein et al and were reported to differentiate into bone and cartilage cells (Friedenstein et al., 1987). MSC have been studied extensively for their differentiation potential and have been shown to differentiate into osteocytes, adipocytes, chondrocytes, myocytes, astrocytes, neuronal cells, endothelial cells, and hepatocytes (Caplan and Bruder, 2001)(Figure 1.11). MSC are positive for cells surface markers such as CD13, CD29, CD44, CD73, CD90, CD105, CD146 and human leukocyte antigen-I (HLA-I); and they negative for hematopoietic markers CD34, CD45 and human leukocyte antigen-II (HLA-II) (Hass et al., 2011).

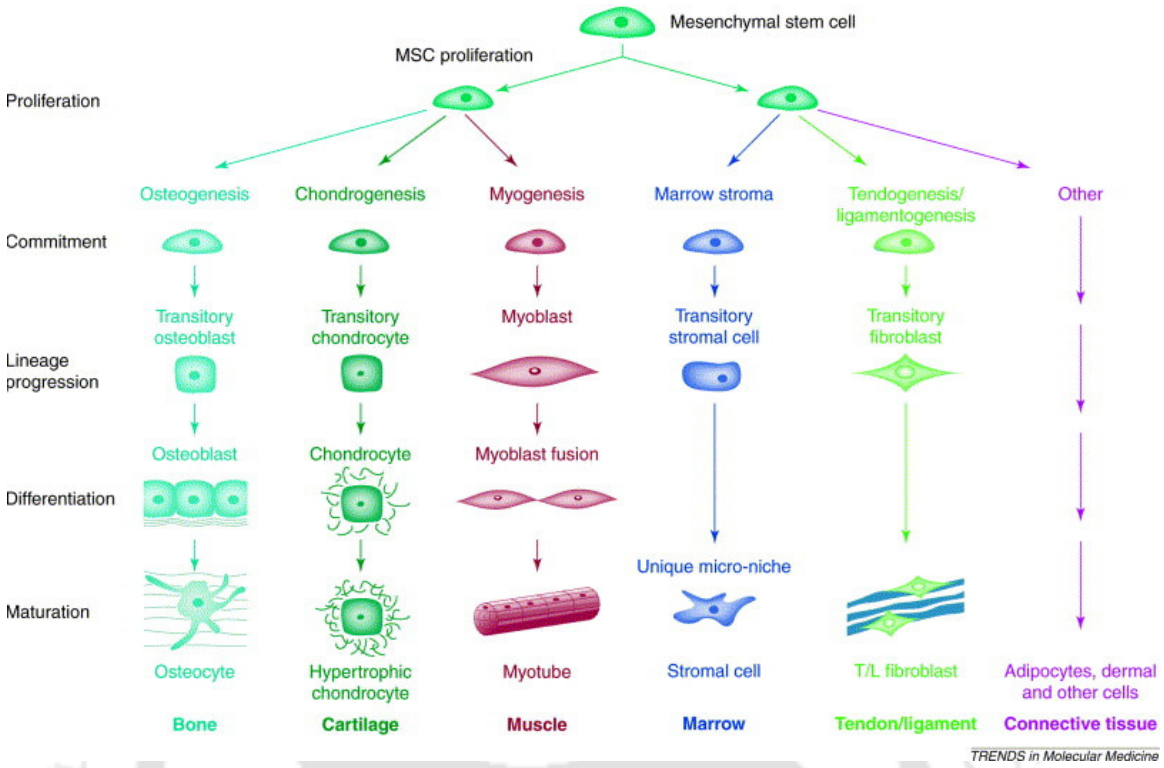

Figure 1.11: *Differentiation potential of MSC into different types of mature cells. From: (Caplan and Bruder, 2001)*

MSC have been reported to secrete several cytokines and growth factors. MSC secreted growth factors and cytokines such as epidermal growth factor (EGF), platelet-derived growth factor (PDGF), vascular endothelial growth factor (VEGF), hepatocyte growth factor (HGF), Angiopoietin-1, fibroblast growth factor (FGF), transforming growth factor β (TGF-β), stem cell derived factor (SDF-1), interleukin-8 (IL-8) are involved in wound healing, tissue repair and angiogenesis (Giacca and Zacchigna, 2012; Lee et al., 2011; Ma et al., 2013). MSC have been shown as a promising candidate for therapy because of their differentiation potential, self renewal capacity, immunomodulatory role and anti-inflammatory properties. MSC secreted cytokines are necessary for their immunoregulatory function (Siegel et al., 2009). MSC either secrete these cytokines on their own or when they are stimulated by other cytokines such as IFNγ, tumor necrosis factor-α (TNF-α) or interleukin-1β (IL-1β), upon which MSC secrete imunomodulatory cytokines such as indolamine 2,3dioxygenase (IDO), prostaglandin E2 (PGE2), nitric oxide (NO) and TGFβ (Bernardo and Fibbe, 2013; Ren et al., 2008; Ren et al., 2012; Ren et al., 2010).

MSC secreted cytokines and factors also play an important role in hematopoiesis. IL-6 is involved in B cell differentiation, megakaryocyte maturation and expansion of HSC (Hirano et al., 1990). FLT3 ligand secreted by the stromal cells acts as growth factor for immature myeloid cells and helps in expansion of CD34+ cells (Gilliland and Griffin, 2002; Shi and Hu, 2011). Thrombopoietin (TPO) regulates proliferation and differentiation of HSC as well as growth of platelets and megakaryocytes (Rappold et al., 1999; Rappold et al., 1998). C-X-C Motif Chemokine Ligand 12 (CXCL12)/C-X-C chemokine receptor-4(CXCR4) signaling axis regulates homing, adherence and migration of HSC (Mendez-Ferrer et al., 2008; Mishima et al., 2010; Sugiyama et al., 2006). Apart from secreted factors, stromal cells interact with HSC via cell surface expressed adhesion molecules such as N-Cadherin (N-Cad) and β integrins.

1.4 Hematopoietic and stromal cell interactions in BM

1.4.1 Stromal components of BM

BM provides a complex microenvironment to HSC which regulates quiescence, self renewal and differentiation of HSC. HSC are present in osteoblastic niche or vascular niche in the BM (Figure 1.12). Osteoblastic or endosteal niche corresponds to the bone-BM interface area where HSC closely interact with osteoblasts cells. Vascular niche is the sinusoidal perivascular area in the BM.

Recent studies have reported an increasing heterogeneity among the stromal populations present in the BM (Figure 1.12). HSC reside in the BM in contact with the osteoblasts via N-Cad and integrins which is very crucial for quiescence and dormancy of HSC. (Trumpp et al., 2010). Nakamura et al investigated different subpopulations of stromal cells in the endosteal based on the expression of Activated leukocyte cell adhesion molecule (ALCAM) and Stem cells antigen-1 (SCA-1), for their capacity to support and maintain HSC. All the three fractions ($ALCAM^{-}SCA^{+}$, $ALCAM^{+}SCA^{-}$, $ALCAM^{-}SCA^{-}$) were found to support long-term reconstitution (LTR) ability of HSC *in vitro*. However, $ALCAM^{+}SCA^{-}$ fraction expressed higher levels of cell adhesion markers Cdh2, Cadherin 11 and ALCAM which significantly increased the LTR ability of HSC compared to $ALCAM^{-}SCA^{+}$ fraction which expressed cytokines and growth factors at higher levels

(Nakamura et al., 2010). Nestin+ MSC which were identified recently, reside in the perivascular niche at higher frequency and at a lower frequency in the endosteal niche. Nestin+ MSC express high levels of HSC maintenance genes such as CXCL-12, SCF, Angiopoietin-1,IL-7 and Vascular cell adhesion protein-1 (VCAM-1). Nestin+ MSC can grow *in vitro* as mesenspheres and maintain their self-renewal capacity. These cells were shown to co-localize with HSC in the vascular niche (Mendez-Ferrer et al., 2010). CXCL12-abundant reticular (CAR) cells present in both endosteal and vascular niches were shown to interact closely with HSC in both the niches and regulate HSC cycling and self renewal (Sugiyama et al., 2006). Self-renewing CD146+ osteoprogenitors are capable of establishing hematopoietic microenvironment in the BM *in vivo. CD146*+osteoprogenitors support sinusoidal angiogenesis which further supports hematopoiesis (Sacchetti et al., 2007). Osteoclasts, a subpopulation of macrophages, which are responsible for bone resorption, upon activation by RANKL resulted in mobilization of HSC from BM (Kollet et al., 2006). However, loss of osteoclast activity is associated with defective HSC niche formation in mouse model. In the absence of osteoclast activity the number of mesenchymal progenitor cell increased, however, their osteoblastic differentiation was reduced. This led to impaired homing of HSC to the BM (Mansour et al., 2012). Osteomacs, which are also a subpopulation of macrophages, are present near the endosteal niche and their depletion upon Granulocyte-colony stimulating factor (G-CSF) treatment led to osteoblastic depletion and HSC migration(Winkler et al., 2010).

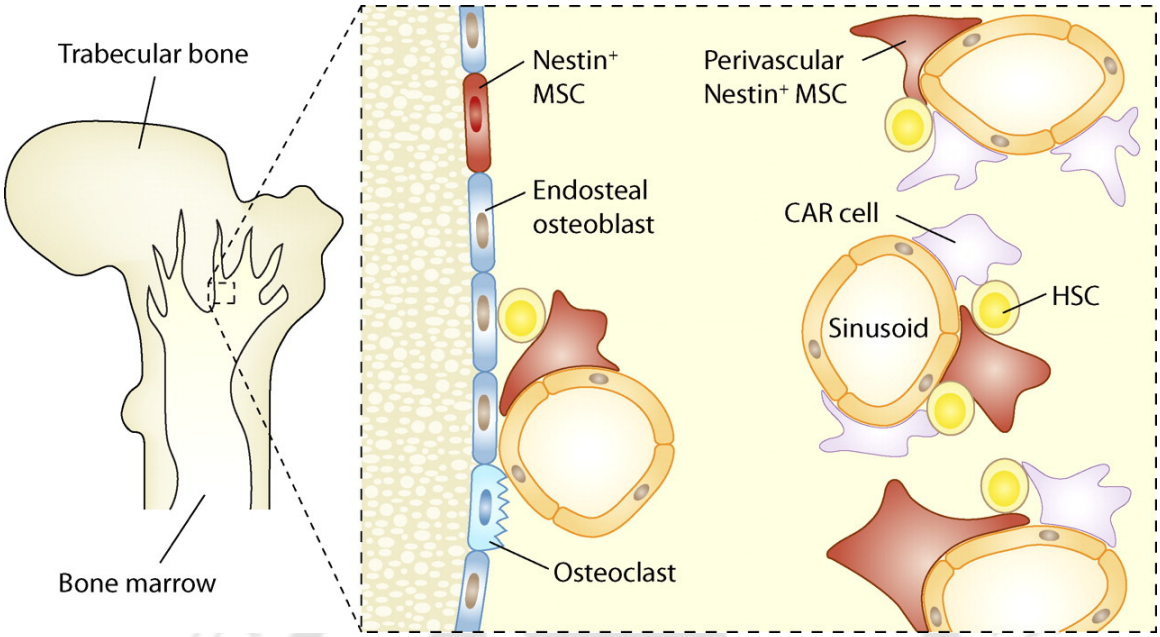

Figure 1.12: *Different cellular components of the BM niches. From (Levesque et al., 2010)*

1.4.2 Molecular signaling pathways in the BM niche

The cellular components of the BM interact with HSC through various signaling molecules (Figure 1.13). Secreted ligands from the stromal cells such as CXCL-12, SCF interact with their receptors on the HSC and are crucial for HSC maintenance. CXCL-12 (or SDF1) secreted by endosteal as well as vascular niche cells was shown to regulate HSC localization, homing and quiescence (Greenbaum et al., 2013). Osteoblasts, Nestin+ MSC and CAR cells secrete CXCL-12, which is the ligand for CXCR4 present on the HSC surface. SCF expressed by endothelial and perivascular stromal cells was shown to be important for cKit+ HSC maintenance as conditional deletion of SCF from these cells led to depletion of HSC population (Ding et al., 2012).

Notch signaling has also been implicated in hematopoiesis, although its role has been debatable. Transduction of Lineage negative (lin-), c-kit positive, Sca-1 positive (LSK) HSC with active Notch1 intracellular domain regulated their self renewal and maintained HSC in undifferentiated state (Varnum-Finney et al., 2000a; Varnum-Finney et al., 2000b). Further studies showed higher Notch signaling levels in LSK-HSC compared to other compartments of HSC. HSC with high Notch signaling could differentiate into multiple cell type colonies and had higher LTR ability. Notch signaling inhibition

resulted in differentiation of HSC (Duncan et al., 2005; Wu et al., 2007). Notch ligands delta-1 and Jagged-1(JAG-1) are expressed by osteoblasts and parathyroid hormone activated osteoblasts increased HSC number by Notch signaling upregulation (Calvi et al., 2003). Jag-1 is also present on CD146+ stromal cells which can support HSC maintenance (Sacchetti et al., 2007). However *in vivo* studies reported the role of Notch signaling to be dispensable for HSC maintenance. Inducible inactivation of JAG1 in bone marrow stromal cells did not result in impaired HSC self renewal and differentiation (Mancini et al., 2005).

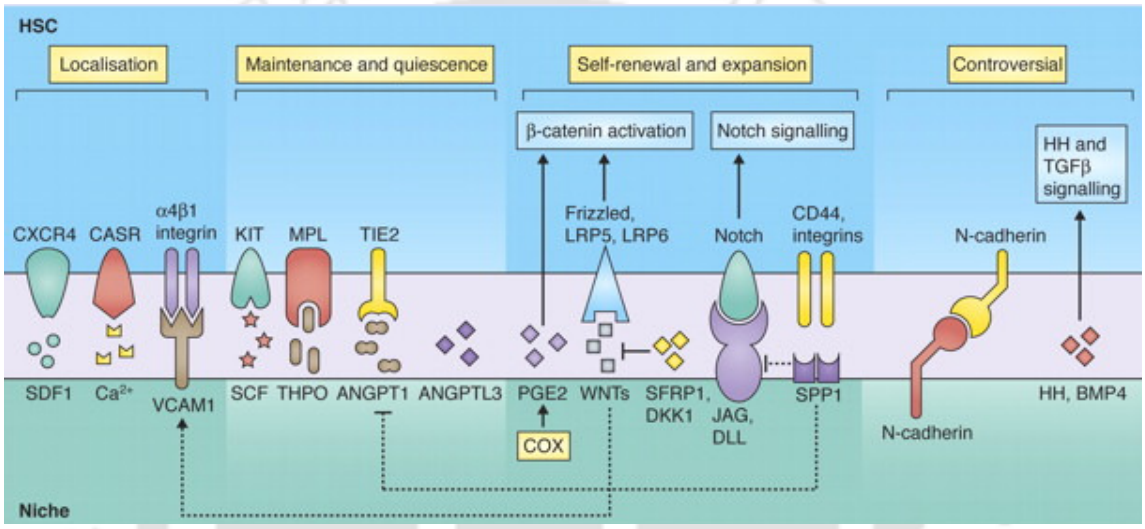

Figure 1.13: *Interactions between HSC and BM niche cells. From (Lo Celso and Scadden 2010)*

Niche mediated Wnt signaling also plays an important role in HSC maintenance. c-Kit+ Thy-1.1lo Lin-/lo Sca-1+ (KTLS) HSC transduced with constitutively active β-catenin, an important component of Wnt signaling, could be maintained longer in *in vitro* culture and had higher short term growth properties. Transduced HSC maintained immature phenotype in long-term *in vitro* culture as well (Reya et al., 2003) Wnt3a deletion in mouse embryo resulted in deficient number of HSC in fetal liver. Loss of function HSC had low LTR ability (Luis et al., 2009). Osteoblast specific promoter driven expression of a canonical Wnt signaling inhibitor dickkopf homolog 1 (DKK1) resulted in increased rate of cell cycle, decreased self renewal and regenerative capacity of HSC, via inhibition of Wnt signaling in HSC (Fleming et al., 2008) Similar results were reported in transgenic mice expressing Wnt inhibitor factor 1 (Schaniel et al., 2011) .

TGF-β in the BM niche helps in HSC self renewal and dormancy through TGF-β-Smad signaling. TGF-β signaling is context dependent in regulation of HSC self-renewal and differentiation (Larsson and Karlsson, 2005). TGF-β has differential effects on myeloid biased HSC (My-HSC) and Lymphoid biased HSC (Ly-HSC). TGF-β signaling increased the proliferation of My-HSC *in vitro* and *in vivo* but inhibited the proliferation of Ly-HSC suggesting that TGB-β signaling in the BM niche regulates the cross talk between different subtypes of HSC and maintain their populations (Challen et al., 2010).

Hedgehog (HH) signaling was implicated in regulation of HSC proliferation by activation of bone morphogenetic protein (BMP4) signaling. This effect could be abrogated by inhibiting either HH or BMP4 (Bhardwaj et al., 2001). BMP4 plays an important role in embryonic hematopoiesis (Zhang and Li, 2005). In adult BM, BMP4 is expressed by the BM stromal cells such as osteoblasts and endothelial cells. In BMP4 deficient mice, number of LSK-HSC was reduced as a result of microenvironmental defects. Normal HSC transplanted into BMP4 deficient mice had reduced LTR activity (Goldman et al., 2009). Recently, inhibition of Smad dependent BMP signaling by noggin was reported to increase CXCL-12 production in the BM. Modulation of CXCL-12 expression by BMP signaling regulated HSC homing, engraftment and migration (Khurana et al., 2014).

Adhesion molecules also play an important role in the HSC interaction with the BM stroma (Zhang et al., 2003). The increase in number of N-Cad expression by osteoblasts was found to correlate with the number of HSC in the BM. N-Cad expression on HSC corresponded to the reconstitution ability of HSC. Differential expression of N-Cad on HSC represented functionally different populations of HSC. N-Cad-low HSC population had high stem cell reconstitution ability compared to the N-Cad-high or N-Cad-intermediate HSC populations (Haug et al., 2008). Osteopontin is an ECM protein secreted by osteoblasts lining the endosteal niche. Adhesion of HSC to osteopontin via β1 integrins inhibits HSC proliferation and regulated HSC localization (Nilsson et al., 2005). Expression of Very Late Antigen-4 (VLA-4) i.e. Integrin α4β1was reported to be important for HSC homing, HSC retention in the BM and short term engraftment of HSC. Integrin α4β1 binds to VCAM1, which is expressed on BM stromal cells, and regulates

HSC homing. Inhibition of VLA4 resulted in HSC mobilization (Ramirez et al., 2009; Rettig et al., 2012).

HSC and BM stromal interactions with each other depend on several molecules and are highly complex. In the table below several components of HSC-BM stromal signaling are listed.

Components	***Effects in vivo or in vitro***
Proteins	
Angiopoietin-1	Overexpression in HSC increases HSC quiescence and recovery from cytotoxic insult and irradiation
Transmembrane KIT-ligand	Lack of expression in host causes severe anemia and reduced HSC lodgment into endosteal niches
Thrombopoietin	Anti-Mpl antibody increases HSC proliferation *in vivo*. TPO administration increases the number of quiescent HSC *in vivo*
BMP-4	Deletion in host increases HSC proliferation, but decreases serial reconstitution (HSC self-renewal)
Sfrp1	Deletion in host decreases HSC proliferation and serial reconstitution (self-renewal)
Connexin-43	Deletion compromises recovery from cytotoxic insult
CXCL12	Conditional deletion of the receptor CXCR4 causes HSC to enter cell cycle, compromise recovery from cytotoxic insult and mobilize into the blood
Osteopontin	Gene deletion causes increased HSC proliferation, accumulation in BM and reduced lodgment to the endosteum following transplant
VCAM-1	Deletion of *VCAM-1* gene induces HSPC mobilization. Deletion of its receptor on HSC reduced HSC lodgment into endosteal niches
N-cadherin	N-cadherin knockdown or overexpression of dominant-negative mutant in HSC increases HSC proliferation, reduces lodgment to the endosteum and compromises long-term reconstitution
Annexin II	Anti-annexin II antibody treatment of HSC reduces HSPC homing to the BM, and long-term reconstitution following transplant. HSPC adhere less to annexin II-deficient osteoblasts
Pathways	
Notch signaling	Inhibition compromises HSC self-renewal and increases differentiation
Wnt signaling	Overexpression of Dikkopf-1 in osteoblasts to inhibit Wnt signaling increases HSC proliferation and decreases serial reconstitution (HSC self-renewal)

Physicochemical properties	
Soluble calcium ion	HSC lacking the calcium receptor have hypocellular BM with reduced number of HSC. They fail to lodge near endosteum upon transplantation
Low blood perfusion, hypoxia	Dormant serially transplantable HSC reside in poorly perfused hypoxic niches and the endosteal niches are hypoxic

Table 1.3. *Bone marrow niche factors. From (Levesque et al., 2010)*

1.5 BM niche in CML chemoresistance

Even though several aspects of HSC-stromal interactions in the BM are still unresolved, a crucial role of microenvironment in hematopoiesis has already been established. However, recently a great interest and curiosity has been generated in understanding the role of microenvironment in hematological malignancies. An important role of BM stroma in leukemia initiation, progression, chemoresistance and relapse has been reported by several groups.

LSC were first reported in AML as a phenotypic subpopulation of leukemic cells. Within the leukemic cells the phenotypic subpopulation which could engraft SCID mice and give rise to colony forming cells was within the CD34+CD38- cell compartment (Lapidot et al., 1994). Later, CD34+CD38- cells were shown to initiate AML in NOD/SCID mice and differentiate *in vivo* to reestablish the disease phenotype in mouse model (Bonnet and Dick, 1997). LSC are similar to HSC in exhibiting potential for self-renewal, dormancy and multi-lineage differentiation. Like HSC, LSC also depend on BM stromal microenvironment for localization, survival and differentiation. Development of malignant niche which differentially supports leukemic cells was also suggested early on (Duhrsen and Hossfeld, 1996). Even though LSC and HSC share several key properties and are dependent on stromal signaling, LSC and its progenitors because of abnormal proliferation advantages can outgrow normal hematopoietic progenitors and manipulate the stromal cells and hijack the BM (Duhrsen and Hossfeld, 1996).

Most signaling pathways important for HSC survival and maintenance have been shown to be important for LSC as well. LSC and HSC adhesion to stroma is guided by similar adhesion molecules such as N-Cad and β1 integrins. Similarly, LSC also utilize CXCL-

12-CXCR4 signaling axis for homing and migration (Tabe and Konopleva, 2014). However, pathways related to survival and proliferation are abnormally activated in LSC (Tabe and Konopleva, 2014)

IM has been successfully used for treatment of a majority of CP-CML patients. However, several patients develop resistance to IM even after few years of remission, especially after discontinuation of IM intake, suggesting that a subpopulation of leukemic cells evade chemotherapeutic effects of IM and persist in the BM. It is proposed that the interactions between leukemic cells and the BM stromal cells play a crucial role in the development chemoresistance. Therefore, role of BM stromal cells and the mechanisms involved in the persistence of leukemic cells against IM and other TKIs need to be studied in detail.

Cytokines secreted by MSC, osteoblasts and other stromal components have been implicated in CML cell chemoprotection against IM and other TKIs. BM stromal cell conditioned media (CM) as well as addition of individual cytokines IL-6, IL-8, IL-11, macrophage colony-stimulating factor (M-CSF), granulocyte-macrophage colony-stimulating factor (GM-CSF) and SDF-1 increased proliferation of CML cells and partially protected CML cells from the inhibitory effect of IM. The combination of these cytokines was more effective than individual cytokines indicating a cumulative role (Weisberg et al., 2008). MSC co-cultured with CML cells in a transwell system without direct physical contact had higher gene expression of IL-17 signaling related inflammatory cytokines such as IL-8, IL-1B and CCL2. Similar changes were observed when MSC were co-cultured in physical contact with CML cells (Civini et al., 2013). CM media from stromal cell line HS-5, protected K562 cells from IM, Nilotinib (NI) and Dasatinib (DS) induced cell death. Stromal CM increased the phosphorylated levels STAT3 in CML cells which was independent of BCR-ABL activity. K562 cells had increased protein levels of anti-apoptotic regulators BCL-xl, MCL-1 and Survivin when cultured in stromal CM and treated with IM (Bewry et al., 2008). In a recent study, a stroma secreted cytokine FGF2 was reported to protect K562 cells from IM induced cell death and confer IM resistance to K562 cells in long term culture. The IM resistance in K562 cells in presence of FGF2 could be abrogated by inhibition of FGFR and ABL

tyrosine kinase activity in K562 cells. FGFR signaling by FGF2 restored Erk1/2 activity in long term K562 cultures in presence of IM which could have played an important role in IM resistance (Traer et al., 2014). Inhibition of stroma secreted placental growth factor (PlGF) slowed the progression of CML without affecting the disease characteristics or homing of the leukemic cells. Leukemia-stromal interaction by VLA-4-VCAM-1 binding upregulated NFkB signaling in the stromal cells resulting in high PlGF expression by the stromal cells. PlGF did not affect STAT5 phosphorylation which is a downstream target of BR-ABL signaling but increased phosphorylation levels of ERK1/2 (Schmidt et al., 2011).CXCR4 is involved in the migration of HSC towards the stromal cell in the BM. CXCL-12 induces migration of leukemic cells *in vitro* (Zeng et al., 2006)which can be effectively inhibited by CXCR4 inhibitor plerixafor (AMD3100). AMD3100 reduced the adhesion of CML cells to fibronectin, endothelial cells and MSC (Weisberg et al., 2012). CD34+ cells from CML-BP patients had lower membrane bound expression of CXCR4 compared to CD34+ cells form CP-CML patients or healthy individuals. BCR-ABL expression was reported to downregulate membrane bound CXCR-4 expression in BCR-ABL transduced MO7e cell line in a dose dependent manner (Geay et al., 2005). Inhibition of BCR-ABL by IM increased CXCR4 expression in presence of MSC which might facilitate the migration of CML cell towards BM stromal cells. IM treatment increased the migration of CML cell towards stromal layer in a transwell assay which was abrogated by CXCR4 antagonist (Jin et al., 2008). CXCR4 antagonist AMD3100 reverted the chemoprotective effect of stromal cells on CML cells treated with TKIs (Dillmann et al., 2009; Weisberg et al., 2012). It was hypothesized that post IM treatment CML cells migrate towards the chemoprotective environment of the stromal cells which express copious amounts CXCL-12. And hence a combinatorial therapy using CXCR4 antagonist along with IM was proposed (Beider et al., 2014; Jin et al., 2008).

Physical interaction of CML cells with stromal microenvironment depends on adhesion molecules such as VLA-5, CD44, N-Cad. CD44 adhesion molecule which binds to E-selectin expressed on endothelial cells in the BM, was reported to be highly expressed in CML stem and progenitor cells. BCR-ABL+ CML cells lacking CD44 expression had reduced homing and engraftment in mouse model (Krause et al., 2006). Similarly lack of E-selectin in the recipient BM led to reduced engraftment of BCR-ABL+ cells (Krause et

al., 2014). TKI treatment along with CD44 monoclonal antibody targeting significantly reduced CML-LSC *in vivo* in mouse model (Hellqvist et al., 2013).

Adhesion of CML cells to fibronectin via VLA-5 was implicated in adhesion dependent chemoprotection of CML cells, suggesting the role of ECM in CML chemoresistance (Damiano et al., 2001). CML-stromal interaction via VLA-4/VCAM-1 binding resulted in NFkB activation in stromal cells which led to expression of inflammatory cytokines by stromal cells (Schmidt et al., 2011).

CML and stromal cells also interact with each other via N-Cad which is expressed by CML as well as stromal cells. N-Cad expression in primary CML cells increased post IM treatment in presence of MSC. MSC adherent CD34+ CML cells had higher levels cytoplasmic N-Cad/β-catenin complex as well as nuclear β-catenin levels. Inhibition of Wnt signaling by DKK1 increased apoptosis in CML cells in co-culture with MSC (Zhang et al., 2013). However it was reported later that Wnt signaling is important for intrinsic TKI chemoresistance in CML cells but not for stroma mediated extrinsic chemoresistance (Eiring et al., 2015).

Thus, understanding the signaling mechanisms involved in the development of chemoresistance in CML, especially, the role of closely interacting bone marrow microenvironment will help in developing better therapeutic strategies to complete eliminate the leukemic cells.

2.0 AIMS AND OBJECTIVES

Leukemia is a disease not only of the hematopoietic cells but of the whole hematopoietic system consisting of hematopoietic cells and the associated stromal cells present in the bone marrow microenvironment. The leukemic cells interrupt and modify the microenvironment stromal cells as much as they are modified by their microenvironment. As a result of this reciprocal interaction, a malignant niche is created which support malignant hematopoiesis rather than the normal hematopoiesis. This malignant niche can also protect the leukemic cells from the effect of chemotherapeutic agents.

Thus, this study aims at understanding the effect of chronic myeloid leukemia cells on their stromal microenvironment and the functional and gene expression changes that occur in the stromal cells as a result of this interaction. Additionally, this study also proposes to analyze the effect of stroma derived paracrine factors and direct cell-cell interaction in chemoprotection of leukemic cells. Chemoprotection leads to the development of chemoresistance in leukemic cells and several signaling molecules are aberrantly regulated during this process. So, this study also aims to find out the key signaling molecules that are important in development of stroma mediated chemoresistance in leukemic cells and the role of pathway inhibitors in chemosensitizing the chemoresistant cells as a therapeutic option. Thus, the following objectives were formulated for this study:

1. To study the characteristics of stromal microenvironment in chronic myeloid leukemia (CML)
2. To understand the role of stroma derived paracrine factors in CML chemoprotection
3. To study the effect of cell-cell interaction between leukemic cells and the stromal cells in CML chemoprotection
4. To derive microenvironment mediated chemoresistant CML cell line and to study the aberrant signaling pathways in the chemoresistant cells

3.0 Materials and Methods

3.1 List of antibodies

3.1.1 Cell surface marker antibodies

Antibodies against the following human cell surface antigens were used for the study.

Sl.No	Antigen	Clone	Company
1	CD13	L138	BD Biosciences
2	CD29	MAR4	BD Biosciences
3	CD34	8G12	BD Biosciences
4	CD44	C26	BD Biosciences
5	CD49A	SR84	BD Biosciences
6	CD49B	AK7	BD Biosciences
7	CD49C	C311.1	BD Biosciences
8	CD49D	9F10	BD Biosciences
9	CD49E	IIA1	BD Biosciences
10	CD49F	GoH3	BD Biosciences
11	CD61	RUU-PL7F12	BD Biosciences
12	CD73	AD2	BD Biosciences
13	CD81	JS-81	BD Biosciences
14	CD90	5E10	BD Biosciences
15	CD95	DX2	BD Biosciences
16	CD104	439-9B	BD Biosciences
17	CD105	266	BD Biosciences
18	CD120A	MABTNFR1-B1	BD Biosciences
19	CD140A	Alpha-R1	BD Biosciences
20	CD200	MRC OX-104	BD Biosciences
21	CD253	RIK-2	BD Biosciences
22	Ki67	7B11	Invitrogen

3.1.2 Phospho antibodies

Antibodies against the following human phospho proteins were used for the study.

Sl. No	Phospho protein	Clone	Company
1	pERK1/2 (pT202/pY204)	20A	BD Biosciences
2	pNFκB p65 (pS529)	K10-895	BD Biosciences
3	pP38 MAPK (pT180/pY182)	36/p38	BD Biosciences
4	pSMAD1 (pS463/pS465)/SMAD8 (pS465/pS467)	N6-1233	BD Biosciences
5	pSTAT3 (pS727)	49	BD Biosciences
6	pSTAT5 (pY694)	47/Stat5	BD Biosciences

3.2 List of primers

3.2.1 Real-time PCR primers for human genes

Sl. No	Gene	Primer sequence
1	BAP1-Forward	ATCTGGGTCCTGTCATCAGC
2	BAP1-Reverse	GCTGCCTTGGATTGGTCTG
3	BMP2-Forward	CTGTCTTCTAGCGTTGCTGCT
4	BMP2-Reverse	CCTCCGTGGGGATAGAACTTA
5	BMP4-Forward	GACTTCGAGGCGACACTTCT
6	BMP4-Reverse	TGCTGCTGAGGTTAAAGAGGA
7	BSP-Forward	TGGCACAGGGTATACAGGGT
8	BSP-Reverse	CTGCCTCTGTGCTGTTGGTA
9	CAT-Forward	GCCTGGGACCCAATTATCTT
10	CAT-Reverse	GAATCTCCGCACTTCTCCAG
11	CD47-Forward	AGCTCTAAACAAGTCCACTGTCCC
12	CD47-Reverse	TCCTGTGTGTGAGACAGCATCACT
13	GDF3-Forward	ATGTACTTCGCTTTCTCCCAGA
14	GDF3-Reverse	CTGACCGCAACACAAACATT
15	IL6-Forward	CTGACCCAACCACAAATGCC
16	IL6-Reverse	GTTGTCATGTCCTGCAGCCA
17	MnSOD-Forward	CTGGACAAACCTCAGCCCTA
18	MnSOD-Reverse	CTGATTTGGACAAGCAGCAA
19	PRKCH-Forward	GTGACTTGATGTTCCACATTCAG
20	PRKCH-Reverse	ATTGTCCAGTTTCAGATCTCTATAG
21	TNF-Forward	ATCTTCTCGAACCCCGAGTGA
22	TNF-Reverse	GAGCTGCCCCTCAGCTTG
23	WNT7B-Forward	GAAGCAGGGCTACTACAACCA
24	WNT7B-Reverse	CGGCCTCATTGTTATGCAGGT

3.2.2 Cloning primers

Sl. No	Gene	Primer sequence
1	hBMP2 F-BamHI	GCGCGGATCCATGGTGGCCGGGACCCGCTGT CT
2	hBMP2 R-BamHI	GCGCGGATCCGCGACACCCACAACCCTCCACAA
3	hBMP4 F-BamHI	GCGCGGATCCATGATTCCTGGTAACCGAATCT
4	hBMP4 R-BamHI	GCGCGGATCCGCGGCACCCACATCCCTCTATA
5	h-GDF3 F-BamHI	GCGCGGATCCATGCTTCGTTTCTTGCCAGATTTG
6	h-GDF3 R-BamHI	GCGCGGATCCCTACCCACACCCACATTCATCGACT

3.3 Cell culture methods

3.3.1 Culture of K562 CML cells

BCR-ABL positive chronic myeloid leukemia (CML) cell line K562 was procured from National Centre for Cell Sciences Pune, India. The cells were cultured in RPMI media (Sigma) supplemented with 10% fetal bovine serum (Thermo Fisher Scientific) and 1X Penicillin/Streptomycin solution (Thermo Fisher Scientific). The cells were maintained at a minimum cell density of $1x10^5$ cells and a maximum density of $1x10^6$ cells. The cells were sub-cultured every 3-4 days to maintain the cell density and to avoid the induction of cell differentiation.

3.3.2 Isolation of primary CML cells

Primary CML cells were isolated from the bone marrow (BM) of patients diagnosed for CML and referred to the Hematology Department of Gauhati Medical College Hospital, in collaboration with Dr. Jina Bhattacharyya and Dr. Damodar Das. Bone marrow was collected from the patients after obtaining ethical clearance from the hospital and IIT Guwahati for the study. Informed written consent was obtained from the patients to utilize the cells left after the diagnosis for research purpose. Bone marrow was also obtained during routine testing for treatment outcome and during remission, following ethical committee guidelines.

The BM samples were transferred to the lab on ice and processed the same day or within 24 hours (hrs) after BM collection. First, the cells were subjected to red cell lysis (RBC) using RBC lysis buffer (10mM Potassium Carbonate, 150mM Ammonium Chloride, 0.1mM EDTA, pH 8.0) on ice, at the ratio of 1:5 (bone marrow: RBC lysis buffer) for 7 minutes (mins). The RBC lysis was terminated by addition of 10% FBS (v/v) and centrifugation. The resulting cell pellet was resuspended in appropriate buffer and mononuclear cells were counted using hemocytometer.

3.3.3 Isolation and culture of bone marrow derived mesenchymal stem/stromal cells (MSC)

MSC were isolated from patients diagnosed for hematologic malignancies and referred to Department of Hematology, Gauhati Medical College Hospital for bone marrow analysis.

The cells were obtained after informed written consent from the patient following institutional ethical guidelines. The BM cells were subjected to RBC lysis and centrifugation. The cell pellet was resuspended in growth media consisting of DMEM low glucose media supplemented with 10% FBS and 1X Penicillin/Streptomycin solution. The cells were plated at a density of $1x10^5$ cells/cm^2 in tissue culture flasks coated with fibronectin (20ng/cm^2 for 1hr at 37°C). Media was changed after 24 hrs and thereafter every 3-4 days until spindle shaped colonies appeared. After the cells reached 70% confluency, they were sub-cultured and later used for experiments.

3.3.4 MSC-CML cells co-culture

To co-culture CML cells (primary samples, K562 CML cell line) with MSC stromal layer, the stromal cells were seeded in tissue culture dishes at a concentration of 10,000 cells/cm^2. The cells were allowed to attach for 24 hrs. Leukemic cells were added to the stromal layer at a ratio of 1:10 (stromal cell: leukemic cells) and co-culture system was established for allowing the cells to attach and proliferate for 48 hrs. For long-term co-culture, media change was performed every 3 days. The adherent leukemic cells were also passaged onto new stromal layer whenever required.

3.3.5 Separation of adherent and suspension CML cells from stromal co-culture

In co-culture conditions, a fraction of leukemic cells were attached to the stroma and rest of the leukemic cells were present as suspension cells. The suspension and adherent fractions of leukemic cells were separated for cell counting, apoptosis analysis, signaling pathway analysis, gene expression studies and for further sub-culture into new stromal layer.

For separation of adherent and suspension leukemic cells, initially the suspension cells were collected along with the media from the co-culture system into a separate tube. The cell layer was gently washed with PBS twice to remove all the suspension cells which were not firmly attached to the stromal cell layer and added to the same tube.

After removal of the suspension cells, the stromal layer was washed once with PBS. To remove the stroma adherent leukemic cells, 0.05% trypsin was added to the co-cultured cells and incubated for up to 30 seconds at room temperature while monitoring the

leukemic cell detachment from the stromal layer microscopically. Once the cells had detached, the trypsin solution along with the cells were collected in a tube containing FBS to inactivate the trypsin action. The remaining leukemic cells were collected again by washing the stromal layer with ice cold PBS.

3.3.6 Adherent versus suspension cell ratio determination

To determine the ratio of adherent versus suspension CML cells, equal number of CML cells was added to all the co-culture conditions. After 24hrs, the suspension cells were removed from the co-culture and added to a separate tube and the adherent cells were collected in a separate tube. The cells were centrifuged and cell pellet was resuspended in 1ml of growth media and the cells were counted using hemocytometer. To differentiate between the live and dead cells, equal amount of 0.4% trypan blue solution was added to the cells and trypan blue negative cells were counted as live cells. The ratio or percentages were calculated using the formula:

Adherent/Suspension cell ratio=

Number of adherent cells/Number of suspension cells.

Adherent cells percentage=

(Number of adherent cells)/(Number of adherent cells+ Number of suspension cells)

3.3.7 Sub-culturing of co-cultured CML cells

Stroma co-cultured CML cells were transferred to a new stromal layer for long-term experiments. In this case, only the stroma adherent cells were passaged. As mentioned in the earlier section, the suspension and adherent leukemic cells were separated from the stromal layer. The adherent leukemic cells were counted and seeded onto a fresh confluent stromal layer.

3.3.8 Separation of stromal cells from leukemic cells after co-culture

Stromal cells were analysed for gene expression, cell surface marker expression and IL-6 secretion after co-culture with the leukemic cells. As described in the previous sections, the adherent and suspension leukemic cells were removed from the stromal cell layer. The stromal cells were washed with PBS and checked under microscope to ensure

complete removal of all the leukemic cells. The cells were treated with 0.05% trypsin for 5-7 mins at 37ºC, the cells were checked under microscope for detachment from the tissue culture surface. Trypsinization was stopped by addition of serum and the cells were further processed for the experiments.

3.3.9 Long-term co-culture

To understand the interaction of leukemic cells with the stroma, long-term co-culture of leukemic cells with the stroma was performed. First, the MSC were seeded in plates or dishes. After the cells reached 100% confluency, the leukemic cells were added to the stromal layer in RPMI growth media and the co-culture system was maintained for 5-7 days. As the leukemic cells proliferated, several cells were present in suspension and the rest were adhered to the stromal layer. After establishment of co-culture system for 5-7 days, suspension cells were removed and IM(10µM) treatment was initiated. The suspension cells were regularly removed and fresh media with IM was added every 3-4 days. Hence the leukemic cells were maintained continuously in presence of IM (10µM). After 5 weeks of IM treatment initiation, depending on the experimental conditions, the adherent leukemic cells were treated with additional pathway inhibitors; transferred to a fresh stromal layer; used for analysis or maintained further in presence of IM on the same stromal layer.

3.3.10 Cobble stone area forming culture

To identify the presence of hematopoietic/leukemic stem cells, cobble stone forming assay was performed. The stromal layer cells were seeded and grown to confluency and mononuclear cells from the bone marrow were added to the stromal layer. The cells were cultured for 2 weeks and cobble stone forming areas were documented microscopically.

3.3.11 Collection of conditioned media from adherent MSC

MSC were seeded in tissue culture treated plates in normal growth media and allowed to grow to 100% confluency. After the cells reached confluency, fresh complete media was added to the cells. The conditioned media (CM) containing secreted factors was collected after 3 hrs, centrifuged to remove cell debris and filtered through 0.2um filter. CM was aliquoted and stored at -80°C until further use. For identification of secreted factors

through ELISA, serum free media was added instead of growth media.CM containing secreted factors was collected after 24 hrs and centrifuged to remove the cell debris.

3.3.12 Collection of conditioned media from suspension cells

Suspension cells were counted and seeded at a density of $1x10^6$ cells/ml in fresh growth media. After 3 hrs of incubation at 37°C, CM was collected by centrifugation to remove the cells. The supernatant was filtered through 0.2 um filter, aliquoted and stored at -80°C until further use. For ELISA experiments, the conditioned media was collected by adding serum free media to the cells and collected after 24 hrs.

3.4 Cryopreservation of cells and thawing

3.4.1 *Cryopreservation*

BM samples, isolated MSC or the leukemic cell lines were cryopreserved for later use. Briefly, adherent cells were trypsinized by addition of 0.05% trypsin solution (Thermo Fisher Scientific) for 5-7 mins and centrifuged. In case of suspension cells, the growth media was removed by centrifugation. The cells were washed once with ice-cold phosphate buffered saline (PBS, 137mM NaCl, 2.7mM KCl, 10mM Na_2HPO_4, 2mM KH_2PO_4, pH 7.0), resuspended in 100% FBS and transferred to cryovials. To each vial an equal volume of FBS with 20% (v/v) DMSO was added, the vials were transferred to cryo chill container and placed in -80°C deep freezer for 16 hrs. The cells were transferred to liquid nitrogen container for long-term storage.

3.4.2 Thawing of cryopreserved cells

The cryovials were taken from the liquid nitrogen container and immediately transferred to 37°C waterbath. Once the contents of the vials were thawed, the cell solution was transferred to a 15ml tube and warm media at 37°C was added drop-wise. The cells were centrifuged to remove DMSO, resuspended in growth media and plated in tissue culture flasks.

3.5 Differentiation into various lineages

3.5.1 Adipogenic differentiation

MSC obtained from the bone marrow were tested for adipogenic differentiation. The cells were plated at a density of 20,000 cells/cm^2 in tissue culture flask/dishes in growth media. After 24hrs, the media was removed and adipogenic induction media (DMEM high glucose with 10% FBS containing 1uM dexamethasone, 0.2mM indomethacin, 10mM Insulin and 0.5mM 3-isobuty-1-methylxanthine) was added to the cells. The media was changed every 3-4 days until 21 days to obtain differentiated adipocytes. The adipogenic differentiation was confirmed by staining the cells with Oil-Red O solution (1% w/v in isopropanol) and counted microscopically. Oil-Red O staining in the cells was also quantified by isolating the stain with 100% isopropanol and measuring the absorbance at 500nm.

The expression of adipogenic differentiation specific genes *ADIPOQ*, *PPARG* was determined by real-time PCR in the adipo differentiated cells and compared with control cells.

3.5.2 Osteogenic differentiation

Osteogenic differentiation of MSC was performed by seeding the cells at a density of 5000 cells in growth media. 24 hrs later, the growth media was replaced with osteogenic induction media (DMEM high glucose supplemented with 10% FBS, 0.1uM dexamethsone,10mM b-glycerolphosphate and 50uM ascorbic acid-2-phosphate). Fresh osteogenic media was added every 3-4 days for 21 days. The osteogenic differentiation was assessed by staining the differentiated cells for the presence of alkaline phosphatase using leukocyte alkaline phosphatase kit (Sigma) following the manufacturer's instructions. The extracellular calcium deposition was analysed by staining with Alizarin Red solution (40mM) The alizarin red staining was quantified by extracting the stain with Cetylpyridinium chloride and absorbance measurement at 562 nm.

The expression of osteogenic differentiation specific genes were analysed by detecting the expression levels of *OSTEOCALCIN* and *BSP* through real-time PCR.

3.6 Cell proliferation and cell death analysis

3.6.1 MTT assay

Equal numbers of cells were seeded in a 96-well plate and MTT assay was performed as per the manufacturer's instructions (EZcount MTT assay Kit, Himedia Laboratories). Briefly, MTT reagent was added to the cells and incubated at for 4-6hrs. The plate was checked under the microscope for the formation of formazan crystals. The formazan crystals were dissolved with DMSO and absorbance was measured at 570nm.

3.6.2 Annexin-V/Propidium iodide staining

Apoptosis analysis was performed by staining the cells with Annexin-V and PI (Annexin-V staining kit, Invitrogen – ThermoFisher Scientific) according to the manufacturer's instructions and analysed using flow cytometry. Briefly, the cells were collected and washed with ice-cold PBS. The cells were resuspended in100 µl of 1X Annexin V binding buffer at a concentration of $1x10^5$ cells/100µl buffer, anti annexin V antibody was added to the cells and incubated in dark for 15 mins at room temperature. Additional 200 µl of annexin-V binding buffer containing PI was added to the cells and analysed with FACSCalibur.

During analysis the cells were visualized in FSC versus SSC plot and gated to select the cells and to remove the cell debris. The gated population was plotted in FL1 versus FL3 to visualize the fluorescence in respective channels. Quadrant gate was created to separate the live cells, early apoptotic, late apoptotic and dead cells.

3.6.3 Active-caspase-3 staining

Cell death was further confirmed by staining for active form of caspase-3 and anlaysis through flow cytometry. Active caspase-3 staining was performed using Active caspase-3 apoptosis kit (BD biosciences). For this, cells were collected and washed twice with PBS. The cell pellet was resuspended in BD cytofix/cytoperm fixation/permeabilization buffer and incubated for 20 mins on ice. The cells were pelleted by centrifugation and the supernatant was discarded. The cells were washed twice with 1X BD perm/wash buffer and resuspended again with the recommended volume of BD perm/wash buffer and fluorescent conjugated anti-active caspase 3 antibody was added to the cells. The cells

were incubated in dark at room temperature for 30 mins. The cells were washed and analyzed with FACSCalibur.

3.7 Flow cytometry analysis

3.7.1 Cell surface marker/antigen expression analysis

The cell surface antigen expression was analysed by flow cytometry. Adherent cells were trypsinized and suspension cells were collected through centrifugation. The cell pellet was washed once with ice cold PBS to remove the media and resuspended in the staining solution (2% FBS in PBS) at a density of $1x10^5$ cells/100ul. In case of less number of cells, the cells were resuspended in a minimum volume of 50ul of staining solution. Fluorescent dye conjugated monoclonal antibodies against the specific cell surface antigen or isotype control was added to the cells and incubated on ice in dark for 30 mins. The cells were washed once, resuspended in the staining solution and analyzed by FACSCalibur (BD biosciences). Propidium iodide (PI) was added for live/dead discrimination.

First the cells were gated for live cells and the gated cells were plotted into FSC versus SSC plot. The cells were again gated to remove cell debris and the viable cells were visualized in the fluorescent channels for which the cells were stained. Gating for the positive cells were done based on the isotype control.

3.7.2 Phospho flow analysis

The phosphorylated levels of signaling proteins were analysed through phospho flow cytometry by specifically staining with antibodies against the phosphorylated forms of the proteins. The cells were fixed with 2% formaldehyde at 37°C for 10 mins, washed and permeabilised with 100% ice cold methanol for 15 mins on ice. The cells were washed with staining solution [0.5% Bovine serum albumin (BSA)], counted and equal number of cells from different treatments were added to the FACS tubes. Equal amount of fluorescent conjugated phospho specific antibodies (BD Biosciences) were added to the samples and incubated at room temperature for 1 hour. The cells were washed with the staining solution and analyzed with FACSCalibur.

3.8 Cell cycle analysis

3.8.1 Cell cycle through Cycle Trak expression

The cell cycle stage of leukemic cells K562 which were adherent to the stromal layer was determined real-time through the expression of cell cycle reporter plasmid CycleTrak (a kind gift from Dennis Ridenour, Stowers Institute for Medical Research, USA). The plasmid was packaged using the second-generation packaging plasmids and the target cells were transduced as described earlier.

3.8.2 Ki67 staining

The G0 cell cycle stage of the cells was analysed by Ki67 staining. The cells were pelleted by centrifugation and washed with PBS. 70% ice-cold ethanol was added to the cells drop wise while vortexing and incubated at -20ºC for 2 hrs. The cells were washed with excess amount of PBS and resuspended in 100µl staining buffer (2%FBS in PBS). FITC conjugated Anti-Ki67 antibody (BD Biosciences) was added to the cells at the recommended concentration and incubated at room temperature for 1 hour in dark. The cells were washed and stained with PI for 15 mins and analysed by flow cytometry.

The cells which were negative for Ki67 at the G0 position of the cell cycle were considered as quiescent or non-cycling cells.

3.8.3 Propidium iodide staining for cell cycle analysis

The cell cycle analysis was performed using propidium iodide (PI) staining. The cells were collected in appropriate manner and washed with PBS. The cells were fixed with ice-cold 70% ethanol. The ethanol was added drop-wise to the cell pellet while vortexing to avoid cell clumping. The cells were incubated at 4ºC for 30 minutes and washed twice with PBS by centrifugation at 2000rpm to pellet the cells. RNase A (50ul of 100ug/ml) was added to the cells and incubated at 37ºC for 30 minutes. PI (200ul of 50ug/ml) was added to the cells and incubated on ice for 20 minutes. The cells were analysed with FACSCalibur to detect PI fluorescence which shows the cell cycle profile.

During FACS analysis, first the cells were gated using forward vs side scatter plot to remove the cell debris. The cells were gated in FL2-area versus FSC height to remove cell doublets. The cell cycle profile was visualized in FL2 channel in the linear scale.

3.9 Gene expression analysis

3.9.1 RNA extraction

The cells were collected and washed with ice-cold PBS. The cell pellet was resuspended in TriZol solution (Thermo Fisher Scientific), mixed by vortexing and incubated at room temperature for 5 mins. Chloroform was added to the trizol mix (Chloroform:Trizol; 1:5) and incubated at room temperature for 5 mins. The samples were centrifuged at 12000xg for 15 mins at 4°C. The transparent aqueous phase was transferred to a fresh tube and an equal volume of 100% of ethanol was added to the sample to obtain final ethanol concentration of 50%. The contents were mixed briefly by vortexing and transferred to a spin cartridge (Pure Link RNA mini kit, Thermo Fisher Scientific). Total RNA extraction was performed as per the manufacturer's instructions and RNA was eluted from the spin column with RNase free water.

RNA was quantified by measuring absorbance at 260nm using Eppendorf Biophotometer (Eppendorf Ltd). The purity of RNA was assessed through 260/280 nm ratioand samples with values between 1.9 to 2.0 were used for further experiments. The RNA samples were stored at -80ºC until further processing.

3.9.2 Reverse transcription

2µg of total RNA was reverse transcribed into cDNA using high capacity cDNA reverse transcription kit (Applied Biosystems) using oligo dT primers. The reverse transcription reaction was performed as follows:

25°C for 10 mins
37°C for 120 mins
85°C for 5 mins

The resulting cDNA samples were diluted if necessary with RNase free water and stored at -20°C.

3.9.3 Real-time PCR

The gene expression at transcript level was assessed by real-time PCR. Real-time PCR was performed with Power SYBR Green real-time PCR mix (Applied Biosystems) using Applied Biosystems 7500 Real-time PCR system.

Real time PCR reaction mix per reaction was as follows:

cDNA: 20ng
Primers (forward and reverse): 500nM each
2X Power SYBR green master mix
Water was added to make up the reaction volume.

Real-time PCR reaction:

Initial stage
50°C for 2 mins
95°C for 10 mins
Cycling stage (35 cycles)
95°C for 15 seconds
55-60°C for 1 minute (temperature as per the primer annealing temperature)
Final extension stage
72°C for 10 mins
Melt curve stage
95°C for 15 seconds
60°C for 1 minute
(ramp rate of 1% to reach 95°C)
95°C for 30 seconds
60°C for 30 seconds

All genes were analysed in duplicates and the gene expression levels were quantified using $2^{\Delta\Delta Ct}$ method and normalized to GAPDH expression levels.

3.10 Gene cloning

3.10.1 Cloning PCR

To study the involvement of BMP signaling, BMP ligand genes*BMP2* and *BMP4* as well as BMP antagonist *GDF3* were cloned in the lentiviral vector. The lentiviral control plasmid had a single restriction enzyme site for BamHI. First, both forward and reverse primers with BamHI site were designed for *BMP2*, *BMP4* and *GDF3* genes. The primers spanned the region from start codon to the stop codon of the target genes. Primers were designed to make sure that the reading frames for the genes were unaffected.

For cloning, initially, total RNA was extracted from human mesenchymal stem cells and mRNA was reverse transcribed as described earlier. The resulting cDNA was utilized for performing the cloning PCR. Since the amplicon size for the genes to be cloned ranged

from 1.2 to 1.5 Kb, Phusion high fidelity DNA polymerase (New England Biolabs, NEB) was used. The cloning PCR reaction and cycling was as follows:

5X Phusion GC Buffer	1X
dNTPs	200 µM
Forward Primer	0.5 µM
Reverse Primer	0.5 µM
Template DNA	250 ng
Phusion DNAPolymerase	0.2 µl
Nuclease free water	to make volume to 20µl

The annealing temperature for the PCR was modified according to Tm of individual primers that were used for cloning.

3.10.2 Ligation and transformation

An aliquot of the PCR product was run on 1% low melting agarose gel to determine the product size and PCR specificity. The PCR products were purified using PCR purification kit (Qiagen) to remove the primers, salts and other impurities before cloning. Since Phusion DNA polymerase produces blunt end PCR products, the purified PCR products were ligated into blunt end Topo plasmid (Topo blunt end cloning kit, Invitrogen). Topo plasmid was used as an intermediate for subcloning to increase the cloning efficiency into the target lentiviral vector which is ~10Kb in size.

The ligated mix was transformed into E.coli DH5a (Top10 bacteria, Invitrogen) by heat shock method and 10 positive colonies were picked from the antibiotic selection plate. The colonies were grown in liquid culture and plasmids were isolated. The isolated plasmids were digested again with BamHI and tested for the presence of the cloned gene. Two clones of each gene that had the gene insert were further expanded and subcloned into the target lentiviral vector. For this, both the target lentiviral vector and the positive Topo plasmids were digested with BamHI and ran in 0.8% low melting agarose gel. The digested target vector and the insert were excised from the gel and the DNA was extracted with gel extraction kit (Qiagen) following manufacturer's instructions. The eluted DNA was quantified and ran in the gel to check the presence of DNA and the size before the final cloning step.

Since the cloning performed in the target lentiviral plasmid utilized a single restriction enzyme, this might result in re-ligation of the target plasmid. To avoid vector re-ligation without the insert, the BamHI digested target vector was dephosphorylated using CIP (calf intestinal phosphatase, NEB). The CIP treated target vector was gel purified (Gel extraction kit, Qiagen) and quantified. Ligation of the insert with the CIP treated target vector was performed using either Quick ligation kit (NEB) or using T4 DNA ligase kit (NEB). The ligated product was trasnsformed in Top10 bacteria using heat-shock and selected on antibiotic plate. The positive clones were analysed for the presence of insert through plasmid isolation and re-digestion with BamHI. Clones containing the plasmid with inserts were further expanded. Since this was a single site cloning, the orientation of the gene cloned could be in the correct or reverse direction. To detect the gene orientation, PCR was performed with plasmid specific forward primer and gene specific reverse primer as well as plasmid specific reverse primer and gene specific forward primer. The products were run on a gel and the plasmid with the correct orientation was sequenced to check for mutations. The plasmid with the gene in right orientation, checked for mutations through sequencing was used for further experiments.

3.10.3 Plasmid isolation

Plasmid was isolated from the transformed bacteria using the plasmid extraction mini kit (Qiagen), Maxi plasmid extraction kit (Thermo Fisher Scientific) according to the manufacturer's instructions.

3.11 Lentiviral packaging and transduction

3.11.1 Transfection of packaging cells

The packaging cells 293FT (Invitrogen) were plated at a density of 5-6x10^4cells/cm^2 in DMEM high glucose media containing 10% FBS, 1X non-essential amino-acids and 1X Penicillin/Streptomycin. The cells were allowed to adhere for 24 hrs and were transfected with the gene transfer plasmid and packaging plasmids using PEI (Polyethylenimine) method. For trasnsfection, the required amount of DNA was added to serum free DMEM high glucose media containing PEI. The PEI solution was mixed with the DNA, vortexed and incubated at room temperature for 10 mins after which required serum free media

was added. The DNA-PEI mix was gently added to the cell layer and incubated at 37ºC. Serum was added to the cells after 2-3 hrs and incubated for 24 hrs.

For a 6 well plate/well
Transfer plasmid: 12µg
pMD.2: 4.2µg
p8.91: 9µg
PEI: 10ug

3.11.2 Virus collection and titration

Fresh media was added 24 hrs after transfection for virus collection and virus was collected after 24 and 48hrs.

The collected virus was aliquoted and stored at -80ºC for further use. The viral particles produced were titrated on the 293T cells before using for the experiments. 293T cells were seeded at 50,000 cells/ well in a 24-well plate and 24 hrs later the viral supernatant was added. Aliquots of viral supernatant were thawed at 37ºC and diluted in growth medium at a ratio of 1:10, 1:100, and 1:1000 before adding to the cells. The diluted viral particles were added to the 293T cells and 48 hrs later, the percentage of reporter gene, GFP was analysed using flow cytometry. The virus titer was determined as follows:

$$= \frac{\text{50,000 (No. of cells seeded) x percentage of GFP positive cells x 1000}}{\text{Volume of virus added}}$$

This will provide the transforming unit (TU) per ml.

3.11.3 Target cell transduction

The titrated virus particles were used for transduction. Adherent cells or suspension cells were seeded at a constant density and viral supernatant was thawed and added to the cells with an MOI of 5-10 in the presence of polybrene (4ug/ml for adherent cells and 8ug/ml for suspension cells) for 24 hrs. The media with virus supernatant was removed and fresh media was added to the cells. The transduction efficiency was analyzed after 48-72 hrs through flow cytometry by determining the percentage of GFP positive cells.

3.11.4 Transduction validation

The transduced cells were validated for the expression of target gene by transcript analysis through real-time PCR or immunocytochemical staining for the target gene.

3.12 RHOA modification and activity assay

3.12.1 RHO GTPase modification

Rho GTPase activity was modified in the cells through the expression of dominant negative or constitutively active RHOA lentiviral vectors(Jaganathan et al., 2013). The constitutively active RHOA which carries V14 mutation (RHOAV14) and dominant negative RHOA which consists of N19 mutation (RHOAN19) were utilized for the study. The mutation at V14 maintains the RHOA GTPase in the GTP bound state and the dominant negative mutation at N19 maintains RHOA in the GDP bound state.

The lentiviral plasmids were packaged with the second generation packaging plasmids (p8.91, pMD.2) in 293FT cells and the target cells were transduced as described earlier. RHOA activity was determined by RHOA GLISA assay (Cytoskeleton Inc.)

3.12.2 RHOA activity analysis

RHOV14, RHOAN19 and control vector (SIEW) transduced cells were expanded. The cells were washed with ice-cold PBS and lysed with the lysis buffer (RHOA GLISA kit, Cytoskelton Inc) containing protease inhibitors. The protein concentration of lysed cells was determined using Bradford assay. Equal amount of protein was taken for each sample in duplicates and RHOA activity was determined using RHOA GLISA kit according to the manufacturer's instructions. The amount of active RHOA was determined by comparing with the standard curve.

3.13 Inhibitor treatment and analysis

3.13.1 Imatinib myselate (IM) treatment

To induce apoptosis in primary CML cells or CML cell line K562 cells, the cells were treated with 10µM of IM (Sigma) for 48 hrs in normal growth media. The cell density at the time induction was maintained at $2x10^5$ cells/ml. In case of chemoresistant K562 derived during the course of study, IM was added to the cells every 72 hrs at a concentration of 10µM.

3.13.2 Pathway inhibitor treatment

Small molecule inhibitors for specific signaling pathways and actin cytoskeleton inhibitor were used to treat the cells to study the role of specific signaling pathways in leukemic cells. The concentration and treatment time varied as per the experimental set up and is mentioned at appropriate places. The following inhibitors were used in the study.

Inhibitors used for the study:

Actin cytoskeleton inhibitor: CytochalasinD (Sigma)(Sonowal et al., 2013)

BMP-Smad signaling inhibitor: LDN193189 (Sigma) (Raymond et al., 2014)

ERK 1/2 MAPK inhibitor: U0126 (Sigma) (Chu et al., 2004)

CXCR4 inhibitor: AMD3100 (Sigma) (Weisberg et al., 2012)

NFkB inhibitor: Bay 11-7082 (Sigma) (Morotti et al., 2006)

P38 MAPK inhibitor: SB203580 (Sigma) (Mayer et al., 2001)

ROCK inhibitor:Y27632 (Sigma) (Jaganathan et al., 2007)

STAT3 inhibitor:5,15 DPP (Sigma) (Sen et al., 2012)

3.13.3 IL-6 receptor(IL-6R)monoclonal antibody treatment

To understand IL-6 signaling in cross-talk between the stromal cells and leukemic cells, the IL-6Rwas blocked using monoclonal antibody against membrane bound and soluble IL-6R (Tocilizumab, Roche). The antibody was used at the concentration of 10-50µg/ml for 6-24 hrs.

3.13.4 Analysis of intracellular concentration of IM

Equal number of cells was cultured in the presence of IM for 3hrs. Cells were harvested, washed with PBS and lysed in the presence of protease inhibitors. 100ul of cell lysate was transferred to a black walled, glass bottom 96 well plate. The absorbance of IM was measured at 258 nm according to the earlier published method (Bourgne et al., 2012)using Tecan multi-plate reader.

3.14 Cytokine quantification

CM from adherent or suspension cells was collected by addition of serum free media for 24 hrs. ELISA was performed according to manufacturer's instructions (Human IL6

ELISA kit, Novex) to detect secreted IL6 levels. The IL6 levels in the samples were quantified by comparing with the standard.

3.15 Mitochondrial ROS and actin staining

3.15.1 Mitochondrial superoxide analysis

The superoxide molecules level produced in the cells by mitochondria was determined using MitoSOX Red mitochondrial superoxide indicator (Molecular Probes). Briefly, the stroma-leukemic co-culture cells were incubated with 1ml of 5µM Mitosox reagent in a 12 well plate. The cells were incubated in the cell culture incubator at 37ºC for 10 mins. The mitosox reagent was removed by centrifugation at room temperature, suspension leukemic cells were collected and cell layer was washed with PBS kept at 37ºC. The adherent leukemic cells were quickly trypsinized with 0.05% trypsin at 37ºC for 30 seconds. The trypsin was washed by centrifugation at room temperature and the cells were resuspensed in warm buffer. The mitosox fluorescence level in the cells was analysed by flow cytometry and compared with the unstained cells as control.

3.15.2 Actin staining

The F-actin levels in the cells were determined by staining the cells with fluorescent conjugated Phalloidin. Phalloidin specifically binds to F-actin and the actin levels in different cells types were quantified using flow cytometry. The cells to be stained were washed with PBS and fixed with 4% paraformaldehyde for 10 mins at room temperature. The fixative was removed and the cells were permeabilised with 0.1% Triton-X 100 in PBS for 15 mins at room temperature. The Triton-X 100 solution was removed and Phalloidin-Atto 488 (Sigma) at a dilution of 1:5000 was added to the cells in PBS+2% FBS and incubated overnight at 4ºC. The cells were washed and resuspended in PBS+2% FBS and analysed by flow cytometry.

3.16 Data analysis

The results are expressed as Mean$\pm$SE. Statistical analysis was performed using SPSS software and P values <0.05 were considered as statistically significant.

The flow cytomtery data was analysed using Flow Jo software (FlowJo). The real-time PCR data was analysed using $2^{\Delta\Delta Ct}$ method.

4.0 RESULTS

4.1 Stromal microenvironment in chronic myeloid leukemia

To study the role of microenvironment in CML progression, mesenchymal stromal cells (MSC) were isolated from the bone marrow (BM) and characterized. The CML derived mesenchymal stromal cells (CML-MSC) were spindle shaped, similar to MSC derived from the healthy individuals. CML-MSC could be cultured up to 8 passages, however, in many cases the cells lost their proliferation capacity at 4-5th passage after which the cells acquired a flat morphology with limited proliferation capacity.

4.1.1 CML derived MSC possess reduced osteogenic differentiation

To understand the differentiation capacity of the CML-MSC, the cells were differentiated into adipocytes or osteocytes by addition of specific induction factors. The cells readily differentiated into adipocytes and osteocytes (Figure 4.1A), however, their differentiation capacity was limited. Although, no significant difference in the adipogenic differentiation potential was identified, there was a significant reduction in the percentage of cells differentiated into osteocytes compared to control stromal cells (Figure 4.1B).

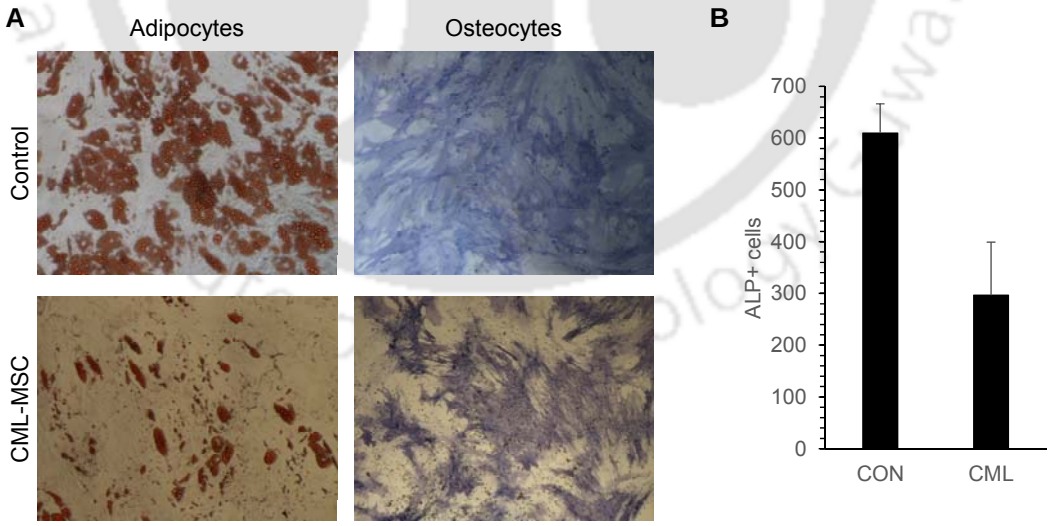

***Figure 4.1: Differentiation of MSC**. (A) MSC derived from the control and CML patient BM were differentiated into adipocytes and osteocytes. MSC were seeded at a density of 20,000 cells/cm^2 for adipogenic and 5000cells/cm^2 for osteogenic differentiation in tissue culture plates. Adipo- or osteo-differentiation specific induction factors were added to the cells and the cells were allowed to differentiate for 21 days. Adipogenic differentiation was determined by Oil Red O staining (red color) and Osteogenic*

differentiation by staining for alkaline phosphatase activity (blue color). Representative microscopic images are shown. Values are mean±SE, n=3-4 samples. (B) The percentage positive cells in both adipogenic and osteogenic differentiation were counted microscopically. The CML-MSC cells showed reduced differentiation into osteogenic lineage as determined by alkaline phosphatase (ALP) staining.

Next, the cell surface marker expression in CML-MSC was analysed. The cells expressed CD13, CD44, CD49E, CD73, CD90, CD95, CD105 and CD120A but were negative for CD34 and CD49D. The cell surface marker expression profile was similar to that observed in control MSC (Figure 4.1.2).

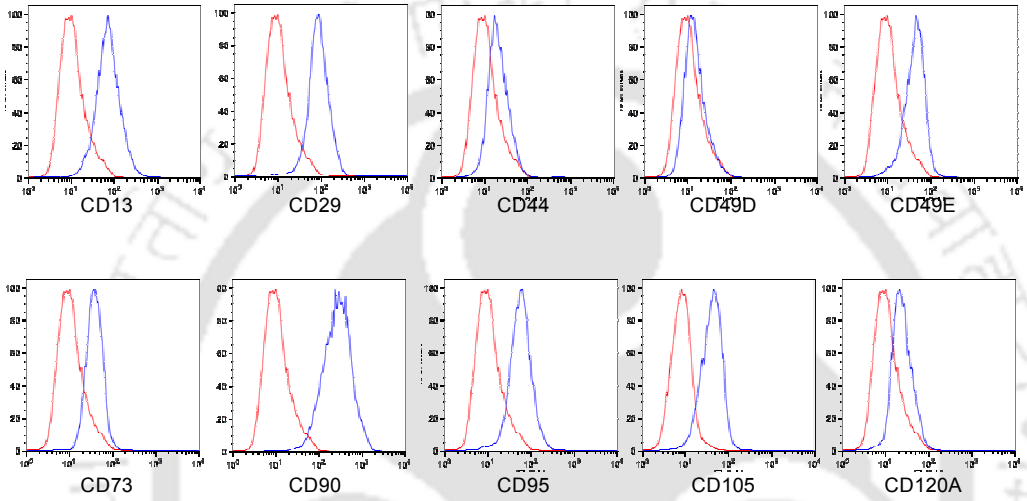

***Figure 4.2: Phenotyping of MSC**. The cells surface antigen expression of CML BM derived mesenchymal stem cells were determined by flow cytometry. The MSC were stained with fluorescently conjugated antibodies against cell surface antigens and they were positive for CD13, CD29, CD44, CD49E, CD73, CD90, CD95, CD105, and CD120A and were negative for CD34 and CD49D. Representative flow cytometric histograms are shown, red color was the isotype control and the blue color was the stained sample.*

4.1.2 CML-MSC show high IL6 expression

Studies have shown that tumor associated stromal cells secrete higher levels of pro-survival cytokines such as IL-6 and IL-8 (Schmidt et al., 2011). In this context, the CML-MSC were analysed to identify the IL-6 expression levels. *IL-6* mRNA levels were detected by real-time PCR and significantly high *IL-6* mRNA levels were seen in CML as well as AML derived MSC (Figure 4.3A). Since MSC differentiate into osteoblasts and adipoblasts in the BM to support the hematopoietic cells, the expression levels of *IL-6* during adipogenic and osteogenic differentiation were analyzed. The expression of *IL-6* was upregulated during osteogenic differentiation whereas it was significantly downregulated during adipogenic differentiation (Figure 4.3B) suggesting a role of osteoblasts in promoting cell proliferation through secreted factors.

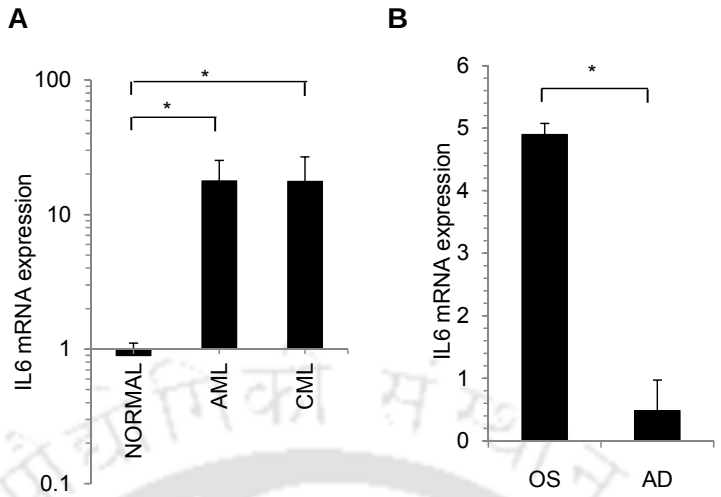

Figure 4.3: IL-6 mRNA expression. *(A) The transcript levels of interleukin 6 (IL-6) in BM MSC derived from control, AML or CML patients were determined by real-time PCR. There was a significant upregulation of IL-6 mRNA levels in AML and CML derived MSC compared to the control MSC. (B) During osteogenic differentiation, IL-6 mRNA levels increased further whereas no change in IL-6 levels was observed during adipogenic differentiation. Values are Mean±SE, n=4-12 samples; *p<0.05*

Next, MSC were differentiated into osteoblasts to identify any possible correlation between osteogenic differentiation potential of MSC and their *IL-6* expression levels. Although the *IL-6* mRNA levels were higher in cells differentiated into osteoblasts, there was no correlation between their *IL-6* expression levels in MSC with their osteogenic differentiation potential (Figure 4.4).

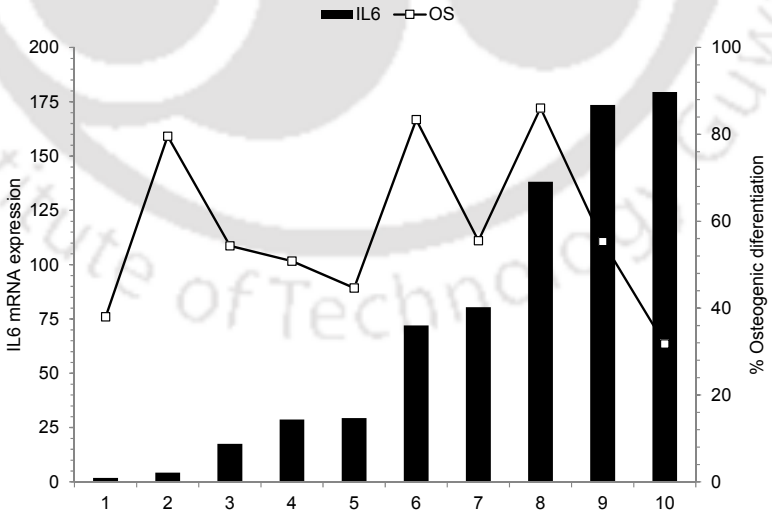

Figure 4.4: Correlation between IL-6 mRNA levels in MSC and osteogenic differentiation potential. *The IL-6 mRNA levels in BM derived MSC were analyzed by real-time PCR. The osteogenic differentiation potential of the cells was determined by differentiating the cells using osteo specific induction factors for 21 days. Differentiation into osteocytes was determined by staining the differentiated cells for alkaline phosphatase activity and the differentiated cells were counted microscopically and the percentage*

differentiation for each sample was determined. The osteogenic differentiation potential of MSC did not correlate with their IL-6 mRNA expression levels. X-axis represents individual samples, primary Y-axis on the left represents IL-6 mRNA level which is represented by the bars and secondary Y-axis on the right shows the osteogenic differentiation percentage represented by the grey line.

Studies have shown that the secretion of cytokines such as IL-6, PIGF was regulated through NFκB pathway (Schmidt et al., 2011). In this context, the expression level of IκB was analyzed and since NFκB pathway can be activated by TNF-α, the expression level of TNF-α was also determined. There was a positive correlation of IL-6 levels with TNF-α and IκB expression levels, as well as positive correlation was identified between IκB and TNF-α expression levels (Figure 4.5).

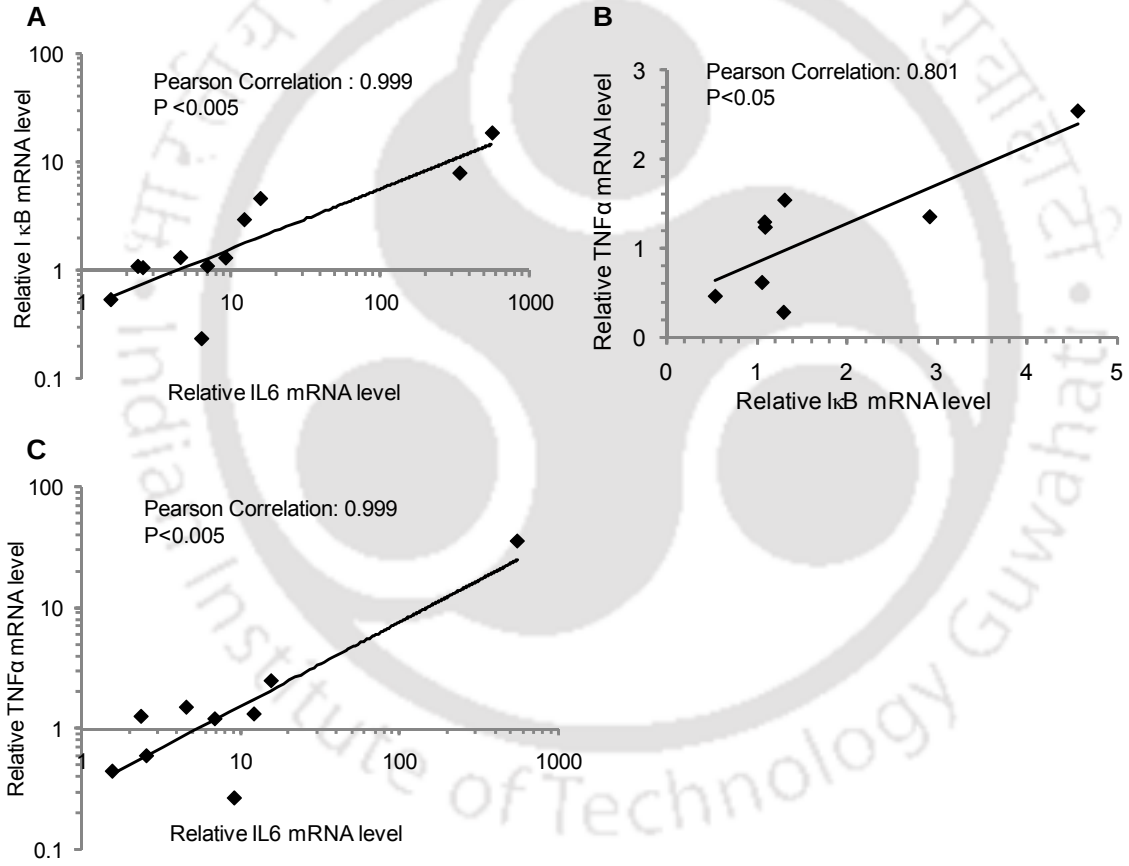

Figure 4.5: Expression levels of IL-6, IκB and TNF-α*. The expression levels of IL-6, IκB and TNF-α in MSC were determined by real-time PCR. The correlation between the expression levels of IL-6, IκB and TNF-α was determined by Pearson co-efficient analysis and a significant positive correlation was seen between IL-6 and , IκB; IL-6 and TNF-α; and IκB and TNF-α expression by MSC. Each dot represents an individual sample.*

To determine whether the CML cells were responsible for the identified changes in the CML-MSC, control MSC were co-cultured with K562 CML cells or treated with conditioned media from K562 CML cells. The co-cultured or conditioned media (CM) treated MSC were subjected to osteogenic differentiation, phenotype and gene expression analysis.

4.1.3 CML cells induce downregulation of cell surface receptors and differentiation genes in MSC

Treatment of MSC with K562 derived CM resulted in the significant downregulation of cell surface markers CD73 and CD90 but CD13 and CD105 expression levels were unaffected (Figure 4.6).

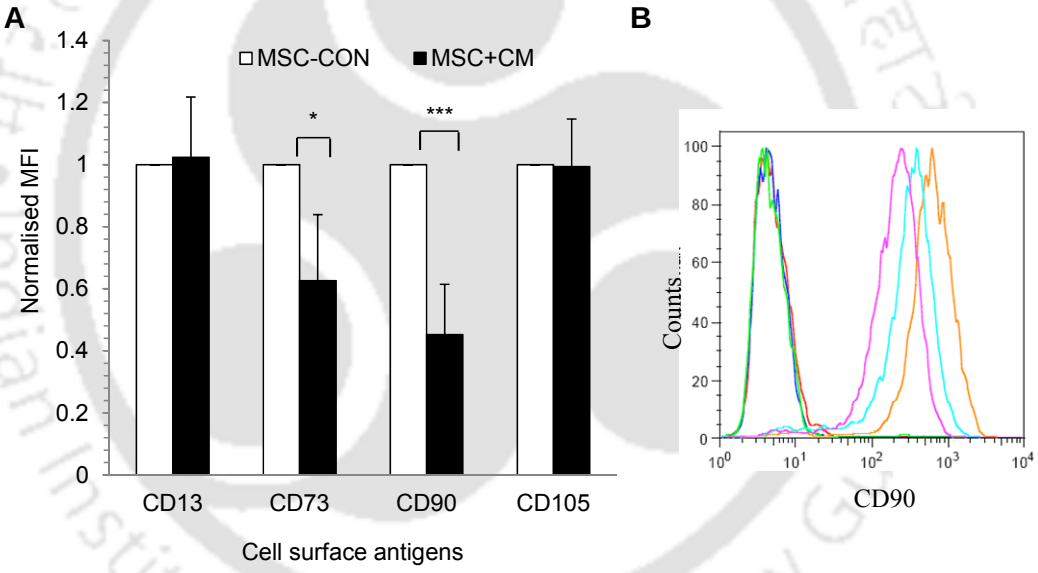

Figure 4.6: Effect of CML paracrine factors on MSC cell surface marker expression. *Conditioned media (CM) from K562 CML cells were added to MSC and cultured for 7 days and the changes in cell surface expression of CD13, CD73, CD90 and CD105 were analyzed by flow cytometry. The expression levels were analyzed by comparing the mean fluorescent intensity (MFI) of isotype control with the sample and values were normalized to the expression levels in control MSC. (A) A significant downregulation of cell surface expression of CD73, CD90 was observed in MSC cultured with K562 cells derived CM (MSC+CM) cells whereas no changes were observed in the expression of CD13 and CD105 compared to the control (MSC-CON). Values are mean±SE; * $p<0.05$, *** $p<0.0005$ (B). Representative flow cytometric histogram of CD90 expression in MSC compared to the control cells. Isotype control (blue, red, green line), control MSC (orange line), CM treated MSC (light blue and pink lines).*

However, when MSC were cultured in direct contact with K562 in a co-culture system, there was a significant downregulation of CD13 and CD90 but not CD73 surface expression (Figure 4.7). When the expression of death receptors that are involved in apoptosis were analyzed, Fas receptor (FasR, CD95) cell surface expression was significantly downregulated in co-cultured MSC (MSC-CC) and but no change in TNFA receptor I, CD120A was observed. Co-culture with K562 cells did not alter the expression levels of integrins CD29, CD49D, CD49E as well as CD105 in MSC.

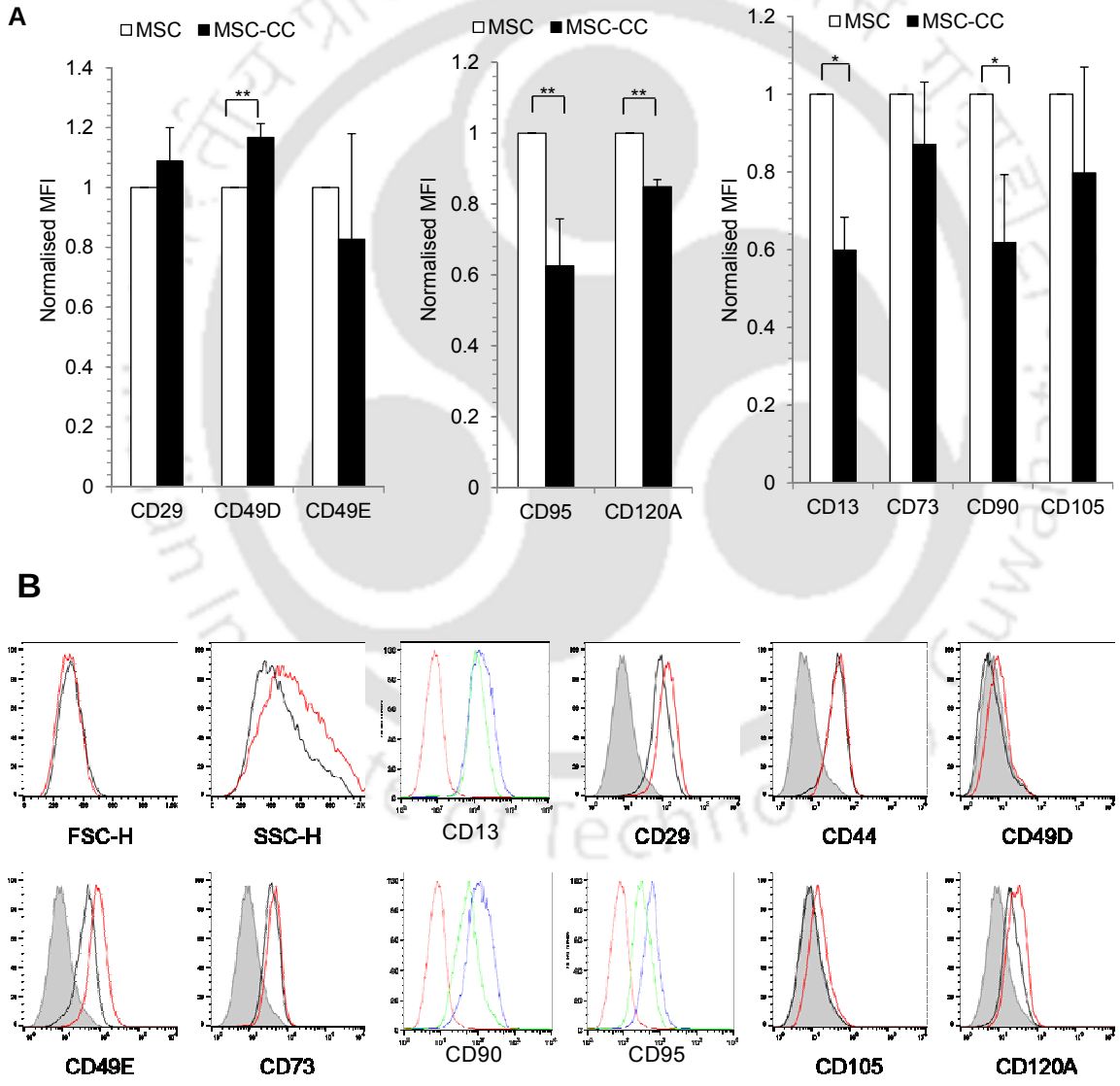

Figure 4.7: Effect of CML co-culture with MSC on MSC cell surface protein expression. *K562 CML cells were co-cultured with MSC (MSC-CC) for 7 days and the changes in cell surface expressions of antigens CD13, CD29, CD49D, CD49E, CD73, CD90, CD95, CD105 and CD120A were analyzed by flow*

cytometry. The expression levels of cell surface antigens were analyzed by comparing the mean fluorescent intensity (MFI) of stained samples with the isotype control and values were normalized to the expression levels in control MSC (MSC). (A) A significant decrease in cell surface expression of CD13, CD90 and CD95 were observed in MSC co-cultured with K562 CML cells (MSC-CC) compared to control MSC (MSC). No change in expression was observed for CD29, CD49D, CD49E, CD73, CD105 and CD120A between the control MSC and MSC-CC. (B). Representative flow cytometric histogram plots of MSC cultured alone or in co-culture conditions with K562 CML cells. For CD13, CD90 and CD95, the red histogram was the isotype control; blue line was stained control MSC and green line was the stained MSC-CC. Other markers, grey filled histogram is the isotype control, black line represents MSC control and red line represents MSC-CC.

Gene expression analysis by real-time PCR showed that there was a downregulation of CD90 gene expression at transcript level when MSC were co-cultured with K562 cells, confirming the reduction in CD90 protein levels analyzed through flow cytometry (Figure 4.8B). Co-cultured MSC also showed significantly lower levels of adipogenic and osteogenic differentiation specific genes ADIPOQ and OSTEOPONTIN respectively (Figure 4.8A).

Nevertheless, transcript levels of secreted factors TNF-α were upregulated in MSC co-cultured with K562 (Figure 4.8B). In addition, the ROS scavenging genes MNSOD and CAT were also significantly upregulated in co-cultured MSC indicating several gene expression changes induced in MSC by CML through direct cell contact or through their secreted factors (Figure 4.8C).

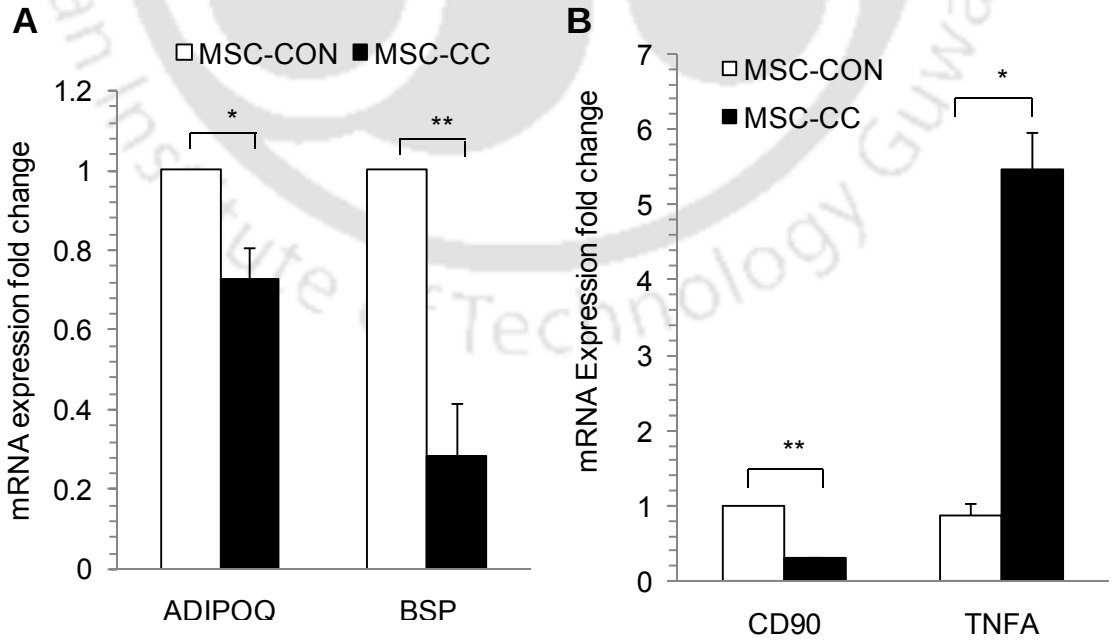

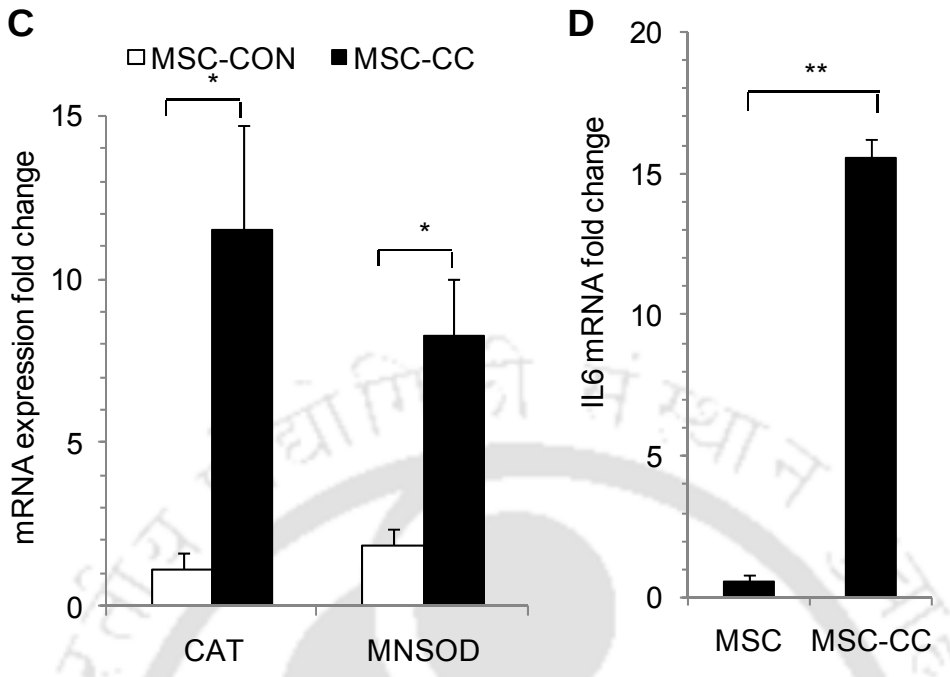

Figure 4.8: Effect of CML cells on MSC gene expression. *K562 CML cells were co-cultured with the MSC (MSC-CC) for 72hrs and the changes in gene expression was analyzed by real-time PCR. The mRNA expression in each sample was normalized to GAPDH expression levels and fold change in expression of each gene in co-cultured MSC (MSC-CC) was compared with the control MSC (MSC-CON). (A) A significant downregulation in the adipogenic lineage gene ADIPOQ and osteogenic lineage specific gene BSP were seen in MSC-CC. (B) Significant downregulation of CD90 transcript levels were seen in MSC-CC whereas a significant upregulation in TNFa mRNA levels was seen in MSC-CC compared with MSC-CON. (C) A significant increase in the mRNA levels of ROS scavenging enzymes CAT and MnSOD were observed in MSC-CC compared to control MSC-CON. (D) A significantly high IL-6 expression levels were seen in MSC-CC compared to MSC-CON. Values are mean±SE, n=3-5; *p<0.05, **p<0.005.*

4.1.4 CML cells induce higher IL-6 secretion in MSC through NFκB phosphorylation

To further understand the role of IL-6 in interaction between the stromal cells and CML cells, the IL-6 secreted levels were quantified in MSC co-cultured with K562 cells. There was a significant upregulation of *IL-6* transcript levels when MSC were cultured in contact with K562 cells (Figure 4.8D). To understand the pathway through which interaction of K562 cells might have increased the IL-6 expression levels in MSC, the co-cultured MSC were analyzed for phosphorylated NFκB levels. There was a significant increase in phosphorylated NFκB levels in MSC when co-cultured in contact with K562 cells for 48 hrs (Figure 4.9).

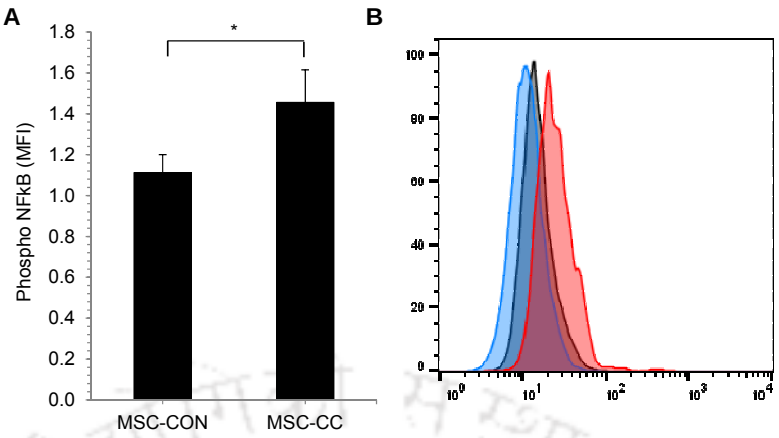

Figure 4.9: NFκB phosphorylation in co-cultured MSC*. MSC were co-cultured with K562 for 48 hrs and harvested after the removal of K562 cells. The phosphorylated levels of NFκB were determined by phospho flow cytometry analysis. (A) A significant increase in the phosphorylated NFκB levels was identified in MSC co-cultured with K562 CML cells (MSC-CC) compared to the control cells (MSC_CON). Y-axis represents the NFκB MFI levels normalized to isotype controls. Values are mean±SE, n=3; * p<0.05(B) A representative flow cytometric histogram showing the increased phospho NFκB in MSC-CC (red line) compared to MSC-CON (dark blue line). Isotype control is (light blue line).*

To study further, the co-cultured MSC were treated with NFκB inhibitor (BAY 11-7082) (10μM) and IL-6 secreted levels were determined. As seen with the transcript levels, there was a significant upregulation of IL-6 secreted levels in MSC co-cultured with K562 cells (Figure 4.10A). However, when co-cultured MSC were treated with BAY 11-7082, there was a significant decrease in the IL-6 secreted levels suggesting the involvement of NFκB pathway in rise in IL-6 secreted levels (Figure 4.10A). In the above experiment, where IL-6 secreted levels were tested, K562 cells were removed from the co-culture, MSC layer was washed with PBS and the conditioned media was collected. This was done to ensure that only the MSC secreted IL-6 levels were determined and not the IL-6 secreted by K562 cells.

Further, when MSC were treated with TNF-α, it increased IL-6 secretion significantly and TNF-α induced increase in IL-6 secretion was downregulated by treatment with BAY 11-7082 (Figure 4.10B). IL-6 secretion was reduced in control MSC as well after treatment with BAY 11-7082. Thus our results strongly indicate NFκB pathway to be the main mediator for increased IL-6 secretion during interaction of MSC with K562 CML cells.

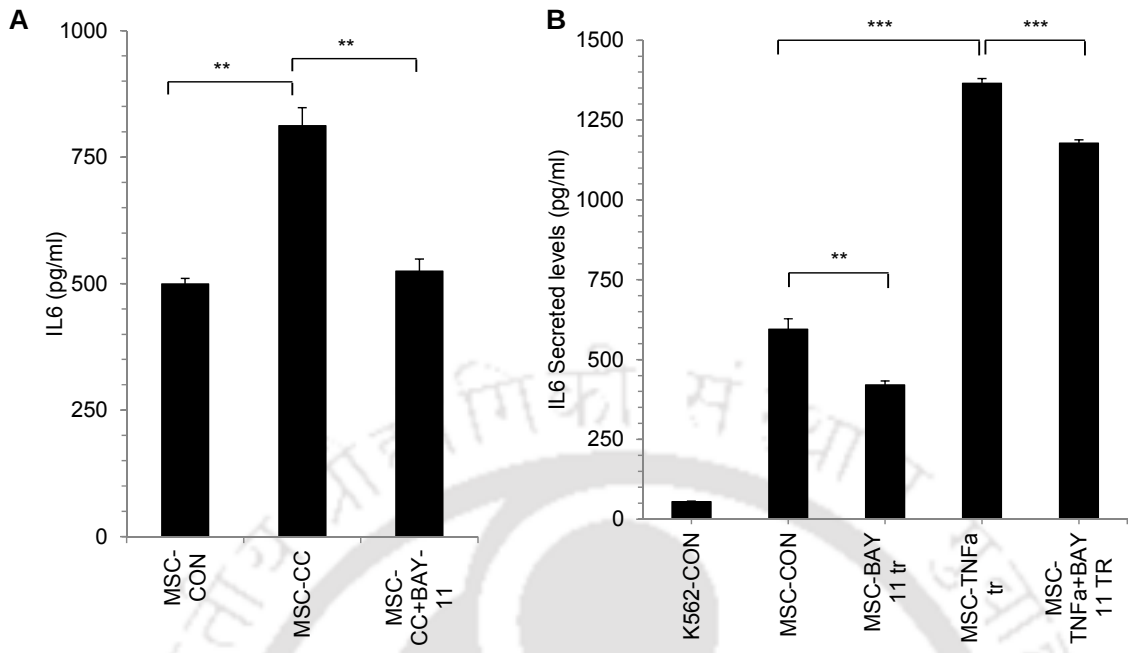

Figure 4.10: IL-6 secretion levels during MSC-CML cells co-culture. *(A) MSC were cultured alone (MSC-CON) or in co-culture with K562 CML cells (MSC-CC) for 48hrs with. The CML cells were discarded and conditioned media was collected from MSC after the addition of serum free media. IL-6 secreted levels in the conditioned media were determined by ELISA. A significant upregulation of IL-6 levels were seen in MSC-CC, which was downregulated on addition of NFκB inhibitor (MSC-CC+BAY-11). (B). IL-6 secreted levels were inhibited in control MSC (MSC-CON) after addition of BAY 11. IL-6 levels further increased when TNF-α was added to MSC (MSC-TNFα tr) before collection of conditioned media and were again inhibited by addition of NFκB inhibitor (MSC-TNFα tr+BAY-11 tr). Values are mean±SE, n=5; ** p<0.005, *** p<0.0005.*

Thus, CML cells modified the BM stromal cells by changing their cell surface protein expression, gene expression and IL6 secretion.

4.2 Stroma derived paracrine factors in CML chemoresistance

4.2.1 MSC derived conditioned media inhibits Imatinib induced apoptosis in CML cells

In this section, the role of stroma in regulating the behavior and function of K562 CML cells was studied. In the section 4.1, several experimental results showed that leukemic K562 cells interact with the MSC to modify their gene expression and function. Similarly, the bone marrow stromal cells also interact with the leukemia cells through their secreted factor and through direct cell-contact to regulate the leukemic cells. In addition to supporting the leukemic cells in proliferation, the stromal cells also chemoprotect the leukemic cells during therapy. This section therefore deals with the role of stroma secreted factors in chemoprotection of CML cells.

Imatinib mesylate (IM) is used as a first line of treatment for CML which arises due to *BCR-ABL* translocation. K562 CML cells harbor *BCR-ABL* translocation and are used as a model system to study CML. Firstly, K562 cells were treated with different concentrations of IM to identify the optimal concentration that can be used for chemo-protection and chemo-resistance studies. Concentrations varying from 1μM to 100μM of IM were added to K562 cells and MTT assay was performed after 48 hours of addition of IM. Concentration of 1, 5 or 10μm had similar growth inhibiting effect (Supplementary Figure 7.3) and 10μM of IM was considered to induce cell death in K562 for further experiments.

On treatment of K562 cells with IM, there was a significant increase in apoptosis and up to 40% apoptotic cells were detected by Annexin-V/PI staining. However when K562 were co-cultured with MSC, there was a significant decrease in IM induced cell death in K562 cells which suggests that MSC through secreted factors or cell-cell interaction offer chemoprotection to K562 cells in the presence of IM (Figure 4.11).

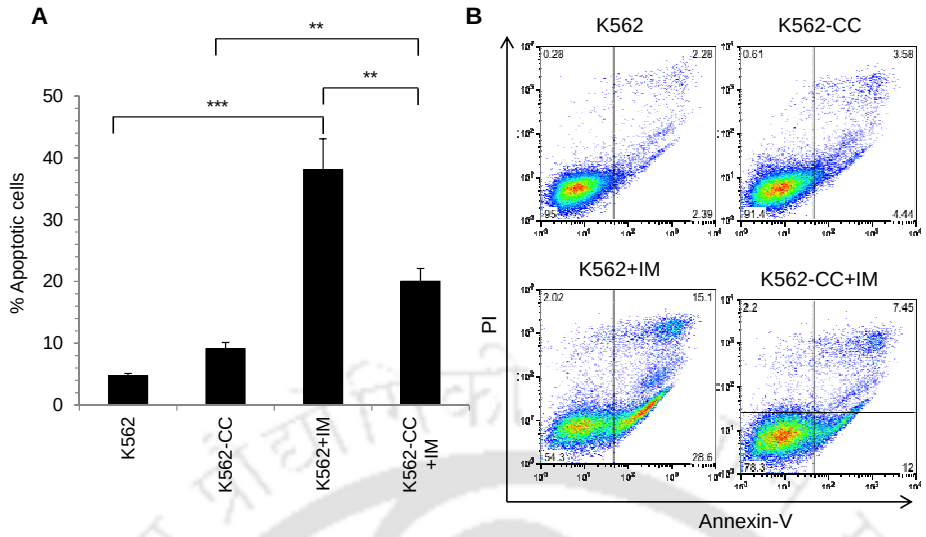

Figure 4.11: Apoptosis in K562 cells during MSC co-culture. *K562 cells were cultured alone (K562) or in co-culture with bone marrow derived MSC (K562-CC) for 48 hours. The cells were treated with IM (10μM) for 48 hours and apoptosis was determined by Annexin-V/PI staining using flow cytometry. (A) Apoptosis in K562 cells treated with IM was determined by calculating the percentage of all Annexin-V positive cells. A significant increase in apoptotic cells were observed when IM was added to control cells (K562+IM) which decreased significantly when K562 cells were co-cultured with MSC (K562-CC+IM). Values are mean±SE, n=3 independent experiments; ** p<0.005, *** p<0.0005. (B) Representative flow cytometric plots showing the Annexin-V/PI staining in K562 cells under different conditions.*

To study whether the secreted factors from MSC were sufficient to chemoprotect K562 cells from IM induced cell death, K562 cells were treated with IM in the presence and absence of conditioned media from MSC (CM). There was a 50% reduction in apoptosis in K562 cells treated with IM in the presence of MSC derived CM (Figure 4.12).

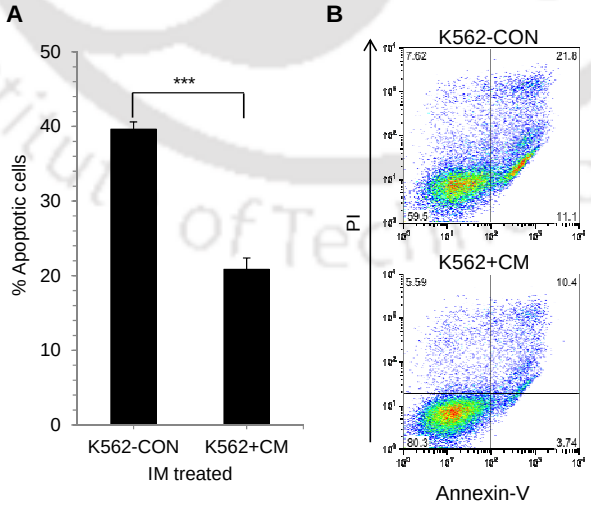

Figure 4.12. Effect of MSC paracrine factors on K562 apoptosis. *K562 cells were cultured in the presence of conditioned media containing paracrine factors derived from MSC. The cells were treated with IM and cell death was analyzed flow cytometrically through An-V/PI staining. (A) A significant reduction*

*in apoptosis of K562 as observed when the cells were treated with IM in the presence of MSC derived conditioned media (K562+CM) compared to control cells (K562-CON). Values are mean±SE, n=3 independent experiments; *** p<0.0005.(B) Representative flow cytometric plots of An-V/PI staining of K562 cells treated with IM in the presence or absence of MSC derived CM.*

4.2.2 MSC derived CM induces STAT3 phosphorylation in CML cells

To understand the signaling pathways that might be activated by MSC derived secreted factors (CM) in K562 cells, phosphorylated levels of ERK1/2 MAPK and STAT3 were analyzed in K562 cells treated with MSC derived CM for 24 hrs and compared them with the control K562 cells. There was no difference in the phospho ERK levels in K562 cells treated with MSC derived factors compared to the control cells (Figure 4.13A, C) but there was a significant increase in phospho STAT3 levels after MSC derived CM treatment (Figure 4.13B).

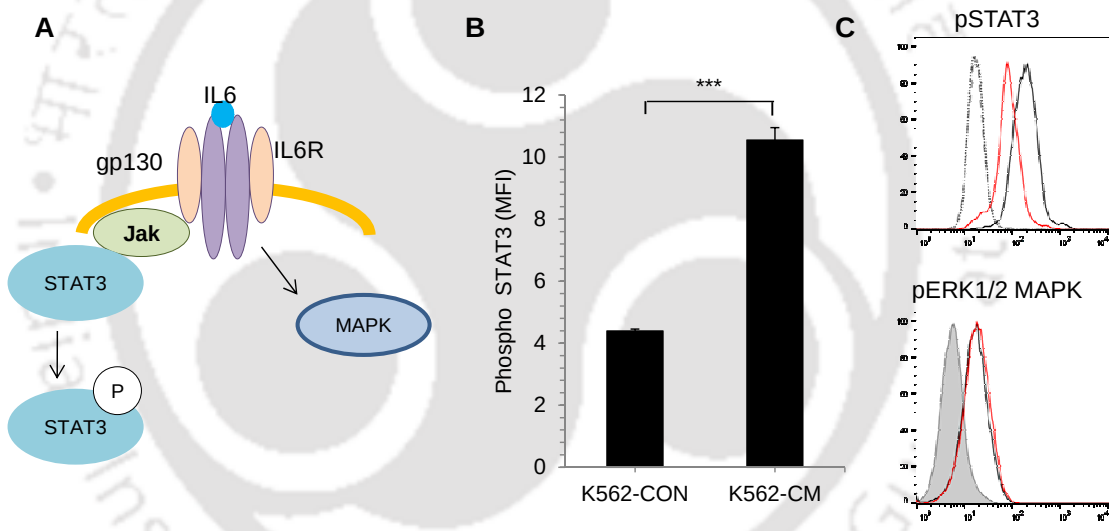

Figure 4.13: Phospho levels of ERK1/2 and STAT3 in K562 cells after MSC derived CM treatment *(A) Figure representing the pathways activated by IL-6 binding to its receptor IL6-R on the cell surface. Figure adapted from (Tawara et al., 2011). (B). When conditioned media (CM) from MSC were added to K562 cells, a significant increase in the phosphorylated levels of STAT3 was seen in CM treated K562 (K562-CM) as measured by intracellular staining analysed through flow cytometer. (C). Representative flow cytometric histograms showing the staining for phospho STAT3 or phospho ERK1/2 MAPK in control (red line) as well as CM treated K562 cells (black line). The isotype control is represented as grey filled histogram. Values are mean±SE, n=3 independent experiments. *** p<0.0005.*

Consequently, ERK inhibition by treating K562 CML cells with U0126 (10µM) did not increase IM induced cell death in cells cultured with MSC derived CM although there was a increase in apoptosis in K562 treated with U0126 in the absence of CM (Figure

4.14). Similarly inhibition of NFκB with BAY 11-7082 (10μM) in MSC derived CM treated K562 cells did not augment the IM induced apoptosis (Figure 4.14).

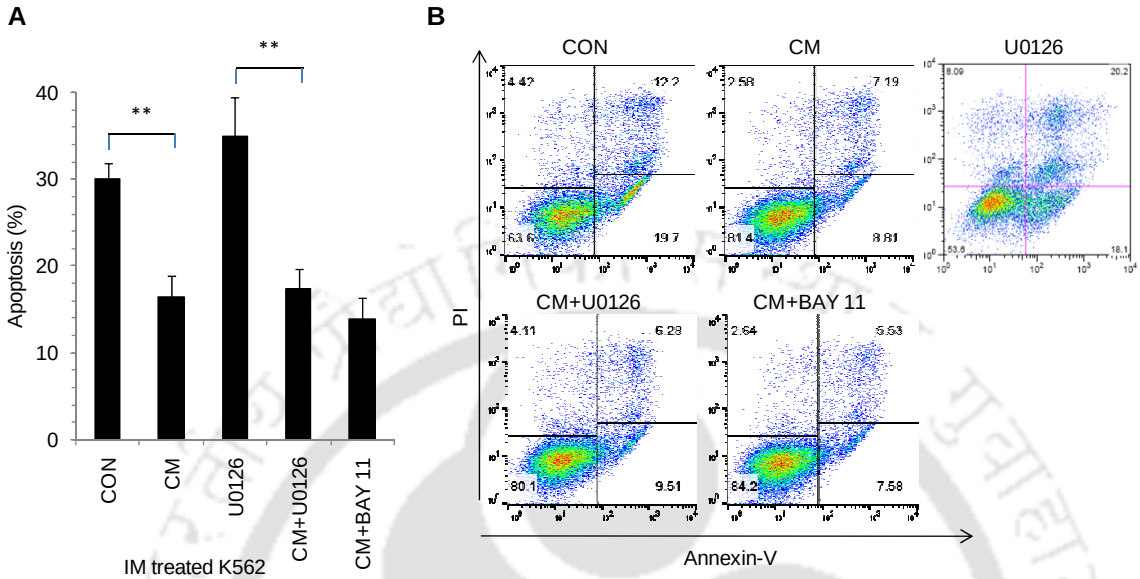

Figure 4.14: Effect of ERK and BMP inhibition on MSC derived CM treated K562 *(A) K562 were treated with IM in the presence of ERK inhibitor (U0126) (10μM) and NFκB inhibitor (BAY 11) (10μM) for 48 hours and apoptosis was analysed by An-V/PI staining. No change in apoptosis percentage was observed in IM treated K562 when co-treated with ERK or NFκB inhibitor upon addition of MSC derived CM. (B) Representative flow cytometric plots showing An-V/PI staining of K562 treated with IM in the presence of ERK or NFκB inhibitor. CON-Control; CM-Conditioned media from MSC; U0126-ERK inhibitor (10μM); BAY 11- NFκB inhibitor BAY 11-7082 (10μM). Values are mean±SE, n=3 independent experiments. ** p<0.005.*

Our earlier results showed that the amount of IL-6 secretion by MSC during co-culture with K562 cells increased significantly compared to the control MSC. To test whether the presence of IL-6 in the MSC derived CM was responsible for chemoprotection of K562 from IM induced cell death, K562 cells were treated with monoclonal antibody against IL-6 receptor (IL-6R) tocilizumab, in the presence or absence of IM. As seen earlier, the conditioned media from MSC chemoprotected K562 from IM induced cell death, however, blocking both secreted and membrane bound IL-6R did not change the IM induced apoptosis percentage (Figure 4.15). This suggests that chemoprotection of K562 cells by MSC secreted factors might be IL-6 pathway independent or might be dependent on multiple cytokines and growth factors in a compensatory mechanism.

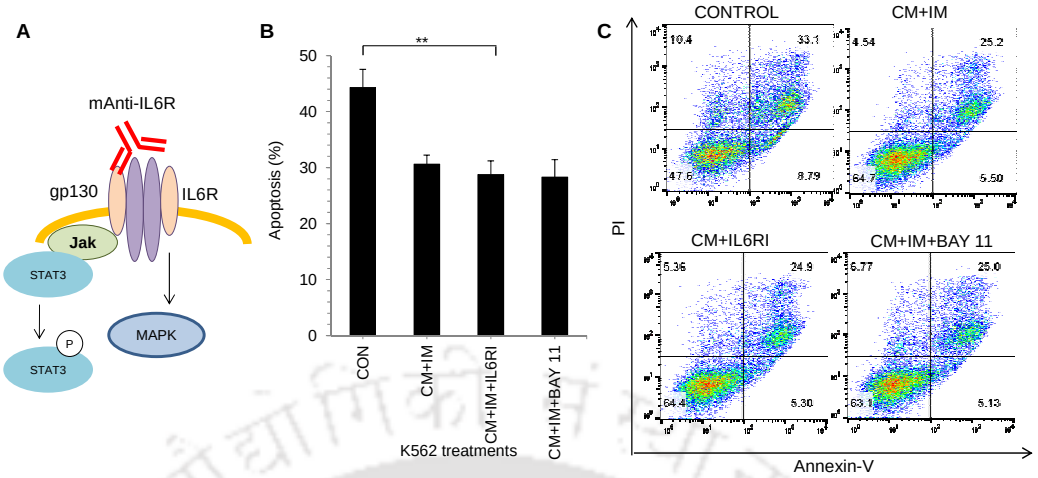

Figure 4.15: Effect of blocking of IL-6R in K562 cells.*(A) K562 cells were treated with monoclonal antibody against IL-6 receptor (IL-6RI) to block the IL-6R induced signaling. (B) IM induced apoptosis in K562 cells treated with IL-6RI (50µg/ml) in the presence of MSC derived CM was determined by An-V/PI staining. IL-6R inhibition or NFκB inhibition (BAY 11) did not change the apoptosis percentage of K562 cells. Values are mean±SE, n=4-5; ** p<0.005. (C) Representative flow cytometric dot plots of K562 stained for An-V/PI treated with IL-6RI or BAY 11and IM in the presence of MSC-CM.*

To confirm further, MSC were treated with TNF-α to increase the IL-6 secreted levels and the resulting CM was added to K562 cells and treated with IM. This increased IL-6 levels did not alter the IM induced cell death percentage (Figure 4.16) further confirming IL-6 independent pathway in chemoprotection of K562.

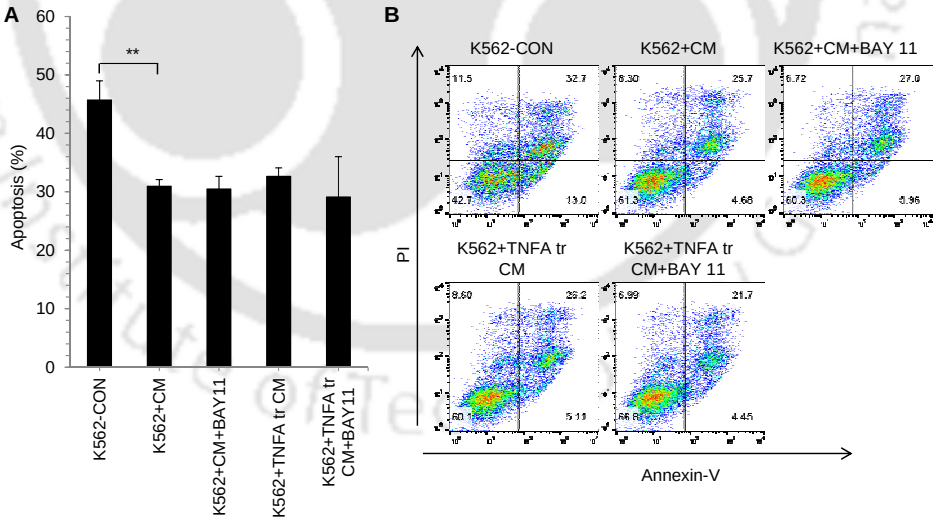

Figure 4.16: Chemoprotection in K562 by MSC derived CM is IL-6 independent*. K562 cells were treated with IM in the presence of MSC derived CM (K562+CM). CM was collected with or without addition of TNF-α. K562 cells were further treated with NFkB inhibitor (BAY 11) in the presence or absence of TNFα treated CM. (A) Apoptosis in K562 cells treated with IM alone (K562-CON) or IM in the presence of MSC derived CM (K562+CM); or CM with NFkB inhibitor (K562+CM+BAY 11); TNFα treated CM (K562+TNFAtr CM); TNFα treated CM with NFkB inhibitor (K562+TNFAtr CM+BAY 11) by An-V/PI staining. TNF-α treatment and NFkB inhibitor treatment did not affect the apoptosis percentage of IM treated K562. (B) Representative flow cytometric plots showing An-V/PI staining of the experimental conditions.*

4.2.3 STAT3 inhibition did not diminish the chemoprotective effect of MSC derived CM on CML cells

Since there was a significant increase in phosphoSTAT3 levels in K562 cells treated with MSC derived CM compared to the control cells, K562 cells were treated with STAT3 inhibitor 5, 15 DPP (10µM). DPP treatment did not affect IM induced apoptosis in the presence or absence of MSC derived CM (Figure 4.17 A). As seen earlier, ERK inhibition with U0126 significantly increased apoptosis percentage in IM treated control K562 but not in CM treated K562 (Figure 4.17 A).

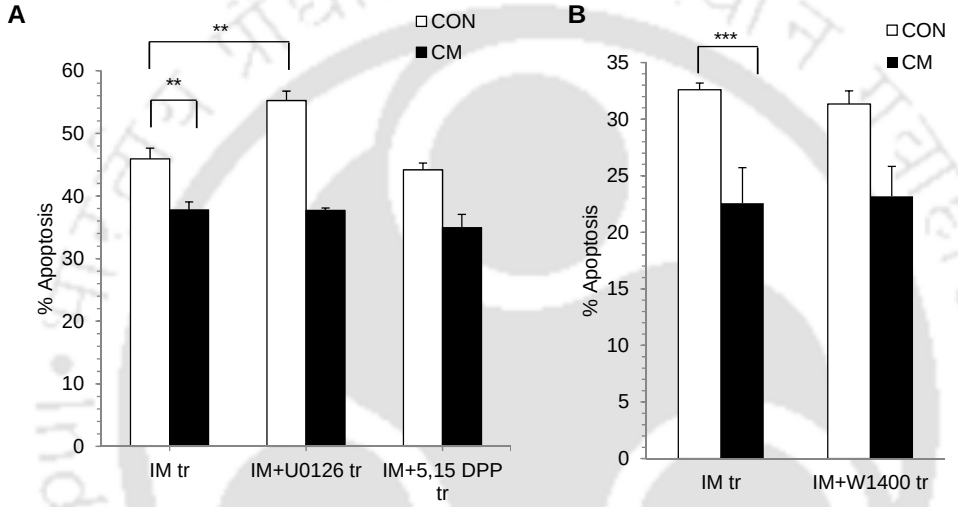

Figure 4.17: Effect of ERK, STAT3 and iNOS inhibition in CM treated K562 cells. *K562 cells were cultured alone (CON) or in the presence of MSC derived conditioned media (CM). (A) ERK inhibitor (U0126) and STAT3 inhibitor (5, 15 DPP) were added to K562 control cells or CM treated cells in the presence of IM and apoptosis percentage was analyzed by Annexin-V/PI staining. (B) Apoptosis was analyzed in CON or CM treated K562 cells treated with IM in the absence or presence of iNOS inhibitor (W1400). Values are mean±SE, n=3 independent experiments; ** p<0.005, *** p<0.0005.*

Some reports also suggest that IL-6 can act acts through iNOS pathway apart from IL-6R pathway (Saini et al., 2014). Since IL-6 receptor blocking with monoclonal antibodies did not affect the apoptosis percentage of IM treated K562 in the presence of MSC derived CM, iNOS inhibitor W1400 (50µM) was added to the cells in the presence of IM. Both in the presence and absence of stroma derived CM, iNOS inhibition did not have any additive effect on apoptosis in IM treated K562 cells (Figure 4.17 B).

Thus, we conclude that CM derived from MSC chemoprotect K562 cells from IM induced apoptosis and which could not be abrogated by inhibition of IL-6R, ERK, STAT3 or iNOS.

4.3 Effect of cell-cell interaction on CML chemoprotection

When K562 CML cells were co-cultured with MSC, the K562 cells were present in suspension (SUS-K562) as well as adherent to the stromal layer (AD-K562). These stroma adherent cells could be removed by a quick trypsinization (30 seconds) and could be separated from the stromal layer and studied.

Earlier studies reported by others and our study showed, that the cell death induced by IM treatment reduced significantly when K562 cells were co-cultured with MSC. The conditioned media from stromal cells was alone sufficient to offer chemoprotection to K562 cells in the presence of IM. However, cell-cell interaction plays a major role in cell signaling and cellular response to therapy induced stress. Therefore in this section; the role of cell-cell interaction between stromal cells and K562 CML cells in chemoprotection against IM treatment was studied in detail.

4.3.1 Cell-cell interaction with stromal cells for chemoprotection of K562 cells during IM treatment

To understand stroma mediated chemoresistance, first, K562 cells were co-cultured with MSC layer and treated with optimal concentration of IM (10µM) as determined earlier to induce apoptosis. After treatment for 48hours with IM, the adherent and suspension fractions of K562 in the co-culture system were separated and percentage of live cells was analyzed through Annexin-V/PI staining. A significantly high percentage of live cells were seen in stroma adherent fraction (AD-K562) compared to suspension fraction (SUS-K562) of co-cultured K562 cells during IM treatment (Figure 4.18).

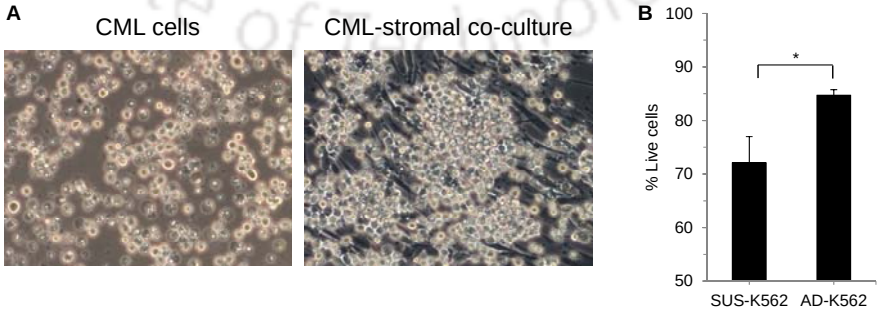

Figure 4.18: Co-culture of K562 cells with MSC. *Representative microscopic images of K562 CML cells cultured in suspension (left) or in co-culture with stromal cells (right) in presence of IM. (B) K562 cells co-cultured with MSC were treated with IM and the cells were separated into adherent (AD-K562) and*

*suspension (SUS-K562) fractions. The percentage of live cells was analyzed by Annexin-V/ PI staining through flow cytometry. A significantly high percentage of live cells were seen in AD-K562 compared to the SUS-K562 cells. Values are mean±SE, n=3; * p<0.05.*

Moreover, the apoptosis percentage during IM treatment in SUS-K562 cells was similar to K562 cultured alone without MSC layer whereas it was significantly lower in AD-K562 cells (Figure 4.19). This suggests that cell-cell interaction protects K562 cells from chemo-drug induced cell death.

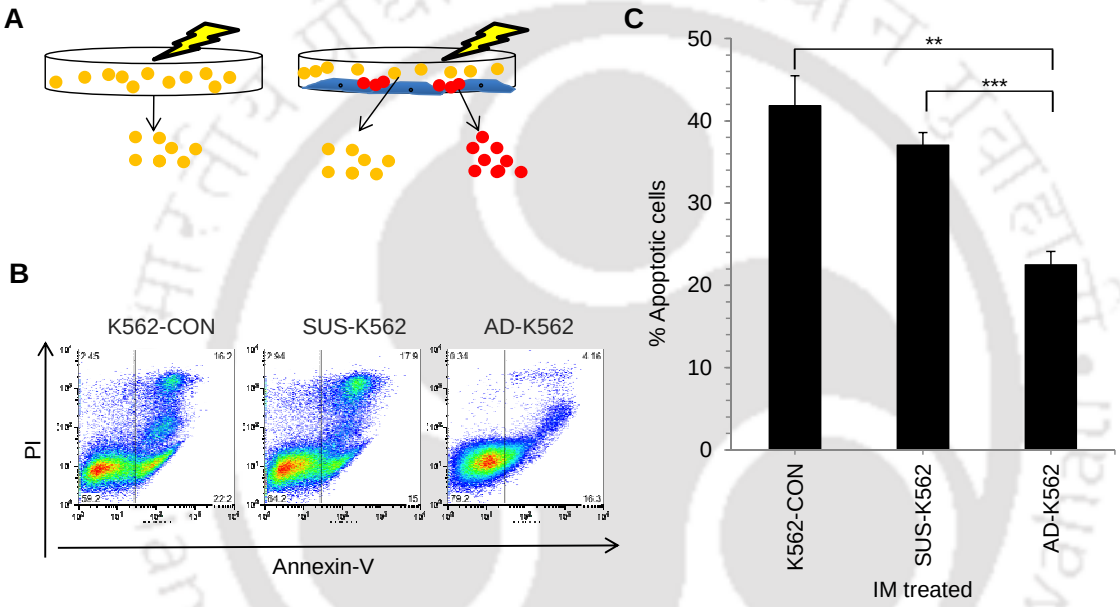

Figure4.19: Cell-cell interaction reduced IM induced apoptosis in K562 cells.*K562 cells were co-cultured with stromal cells and treated with IM for 48 hours. The stroma adherent (AD-K562) and suspension fractions (SUS-K562) were separated and apoptosis was determined by Annexin-V/PI staining and compared with IM treated K562 cells grown without stromal layer (K562-CON). A significant reduction in the apoptosis percentage of IM treated AD-K562 was observed but the apoptosis in SUS-K562 was similar to that seen in K562-CON cells. (A) Pictorial representation of experimental set-up to analyze apoptosis in adherent and suspension cells. (B) Representative flow cytometric plots showing Annexin-V/PI staining in different cell fractions. (C) Graph representing the apoptosis percentage (An-V+PI- and An-V+PI+) of cell fractions after IM treatment. Values are mean+SD, n=5-6; ** p<0.005, *** p<0.0005.*

To find out whether apoptotic pathway was activated in the IM treated AD-K562 and K562-CON cells, active-caspase 3 (active Cas-3) levels in the different cell fractions were detected. There was a significantly high percentage of active Cas-3 positive cells in IM treated K562-CON cells but it was significantly less in AD-K562 cell fraction (Figure 4.20) confirming the above data that cell-cell interaction indeed protects K562 cells from IM induced cell death.

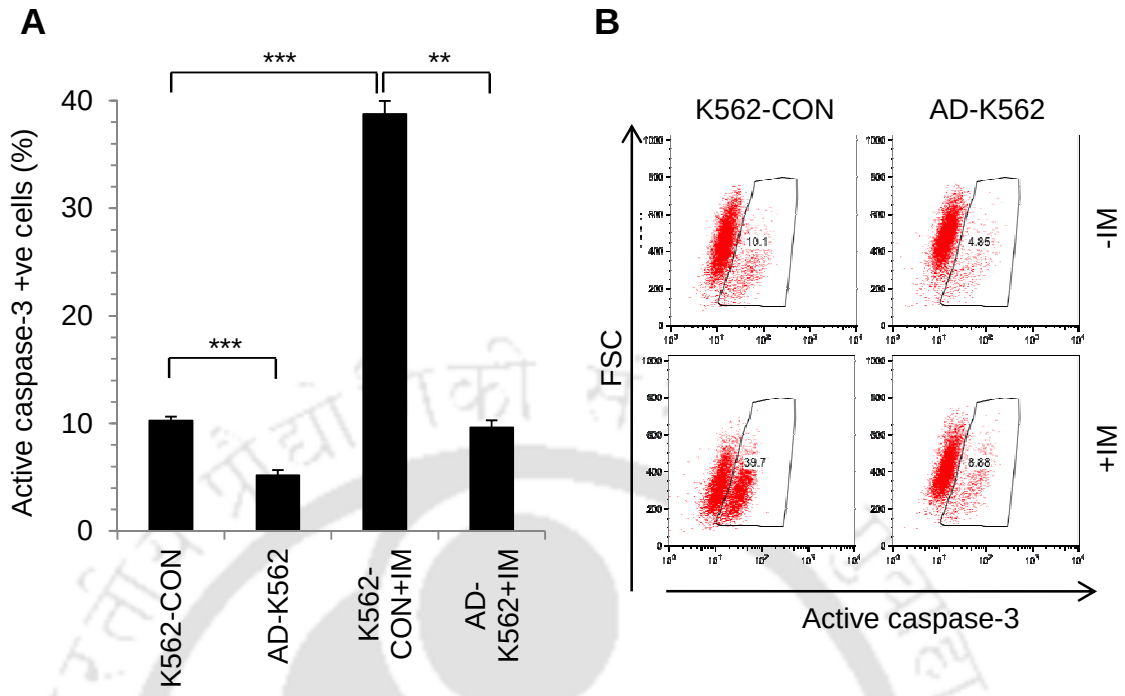

Figure 4.20: Active caspase-3 staining in K562 cells.*K562 cells were grown in co-culture with the stromal cells for 48hrs and stroma adherent (AD-K562) and control (K562-CON) cells were treated without or with IM for 48 hours. The AD-K56) and K562-CON cells were harvested and stained with fluorescently conjugated anti-active caspase-3 antibody. The cells were analyzed by flow cytometry and the percentage positive cells were calculated by gating against isotype stained control cells. (A) A significantly high percentage of active caspase-3 positive cells were seen in IM treated control cells (K562-CON+IM) compared to IM treatedAD-K562 cells (AD-K562+IM). Values are mean±SD, n=3 independent experiments. (B) Representative flow cytometric dot plot showing cells gated for active caspase-3 positive cells; ** p<0.005, *** p<0.0005.*

During co-culture, as discussed before, K562 cells were present as both stroma adherent and non-adherent suspension cells. Hence, it might be possible in co-culture system that IM availability to the adherent K562 might be less due to the interference of suspension cells, because of which reduced cell death was observed in stroma adherent K562 cells. To test this, initially, K562 cells were co-cultured with MSC layer to establish adherent and suspension fraction for 48hrs. After this, the suspension fraction was transferred to a new MSC layer and the adherent fraction was left undisturbed. IM was added to K562 cells present only as adherent cells or as suspension cells (Figure 4.21 A). Analysis of cell death percentage showed that apoptosis in AD-K562 cells was significantly less compared to SUS-K562 cells (Figure 4.21 B, C) confirming the above data that cell-cell interaction of K562 cells with stromal layer protects K562 cells from IM induced cell death irrespective of the drug availability.

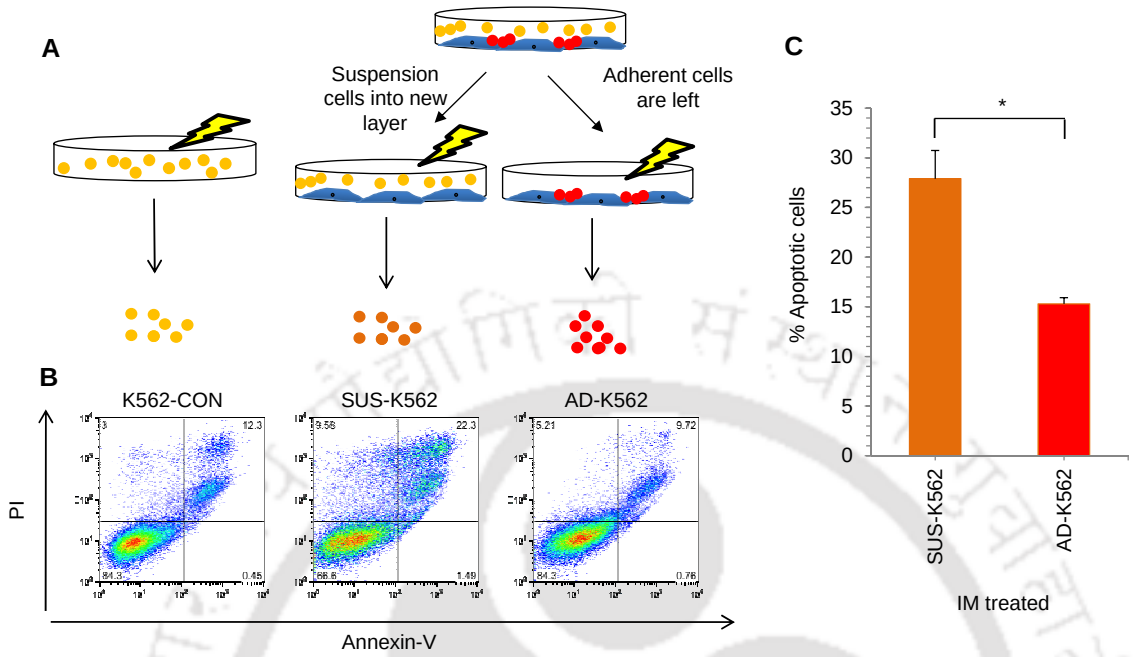

Figure 4.21: Adherent K562 cells were chemoprotected. *(A) Pictorial representation of experimental set-up. K562 cells were cultured in suspension or in co-culture with stromal cells. Only the suspension cells were transferred to a new stromal layer and adherent cells were retained on the same stromal layer. The control and both co-cultured cell fractions were treated with IM for 48 hours and apoptosis was determined by An-V/PI staining. (B) Representative flow cytometric plots showing An-V/PI staining. (C) A significant reduction in the apoptosis of stroma adherent K562 cells (AD-K562) was observed compared to the suspension fraction (SUS-K562). Values are mean±SE, n=3 independent experiments; * p<0.05.*

4.3.2 Disruption of cell-cell interaction diminishes chemoprotection

Since the K562 cells adherent to the stromal cells had significantly less apoptosis when treated with IM, it might be possible that the adherent cells have acquired chemo-resistance or the chemoresistant cell population in fact adhered to the stromal cells. To test this, K562 cells were co-cultured with MSC to establish the adherent and suspension cell fractions. After 48hrs, the SUS-K562 fraction was discarded from the co-culture and AD-K562cells was treated with IM for 48 hours. After IM treatment, the stroma adherent K562 cells were either transferred to a fresh layer of MSC or converted into a suspension culture without MSC. Both the plates containing were treated with IM again for 48hrs and the percentage of live cells was analyzed through flow cytometry (Figure 4.22 A). A significantly high percentage of live cells were found in adherent fraction which continued as stroma adherent throughout the experiment (AD-AD with MSC), whereas

no difference in cell viability was seen between the stroma adherent fractions which were transferred to new stromal layer but later continued as suspension cells (AD-SUS with MSC) or adherent cells which were transferred to stroma free suspension culture (AD-SUS without MSC) and treated with IM (Figure 4.22 B, C).

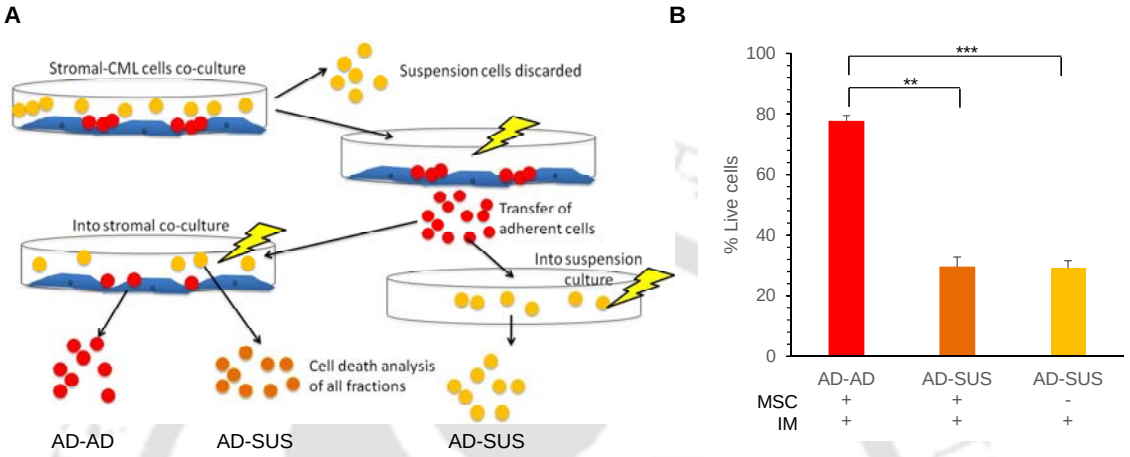

Figure 4.22: Stromal cells mediate chemoprotection. *(A) Pictorial representative of experimental stet-up to determine chemoprotection. K562 cells were co-cultured with stromal cells and the suspension fraction was discarded. The adherent fraction was transferred to a new stromal layer or a suspension culture without the stromal layer.K562 cells in both the conditions were treated with IM. Again, the adherent and suspension fraction were separated and percentage of live cells was analyzed. (B) Percentage of live cells after IM treatment in K562 cells that were maintained as adherent fraction during the course of the experiment (AD-AD) was significantly higher compared to the adherent cells that were made suspension after first IM treatment. The percentage of live cells was similar between adherent cells made into suspension in stromal free culture (AD-SUS; with MSC) compared to adherent cells that later continued as suspension cells in co-culture system (AD-SUS; without MSC). Values are mean±SE, n=4 independent experiments; ** p<0.005, *** p<0.0005.*

The importance of cell-cell interaction in chemoprotection during IM treatment was also tested in primary samples. Primary CML cells obtained from patients in the chronic stage were cultured in the presence or absence of MSC. MSC adherent CML cells (CML-CC) or control CML cells were treated with IM and cell death percentage was analyzed. As seen with K562 cells, there was a significant decrease in cell death in CML cells that were adherent to the stromal layer (Figure 4.23) confirming again that cell-cell interaction with stroma was an important factor for the CML cells to escape targeted cell killing by IM treatment.

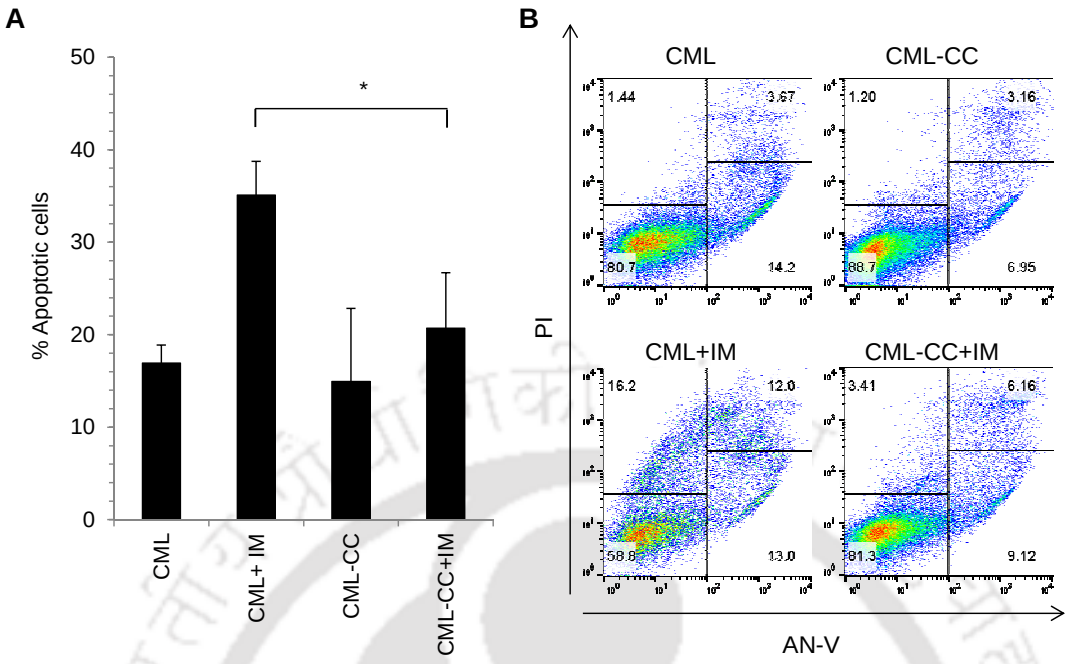

Figure 4.23: IM induced apoptosis in stroma adherent and suspension CML primary cells. *Human primary CML cells were co-cultured with CML BM derived MS, treated with IM for 48 hours and the percentage of apoptotic cells was calculated by An-V/PI staining through flow cytometry. (A) Graph showing the percentage of apoptotic cells in CML cells cultured alone (CML) or in stroma adherent CML cells (CML-CC) with (+IM) and without IM treatment. There was a significantly higher percentage of live cells in IM treated stromal adherent primary CML cells (CML-CC+IM) compared to the control cells (CML+IM). Values are mean±SE, n=3 independent experiments; * p<0.05. (B) Representative flow cytometric plots of An-V/PI staining of IM treated/untreated primary CML cells.*

4.3.3 Stroma adherent CML cells exhibit stem cell-like phenotype

To understand the nature of the stroma adherent CML cells, primary samples from CML patients were co-cultured with MSC which was also isolated from CML BM. The CML cells were allowed to interact and establish adherent and suspension fraction with the MSC layer for 3 days. The stroma adherent (AD-CML) and suspension (SUS-CML) cells from the co-culture were separated and analyzed for the expression of stem/progenitor cell markers CD34 and N-Cad. The AD-CML cells had significantly higher percentage of CD34 positive cells (Figure 4.24A) as well as N-Cad positive cells (Figure 4.24B) compared to the SUS-CML cells suggesting a stem/progenitor-cell like phenotype of the adherent cells.

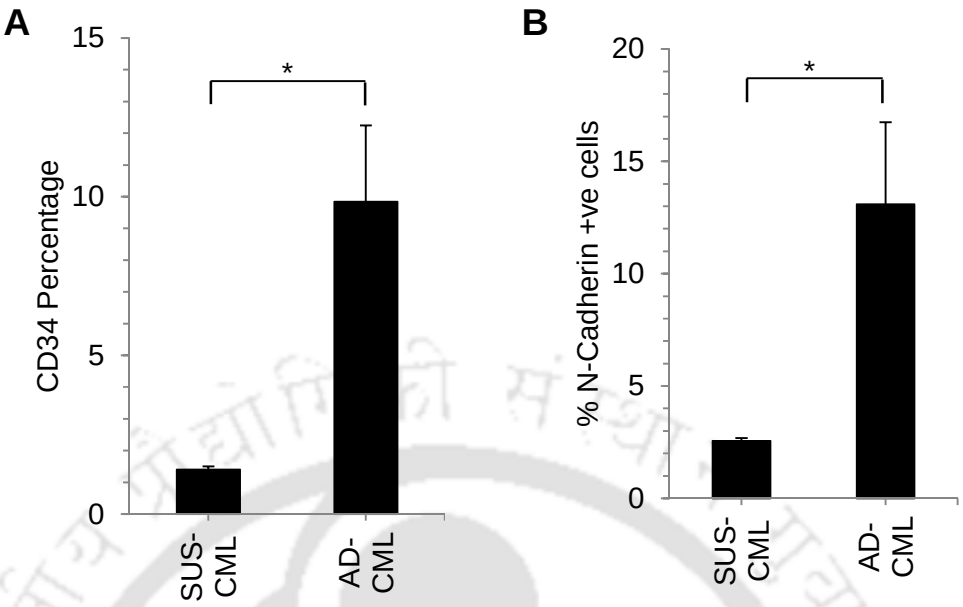

Figure 4.24: Analysis of CD34 and N-Cad positive cells in stroma adherent versus suspension fraction in primary CML samples. *Primary CML cells were co-cultured with CML BM derived stromal cells for 3 days. The CML cells were separated into adherent and suspension fractions and stained with CD34, CD45 and N-Cad fluorescent antibodies. (A) A significantly higher percentage of $CD45^+CD34^+$ cells were seen in the adherent fraction (AD-CML) compared to the suspension fraction (SUS-CML) of primary CML cells in stromal co-culture. (B) A significantly higher percentage of $CD45^+N\text{-}Cadherin^+$ cells were found in AD-CML compared to SUS-CML cells. Values are Mean+SD, n=3 independent experiments; * $p<0.05$.*

4.3.4 Stroma adherent K562 cells exhibit quiescence and reduced ROS production

To further investigate the adherent cells, the cell cycle profile of the stroma adherent CML cells was determined by Ki67 staining. There was a significantly higher percentage of Ki67 negative cells which represents the cells at G0 stage of cell cycle in the stromal adherent K562 cells (Figure 4.25A). The cell cycle status of adherent cells was further confirmed by transducing the K562 cells with cell cycle tracking plasmid Cycle Trak. Most adherent cells were GFP-low and RFP-negative(Figure 4.25B, C),which represents the cells in G0 phase of the cell cycle which is between the M and GI stages, confirming the Ki67 staining results.

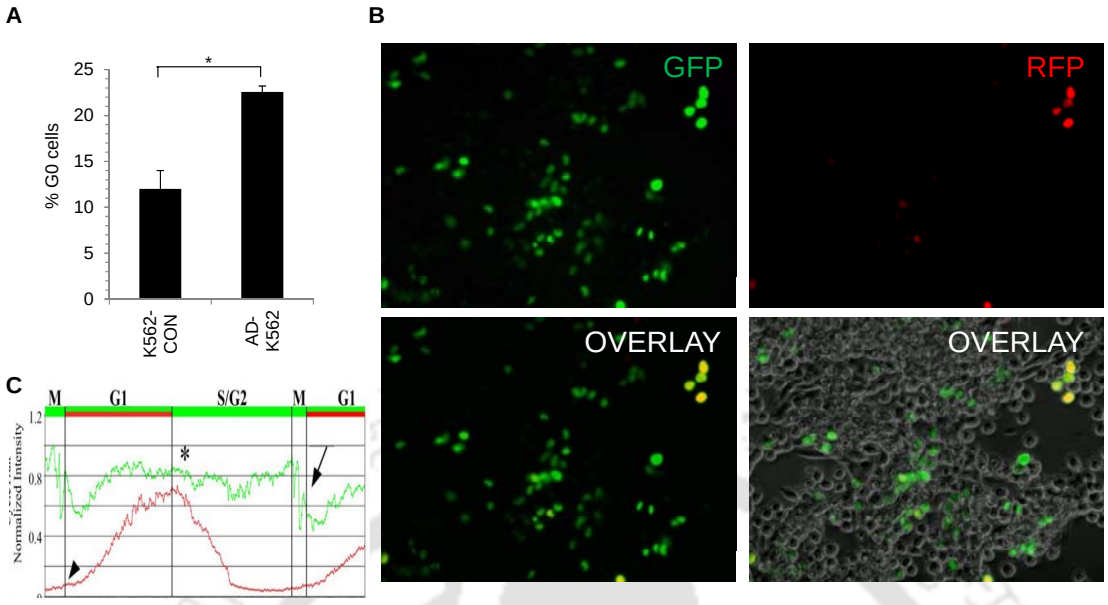

Figure4.25: Cell cycle status of stroma adherent K562 cells. *(A) Graph representing the percentage of G0 cells in K562-CON and AD-K562 cells during stromal co-culture. G0 cell cycle stage was determined by staining with fluorescent conjugated anti-Ki67 antibody and PI and cells at G0 stage were negative for Ki67. (B) K562 cells were lentivirally transduced with cell cycle reporter Cycle Trak and co-cultured with MSC for 3 days. The suspension cells were removed and the adherent cells were imaged for the presence of GFP and RFP using inverted fluorescent microscope (Axio Observer Z1). Representative fluorescent microscopic images of stroma adherent K562 cells expressing GFP or RFP according to their cell cycle stage. The lower panel shows the overlay of GFP and RFP (left), overlay image of K562 cells with stromal layer (right). (C) Representation of GFP/RFP expression during different stages of cell cycle using Cycle Trak plasmid. The green line represents the GFP expression and red line represents the RFP expression.*

The stroma adherent K562 cells were further studied for their metabolic activity by measuring the amount of mitochondrial ROS produced during interaction with stromal cells using mitosox superoxide indicator dye. The adherent cells (AD-K562) were found to have significantly less mitochondrial superoxide levels compared to the suspension K562 (SUS-K562) cells in the stromal co-culture system (Figure 4.26).

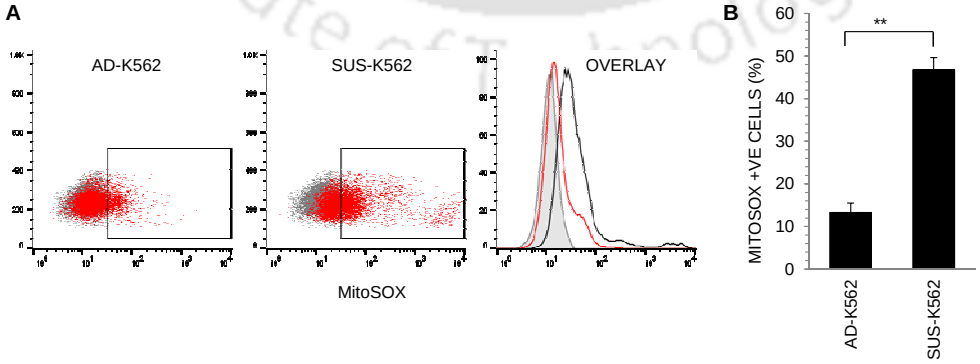

Figure4.26: Mitochondrial ROS production in stroma adherent and suspension fractions of K562. *K562 cells were grown in co-culture with stromal cells for 48 days. Mitosox ROS indicator reagent was added to*

*the cells for 30 minutes and the cells were harvested separately as suspension and adherent fractions. The presence of Mitosox fluorescence and the percentage positive cells were analyzed by flow cytometry. (A) Flow cytometry dot plot showing the mitosox fluorescence in the X-axis and normalized cell count in the Y-axis. Histogram graph shows the overlay of mitosox fluorescence in adherent cells (red line), suspension cells (black line). The grey histogram is the unstained control. (B) Graph representing the percentage of mitosox positive cells in stroma adherent (AD-K562) cells compared to the suspension (SUS-K562) fractions. Values are mean+SD, n=3; ** p<0.005.*

4.3.5 Stroma adherent K562 cells have altered gene expression

Next, the phenotype changes that K562 cells underwent during interaction with the stromal cells were determined. Firstly, the cell surface antigen expression profile of K562 CML cells was studied by flow cytometry. K562 cells were positive for CD29, CD44, CD49E, CD81, CD120A and negative for CD49A, CD49B, CD49C, CD49D, CD49F, CD61, CD73, CD95, CD104, CD140A, CD200 and CD253(Figure 4.27).

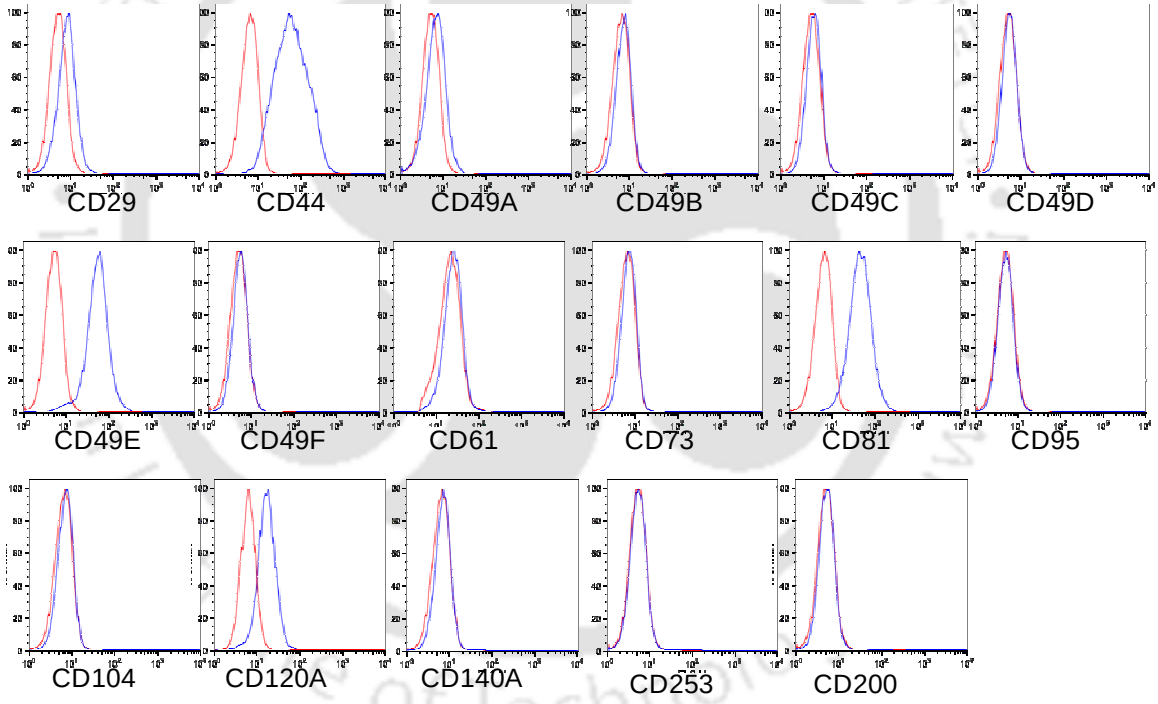

Figure4.27: Cell surface phenotype of K562 CML cells.*K562 cells grown in suspension culture were stained with fluorescently conjugated monoclonal antibodies against CD29, CD44, CD49A, CD49B, CD49C, CD49D, CD49E, CD49F, CD61, CD73, CD81, CD95, CD104, CD120A, CD140A, CD253, CD200. Representative flow cytometric histograms are shown. The red line was the isotype control and the blue line was the stained sample.*

However, during co-culture with MSC, the AD-K562 cells had significantly less CD49E cell surface expression compared to the control cells which were grown in stroma free

suspension culture (Figure 4.28). CD29, CD44 and CD120A cells surface marker expressions were similar in both AD-K562 and K562-CON cells (Figure 4.28).

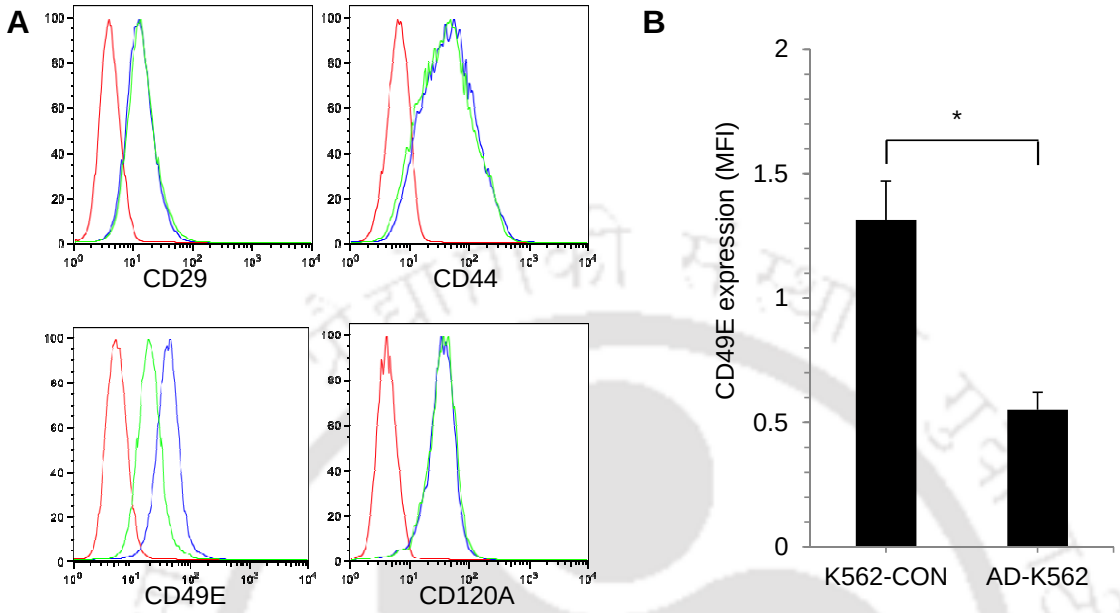

Figure4.28: Cell surface phenotype of stroma adherent and suspension fractions of K562 cells. *K562 cells were co-cultured with stromal cells for 3 days stained with antibodies against cell surface markers. The percentage positive cells and the mean fluorescent intensity (MFI) were calculated for the samples. (A) Representative flow cytometric histograms showing cell surface expression of CD29, CD44, CD49E and CD120A in adherent (green line) and control (blue line) K562 cells. Red line represents the isotype control. (B) Graph showing the MFI ratio of CD49E expression in AD-K562 cells and K562-CON cells. The expression of CD49E is normalized to isotype control. Values are mean±SD, n=4 independent experiment;*p<0.05.*

The AD-K562 cells were further characterized for their changes in gene expression of pro-survival cytokine *IL-6*. When K562 cell were co-cultured with MSC (K562-CC), there was a significant reduction in *IL-6* transcript levels compared to the cells grown in a stroma free culture (K562-CON) (Figure 4.29A). The K562 co-cultured with MSC were further separated into adherent and suspension fractions, AD-K562 and SUS-K562 respectively and their *IL-6* expression levels were tested. The AD-K562 had significantly reduced *IL-6* transcript levels compared to SUS-K562 cells (Figure 4.29B) and *IL-6* transcript levels in K562 cells decreased when they were treated with IM both in the presence and absence of MSC (Figure 4.29C).

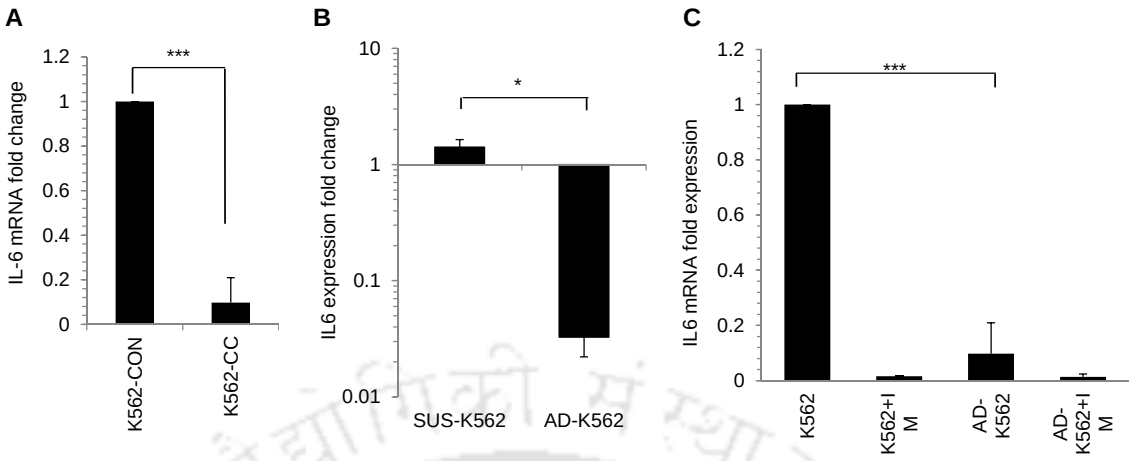

Figure4.29: IL6 mRNA expression. *(A) K562 cells were grown in suspension culture or in co-culture with CML derived stromal cells (K562-CC). The IL6 mRNA expression levels were analyzed by real-time PCR. A significantly reduced IL6 mRNA levels were seen in K562-CC compared to K562-CON cells. (B) The stroma co-cultured K562 cells were separated into adherent (AD-K562) and suspension fractions (SUS-K562) and IL6 mRNA levels were analyzed. There was a significant decrease in the IL6 transcript levels in AD-K562 compared to SUS-K562 cells. (C) K562 cells grown in suspension or in co-culture with stromal cells were treated with IM and IL6 expression levels were analyzed by real-time PCR. A significant reduction in IL6 expression levels were seen in AD-K562 cells which further decreased on IM treatment. Values are Mean±SE, n=3 independent experiments; * p<0.05, *** p<0.0005.*

Also, while there was no difference in the expression levels of inhibitor of apoptosis genes cIAP1 and cIAP2 between K562-CON and AD-K562cells, there was a significant upregulation of cIAP2 levels in AD-K562 cells when treated with IM (Figure 4.30) suggesting a chemoprotective response in stroma adherent CML cells.

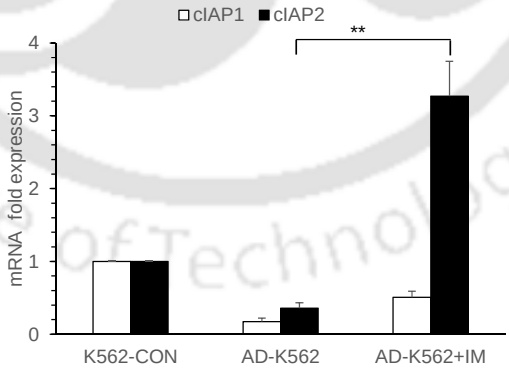

Figure 4.30: IAP expression in stroma adherent K562 cells.*RNA was extracted from control K562 cells and AD-K562 cells during co-culture with MSC after IM treatment. The expression levels of cIAP1, cIAP2 were analyzed by real-time PCR.cIAP1 levels did not change after IM treatment, cIAP2 transcript levels were significantly high in AD-K562 cells when treated with IM (AD-K562+IM) compared with untreated adherent cells (AD-K562) or cells grown in suspension (K562-CON). Values are Mean±SE, n=3 independent experiments; ** p<0.005.*

Further, AD-K562 and SUS-K562 were analysed for expression of genes responsible for scavenging ROS (MNSOD, CAT) or known to have significance in leukemia cell proliferation (PRKCH, WNT7B, BAP1). All these genes were found to be downregulated in AD-K562 cells compared to SUS-K562 which represent the quiescent state of AD-K562 cells and negate the role of these genes in chemoprotection against IM treatment (Figure 4.31).

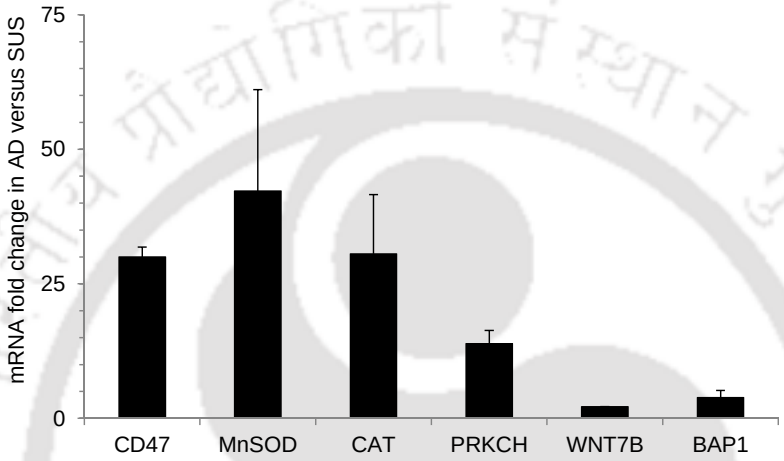

Figure 4.31: Gene expression in AD-K562 versus SUS-K562 cells.*K562 cells were seeded on stromal cells and allowed to interact for 3 days. The adherent and suspension fractions were collected separately and RNA was extracted, reverse transcribed and gene expression analysis was performed for CD47, MnSOD, CAT, PRKCH, WNT17B, and BAP1 by real-time PCR. The expression of each gene was normalized against GAPDH expression levels. Fold change was calculated by normalizing the gene expression levels in adherent cells against the suspension cells. Values are Mean+SD, n=3 independent experiments.*

4.3.6 Imatinib did not facilitate K562 adhesion to stroma

Since it is clear that stroma adherent CML cells are chemo-protected from cell death induced by IM treatment, it was of interest to understand whether IM treatment itself increases CML cell adherence to the stroma to escape the cell death. For this, initially, different serum concentrations were tested to determine the serum percentage which induced higher K562-stromal cell adhesion in the absence of IM. K562 cells attached to the stromal layer at all serum concentrations tested (0.1%, 1%, 5% and 10%) (Figure 4.32), however, significantly higher K562-stroma cell adhesion was observed in higher serum concentration of 10% (v/v) in the culture media (Figure 4.32A). IM treatment significantly inhibited K562 cell adhesion to the stromal layer at all the serum

concentrations (0.1%, 1%, 5%, 10%) tested. However, in presence of IM as well, more cell adhesion was observed at higher serum concentrations (5%, 10%), than at lower serum concentrations (0.1%, 1%) (Figure 4.32 B). This suggests that IM treatment in itself did not induce K562 cell adherence to stromal cells.

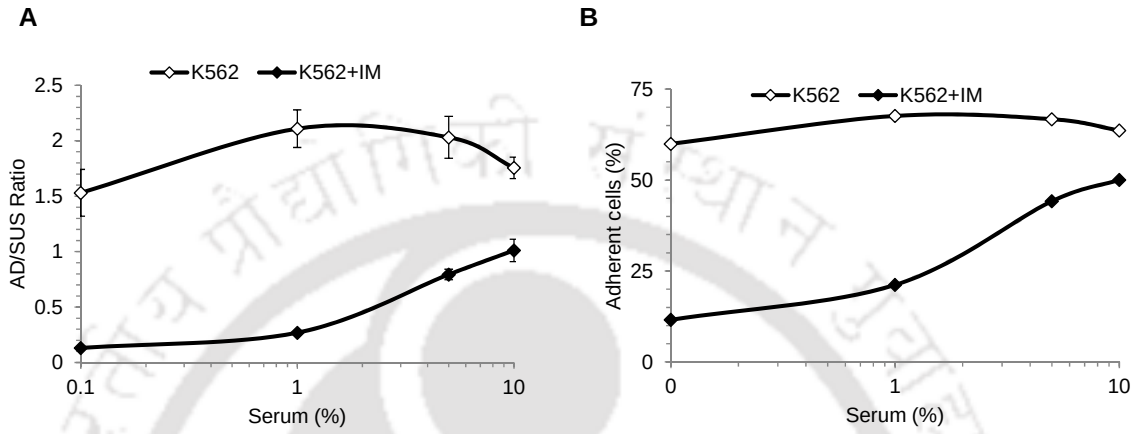

Figure 4.32: Effect of IM treatment on adhesion of K562 cells to stromal layer. *Stromal cells were grown to 100% confluency and K562 cells were seeded on the stromal layer with different serum concentrations (0.1%, 1%, 5%, 10%) in the absence (K562)or presence of IM (10µM) (K562+IM). The K562 cells were allowed to adhere for 24 hours, suspension and adherent cells were collected separately for each condition and counted microscopically. (A) The stroma adherent (AD) versus suspension (SUS) cells ratio for each condition in the presence or absence of IM was calculated and plotted in the graph. There was reduction in the number of adherent cells in the presence of IM at different serum concentrations. (B) The percentage of K562 cells that adhered to stroma was significantly lower than the control cells at low or high serum concentrations. Values are Mean+SD, n=3 independent experiments.*

Next, to identify whether the K562 cells that adhered to MSC layer become more adherent when transferred to a new MSC layer, first, AD-K562 cells were established in a co-culture system with the stromal cells for 24 hrs. The SUS-K562 cells were removed from the co-culture andAD-K562 were harvested. AD-K562 and K562-CON cells were seeded on a fresh stromal layer and the adherent versus suspension (Ad/Sus) ratio in both the conditions was tested (Figure 4.33). The AD-K562 andK562-CON cells had similar Ad/Sus cell ratio when seeded on stromal layer and no difference was observed (Figure 4.33B). To understand further, AD-K562 cells which were treated with IM for 24hrs (AD-K562+IM) or left untreated (AD-K562-IM), were transferred to fresh stromal layer. Ad/Sus cell ratio was found to be same for both the conditions (Figure 4.33C), suggesting that IM treatment did not induce K562 cells to become more adherent to the stromal cells.

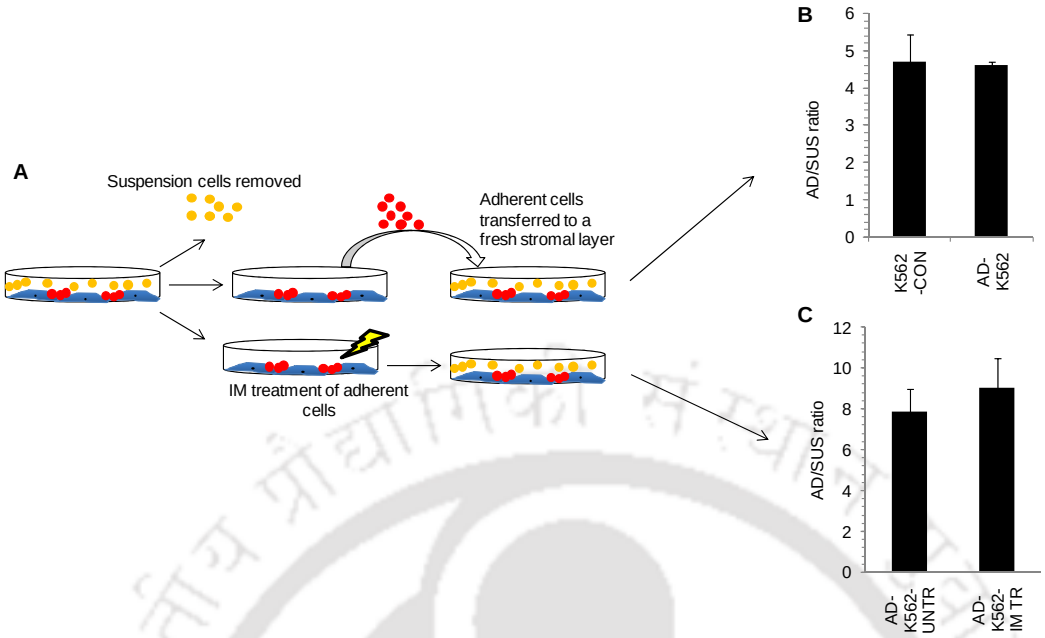

Figure 4.33: Adherence advantage of stroma adherent K562 cells. *(A) Pictorial representation of experimental design. (A) In the first condition, K562 were co-cultured with stromal cells and allowed to interact and 24 hours later, the suspension cells were removed. The remaining adherent cells (AD-K562) and control (K562-CON) cells were seeded onto a new stromal layer. The adherent versus suspension (Ad/Sus) ratio was calculated for each condition after 24 hours. There was no difference in the Ad/Sus ratio between AD-K562 and K562-CON cells after 24hrs. (B) In the second condition, suspension K562 cells were discarded from the co-culture system after 24 hours of seeding. After this, the AD-K562 cells were left untreated (AD-K562-UNTR) or treated with IM (AD-K562-IM TR) for 24 hours. The Ad/Sus ratio was calculated after 24hrs and no difference in Ad/Sus ratio was observed between untreated and IM treated conditions. Values are Mean±SD, n=3 independent experiments.*

4.3.7 CXCR4 and actin inhibition in K562 adherence to stroma

Jin et al showed IM treatment increased surface expression of CXCR4 on CML cells which led to higher migration towards stroma (Jin et al., 2008). To test this condition in our system, K562 cells were added to MSC in the presence of CXCR4 antagonist AMD3100 and a reduction in stroma adhesion was observed at a high antagonist concentration (20-50µg/ml) (Figure 4.34 A). However, there was no increase in apoptosis percentage when CXCR4 was inhibited with AMD3100 addition during IM treatment both in stroma free suspension culture as well as in case stroma adherent K562 cells, showing that CXCR4 inhibition did not sensitize K562 cells to IM treatment (Figure 4.34 B).

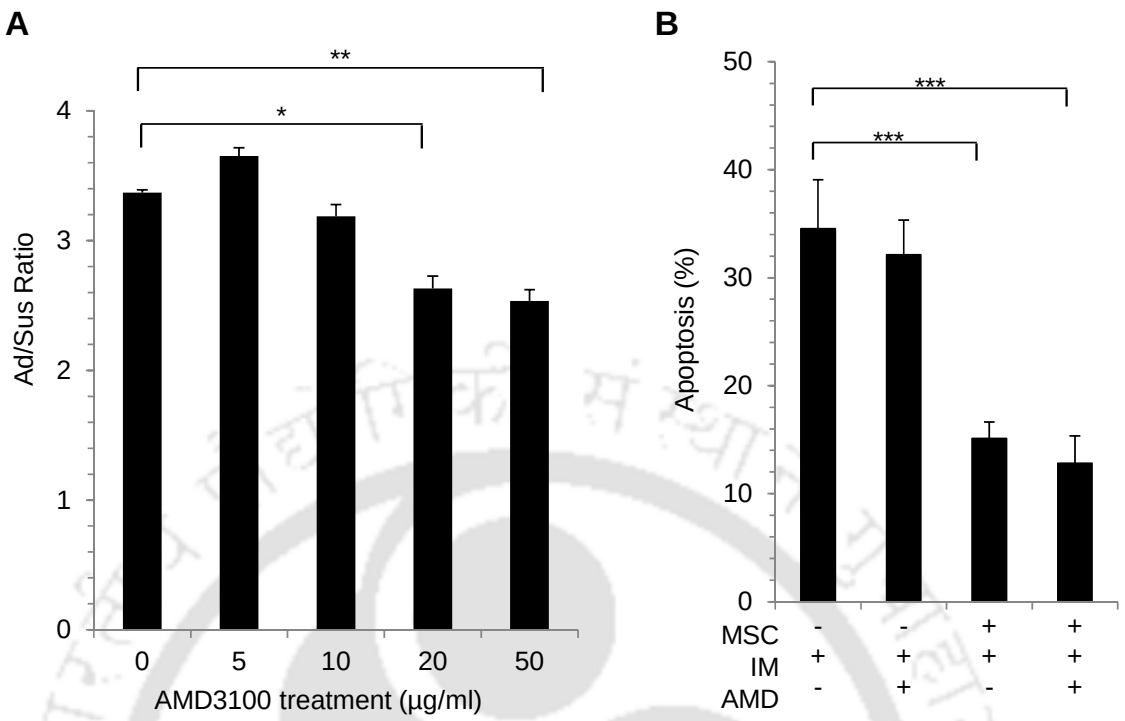

Figure4.34: Effect of CXCR4 inhibition on CML cell apoptosis and adherence to stroma. *(A) Different concentrations of CXCR4 inhibitor AMD3100 was added to K562 cells during co-culture with MSC. At high concentrations of 20ug/ml and 50ug/ml, there was a significant reduction in the adherence of K562 cells to MSC layer. (B) CXCR4 inhibitor was added to K562 cells in suspension or MSC adherent K562 cells in the presence of IM. No change in IM induced apoptosis was observed on addition of AMD3100. Values are Mean+SD, n=3; * p<0.05, ** p<0.005, *** p<0.0005.*

Actin cytoskeleton is one of the major mediators of cell-cell interaction and cell adhesion. To determine the role of actin in regulating adhesion of K562 cells to stromal cells, K562 cells were treated with actin cytoskeleton inhibitor cytochalasin D (CYD) during co-culture with MSC. On treatment with CYD (1000ng), there was a significant reduction in the number of cells that attached to the MSC layer (Figure 4.35 A). Of the different concentrations tested, 300ng/ml of CYD for 24 hours was sufficient to significantly reduce K562 adherence to MSC without compromising their cell viability (Supplementary Figure 7.4).

Next, to find out the effect of actin inhibition in which of the interacting cell types, K562 or MSC have more important role in cell-cell adhesion, K562 cells or the MSC layer were pre-treated with CYD (1000ng/ml)for 24hrs before co-culture. Inhibition of actin polymerization by CYD treatment in both K562 and MSC significantly inhibited cell-cell adhesion. However, CYD pretreated K562 cells had the lower Ad/Sus (Figure 4.35B)

suggesting that actin cytoskeleton in K562 cells might play a major role in cell-cell interaction with MSC. Additionally, post-CYD treatment after establishment of AD-K562 cells in the co-culture system was sufficient to detach AD-K562 cells from the MSC layer (Figure 4.35C). There was ~3-fold reduction in the ratio Ad/Sus cells when CYD treatment was given to AD-K562 cells after 24 hrs of co-culture (Figure 4.35C).

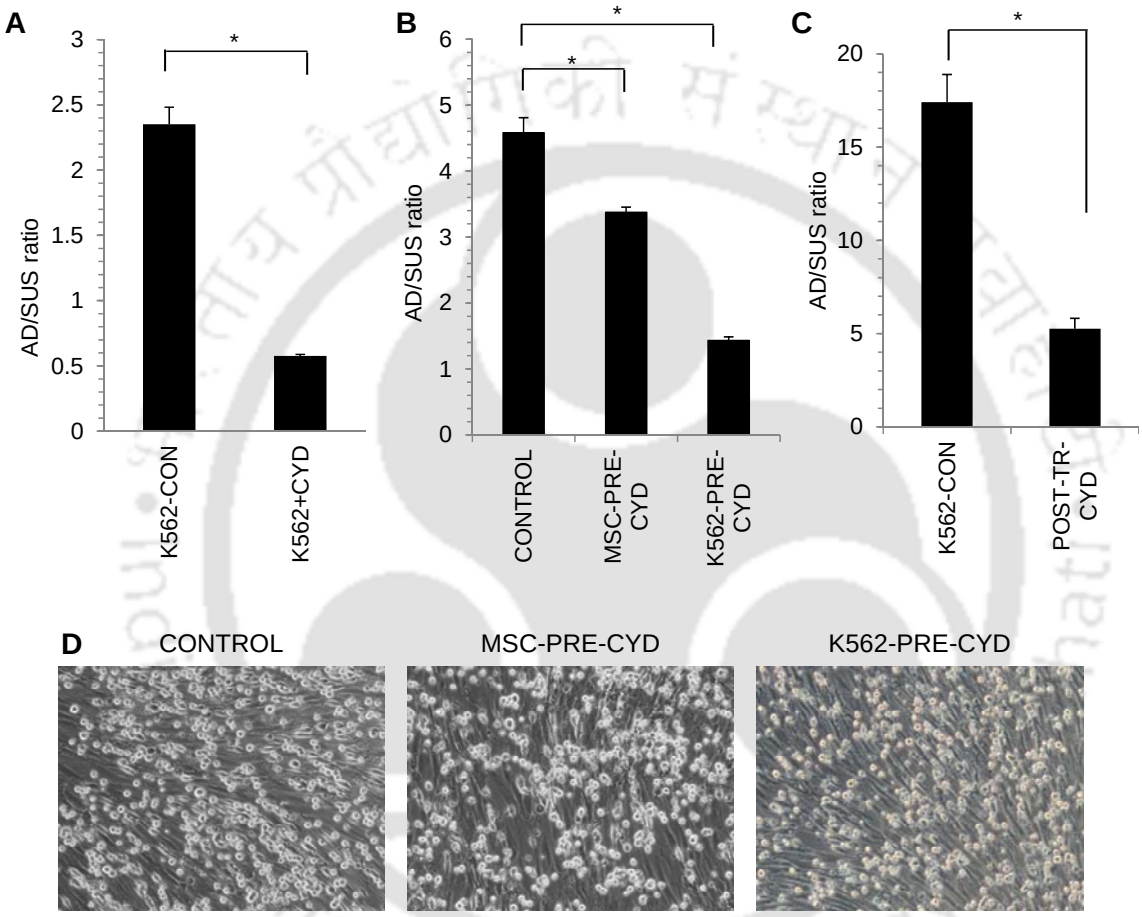

Figure4.35: Effect of actin inhibition on K562 cell adhesion. *(A) K562 cells were added to the stromal cells in the presence (K562+CYD) or absence (K562-CON) of CYD (1000ng/ml) and allowed to interact for 24 hours. The Ad/Sus ratio was analyzed by counting the stroma adherent and non-adherent suspension cells for each condition. CYD treatment significantly decreased K562 cell adhesion to the stromal layer. (B) K562 cells (K562-PRE-CYD) or MSC (MSC-PRE-CYD) were pre-treated for 24 hrs with CYD (1000ng/ml) before initiating the co-culture. The cells were incubated for 24 hours and the adherent and suspension cells were separated, counted and Ad/Sus ratio was determined. A significant decrease in cell adhesion to MSC was observed in both K562-PRE-CYD and MSC-PRE-CYD conditions. (C) K562 cells were cultured with stromal cells for 24 hours to establish cell adhesion and CYD was added for further 24 hours (POST-TR-CYD) to AD-K562 cells and AD/SUS ratio was calculated. There was a significant decrease in K562 adhesion to stroma on CYD treatment. Values are mean±SD, n=5; * p<0.05. (D) Microscopic representative images showing the effect on cell adhesion during pretreatment of K562 or MSC with CYD.*

Since, actin inhibition through CYD decreased the cell-adhesion and cell-adhesion was shown to be necessary for chemoprotection against IM induced cell death in K562 cells, CYD treatment was given to AD-K562 cells to detect their chemosensitization to IM. At high concentrations (1µg/ml), CYD treatment alone was sufficient to induce apoptosis of K562-CON cells in suspension culture (Figure 4.36 A). In the presence of stromal layer, CYD treatment alone at non-toxic concentrations (300ng/ml) did not have a significant apoptotic effect whereas it increased the chemosensitivity of AD-K562 cells to IM induced cell death (Figure 4.36 B). On the other hand, ROCK inhibition by treatment with Y27632 (20µM) did not have any effect on apoptosis (Figure 4.36 B).

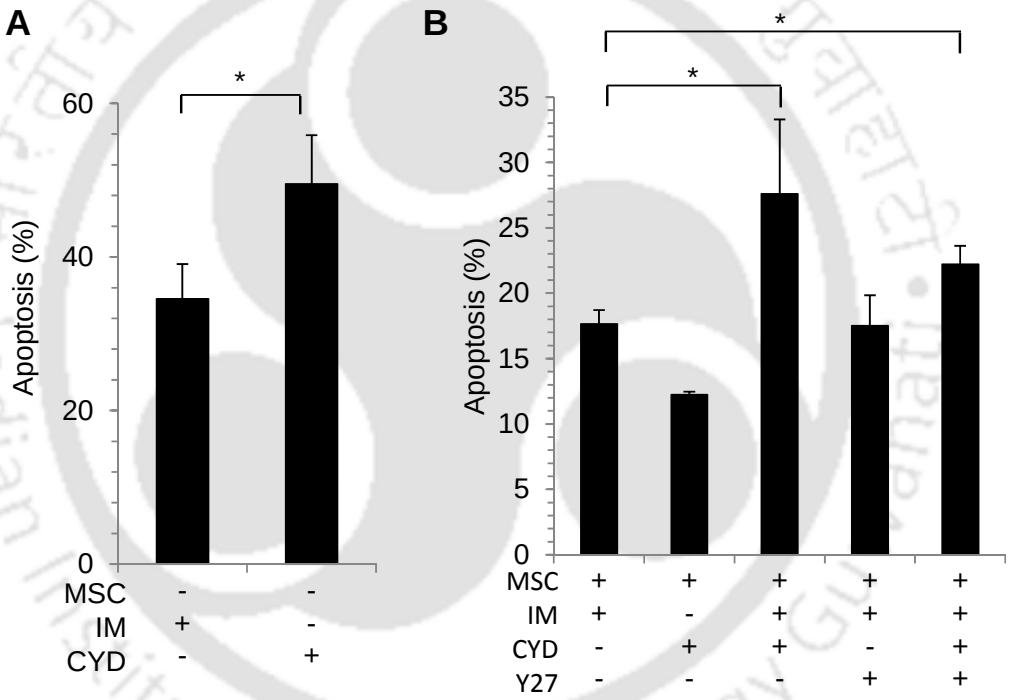

Figure4.36: Apoptosis induced by CYD treatment. *(A) K562 cells in suspension were treated either with IM (10µM) or CYD (1000ng/ml) for 48 hours and the apoptosis percentage was determined by An-V/PI staining. A significant increase in the apoptosis was observed in K562 on treatment with CYD. (B) K562 cells were co-cultured with stromal cells (MSC) for 48 hours. The SUS-K562 cells were discarded and AD-K562 were treated with IM, CYD and Y27632 (Y27) (20µM) alone or in combination with each other as shown for 48 hours. The apoptosis percentage was analyzed by An-V/PI staining using flow cytometry. A significant increase in apoptosis was seen when IM treatment was combined with either CYD, Y27 or in combination of both. Values are mean+SD, n=3; * p<0.05.*

4.3.8 RHOA regulates K562 adherence to stromal cells

To probe the role of actin cytoskeleton further, the role of RHOA GTPase which is a positive regulator of actin cytoskeleton, was studied in cell-cell interaction between K562 cells and MSC. For this, K562 cells were lentivirally transduced with constitutively active RHOA (RHOAV14) or dominant negative RHOA (RHOAN19) and control vector and their effect on K562 cell adhesion to the stromal layer was determined. RHOA modification did not affect the proliferation status of K562 cells (Figure 4.37 A). While RHOAV14 did not alter the K562 cells adhesion to MSC, K562 cells transduced with RHOAN19 significantly decreased K562 cell adhesion to the stroma (Figure 4.37 B). This again confirms that disruption of actin through inhibitors or by modifying RHOA signaling can inhibit cell-cell interaction of K562 cells with the stromal cells.

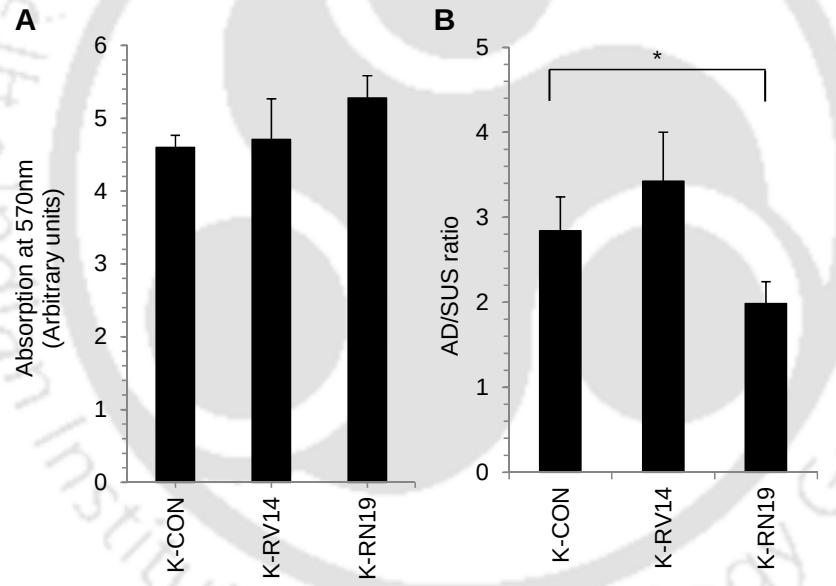

Figure 4.37: RHOA in CML-stromal adhesion.*K562 cells were lentivirally transduced with control vector (K-CON), constitutively active RHOA (K-RV14) or dominant negative RHOA (K-RN19). (A) Cell proliferation in all the transduced K562 cells were analyzed by MTT assay and absorbance was measured at 570nm. RHOA did not affect the proliferation of K562 cells. (B) RHOA transduced K562 were grown in co-culture with MSC for 24 hours and the stroma adherent and suspension cells were counted and ratio was calculated. There was a significant reduction in adhesion of K-RN19 to the MSC layer. Values are Mean±SD, n=3; * p<0.05.*

4.3.9 ERK, SMAD and STAT pathways in adherent K562 cells

As discussed in introduction section, studies have shown that BCR-ABL regulates JAK/STAT, ERK/MAPK, NFκB pathways and cytoskeleton proteins.

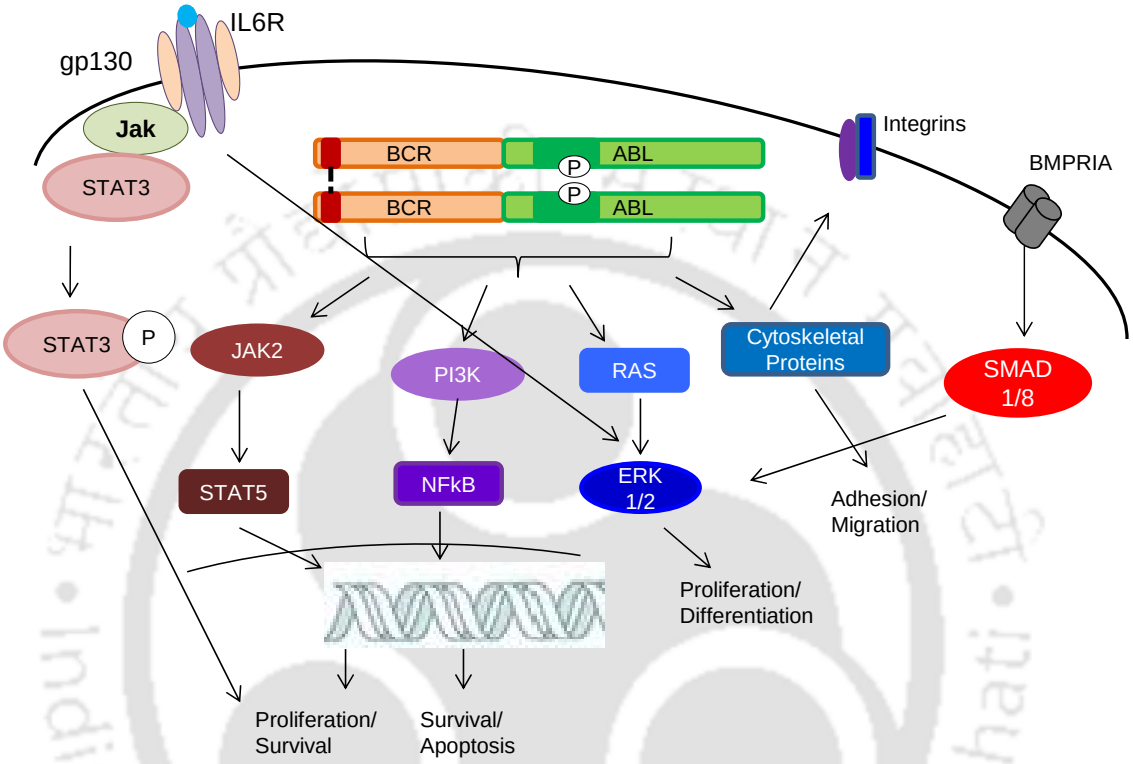

Figure 4.38: Pictorial representation of pathways regulated by BCR-ABL fusion gene and oncogene independent pathways active in CML cells as a result of interaction with stromal cells*. Adapted from (Deininger et al., 2000; Quintas-Cardama and Cortes, 2009)*

To determine whether the BCR-ABL independent signaling resulted in differential aberrant response to IM in AD- K562 cells which can be a source of target for therapy, the phosphorylation status of ERK1/2MAPK, p38MAPK, STAT3, STAT5, NFκB and SMAD1/8 was determined by phospho specific flow cytometric analysis and compared with CON-K562 cells cultured without the stromal layer. P38MAPK was phosphorylated at low basal levels in both adherent and suspension K562 cells indicating low levels of active p38MAPK signaling (Figure 4.39 A). pNFκB levels were similar in both AD-K562 and SUS-K562 cells during co-culture (Figure 4.39 B). While levels of pERK1/2MAPK and pSTAT3 were lower in SUS-K562, it was higher in AD-K562 (Figure 4.39 A, C) andpSMAD1/8 levels were significantly higher in AD-K562

compared SUS-K562 (Figure 4.39 B). No difference in pSTAT5 was observed between AD-K562 and SUS-K562 (Figure 4.39 C). This suggests that ERK1/2 MAPK, SMAD1/8 and STAT3 activity were differentially regulated when K562 directly interacted with the stromal cells.

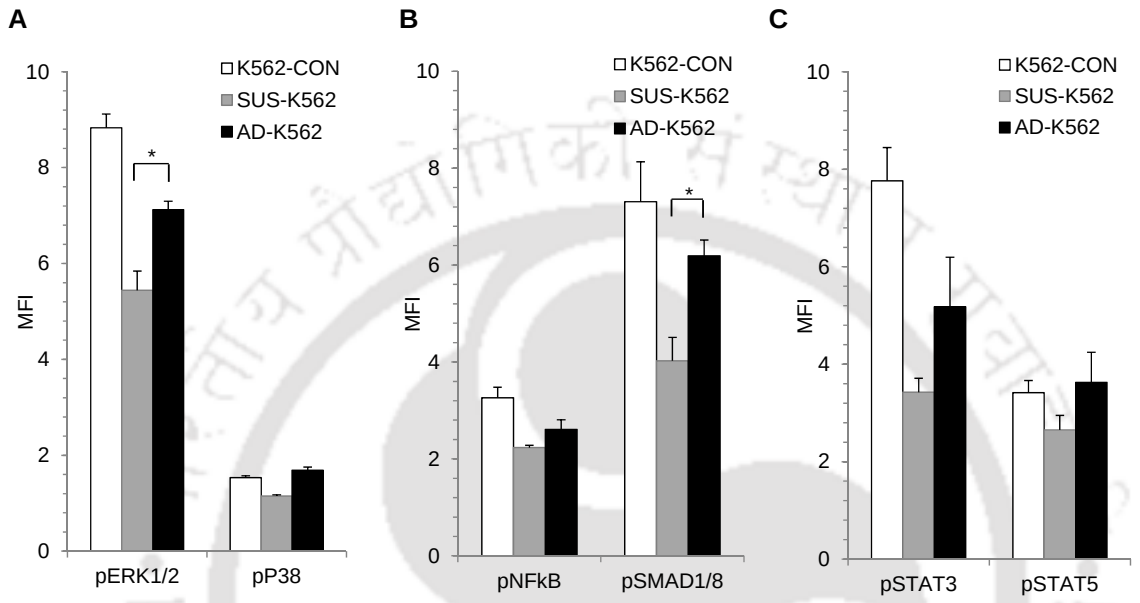

Figure 4.38: Active signaling pathways in K562 cells determined by phospho flow cytometry. *K562 cells 9were cultured alone in suspension (K562-CON) or in co-culture with CML BM derived stromal cells. The co-cultured K562 cells were separated into stroma adherent (AD-K562) and stroma non-adherent suspension cells (SUS-K562). The cells were stained with fluorescent conjugated monoclonal antibodies against phosphorylated form of ERK1/2 MAPK. P38 MAPK, NFkB, SMAD1/8, STAT3 and STAT5. The cells were analysed by flow cytometry and phosphorylated levels were determined by calculating mean fluorescent intensity normalized to the isotype control. Graphs showing phospho protein levels of (A) ERK1/2 MAPK, p38 MAPK, (B) NFkB, SMAD1/8, (C) STAT3, STAT5 in K562-CON, AD-K562 and SUS-K562 cells. Values are mean±SE, n=4-5 independent experiments; * p<0.05.*

Since BCR-ABL regulates several signaling pathways, K562 cells were treated with IM to determine which of the BCR-ABL regulated pathways were downregulated upon IM treatment and whether stroma adherent and suspension cells responded similarly to IM treatment. On treatment with IM, the K562-CON cells showed significant downregulation of phospho levels of ERK1/2 MAPK, STAT3 and STAT5 (Figure 4.40). However, p38MAPK, SMAD1/8 and NFκB phospho protein levels remained unaffected after IM treatment (Figure 40).

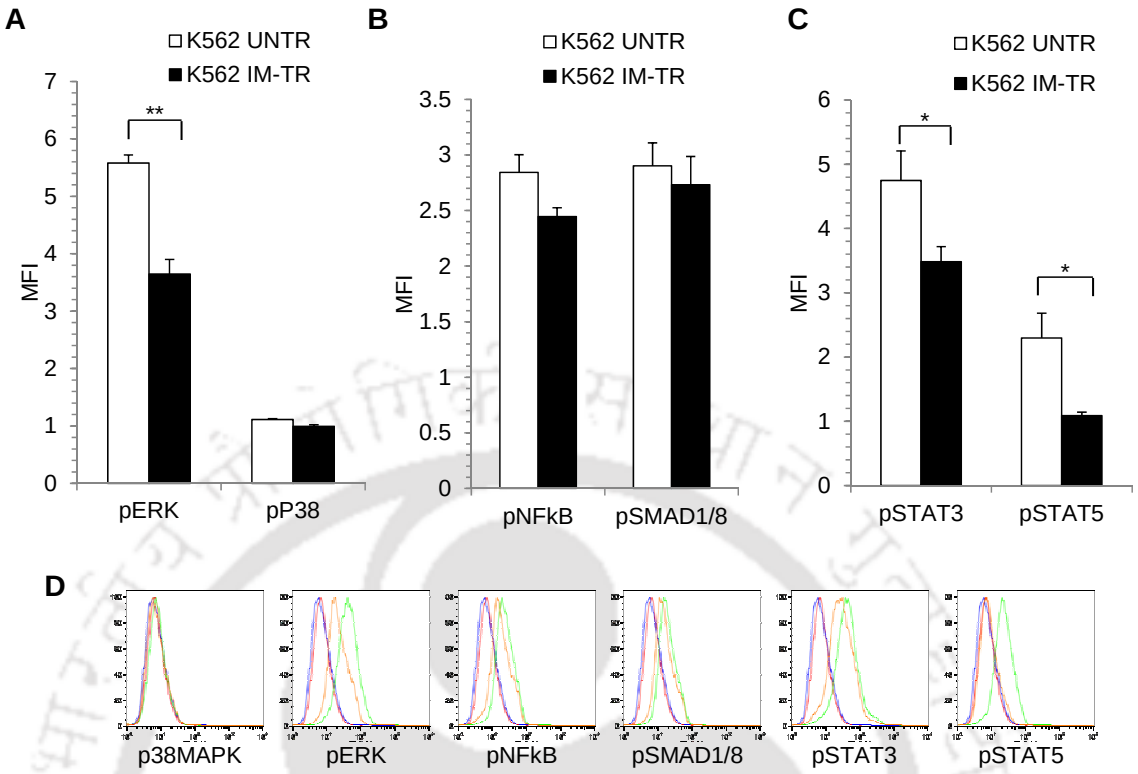

Figure 4.40: Signaling pathways in K562 cells during IM treatment.*K562 cells grown in stroma free culture were treated with IM for 24 hours and stained with fluorescent conjugated monoclonal antibodies against phosphorylated form of ERK1/2 MAPK. P38 MAPK, NFκB, SMAD1/8, STAT3 and STAT5. The cells were analyzed by flow cytometry and expression levels were determined by calculating mean fluorescent intensity normalized to the isotype control. Graphs showing phospho protein levels of (A) ERK1/2 MAPK, p38 MAPK, (B) NFκB, SMAD1/8, (C) STAT3, STAT5 in K562 cells without (K562-UNTR) and with IM (K562 IM-TR) treatment. (D) Representative flow cytometric histograms showing isotype control for CON-K562-UNTR (red line), isotype control for CON-K562 IM-TR (blue line), stained CON-K562-UNTR cells (green line) and stained CON-K562 IM-TR cells (orange line). Values are mean±SE, n=3 independent experiments; * p<0.05, ** p<0.005.*

Next, the phospho levels of signaling molecules were determined in IM treated AD-K562 cells. While the phospho protein levels of p38MAPK, SMAD1/8, NFκB and STAT3 were similar in both untreated and IM treated AD-K562 cells (Figure 4.41), phospho STAT5 levels were significantly downregulated in IM treated AD-K562 cells, indicating BCR-ABL inhibition in AD-K562 cells by IM (Figure 4.41 C). Interestingly, phospho protein levels of ERK1/2 MAPK were significantly upregulated in AD-K562 after IM treatment (Figure 4.41 A) suggesting a possible compensatory mechanism or a drug resistance mechanism through ERK signaling.

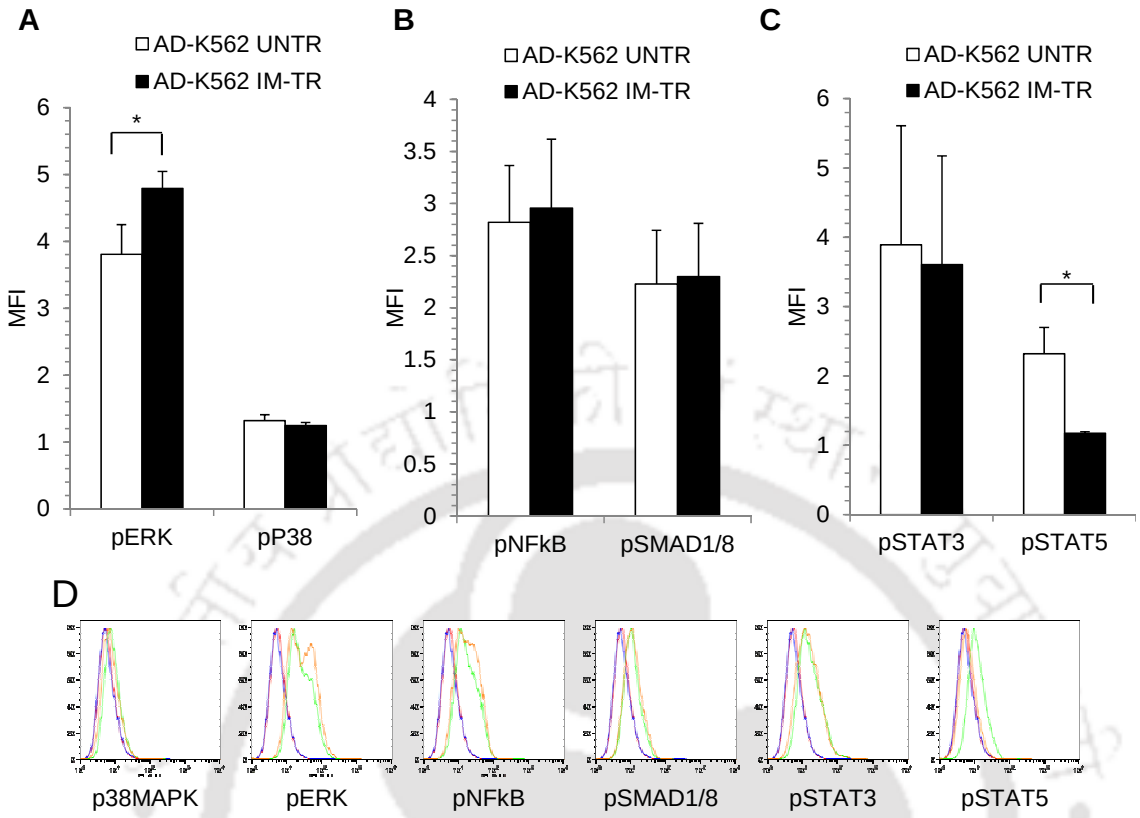

Figure 4.41: Active signaling pathways in stroma adherent K562 cells during IM treatment.*AD-K562 cells cultured in a co-culture system with stromal cells were treated with IM for 24 hours after the removal of suspension cells and stained with fluorescent conjugated monoclonal antibodies against phosphorylated form of ERK1/2 MAPK. p38MAPK, NFκB, SMAD1/8, STAT3 and STAT5. The cells were analyzed by flow cytometry and expression levels were determined by calculating mean fluorescent intensity normalized to the isotype control. Graphs showing phospho protein levels of (A) ERK1/2 MAPK, p38 MAPK, (B) NFκB, SMAD1/8, (C) STAT3, STAT5 in AD-K562 cells without (AD-K562 UNTR) and with IM (AD-K562 IM-TR) treatment. (D)Representative flow cytometric histograms showing isotype control for AD-K562-UNTR (red line), isotype control for AD-K562 IM-TR (blue line), stained AD-K562-UNTR cells (green line) and stained AD-K562 IM-TR cells (Orange line). Values are mean±SE, n=3 independent experiments; * p<0.05.*

To understand the role of these signaling molecules in mediating cell-cell interaction between K562 and MSC, the K562 CML cells were treated with inhibitors for various signaling pathways. K562 cells which were co-cultured with stromal cells were treated with U0126 to inhibit ERK1/2 MAPK, SB 208530 to inhibit p38 MAPK and BAY 11-7082 to inhibit NFκB pathways. Inhibition of p38MAPK, NFκB and ERK 1/2 MAPK with SB 208530, BAY 11-7082and U0126respectively, did not affect K562 adhesion to the stromal cells (Figure 4.42 A). Similarly, addition of SB 208530 and BAY 11-7082 did not affect the viability of control K562 cells whereas the U0126 treatment significantly decreased the viability K562 cells (Figure 4.42 B)

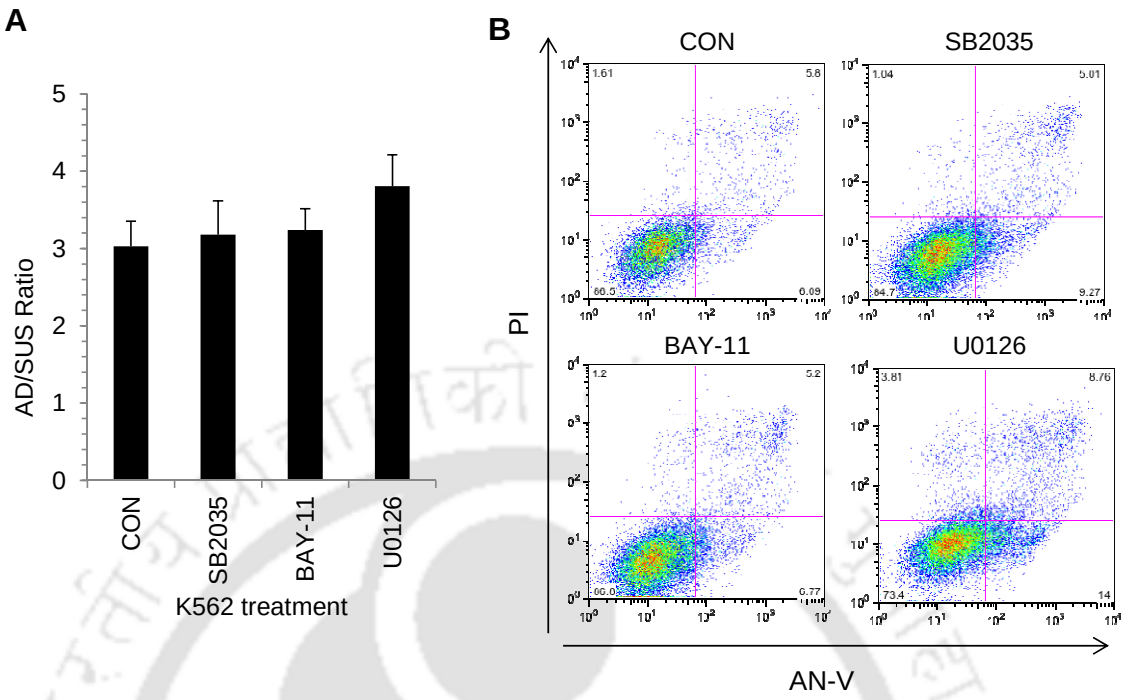

Figure 4.42: Role of signaling pathways in cell-cell interaction.*K562 cells were treated with inhibitors SB203580 for p38 MAPK, BAY 11-7082 for NFκB and U0126 for ERK1/2 MAPK inhibition for 48 hours. The adherent and suspension fractions were collected separately, counted microscopically and the AD/SUS ratio was calculated (A) Inhibition of p38 MAPK, NFκB or ERK1/2 MAPK did not affect the adhesion of K562 cells to the MSC layer. Values are Mean±SE, n=3. (B) Apoptosis was increased during U0126 treatment in K562-CON cells whereas no effect was seen during SB 203580 and BAY 11-7082 as shown in the flow cytometry dot plots*

4.3.10 BMP/Smad and ERK1/2 inhibition reduced stroma adherence and chemoprotection in K562 cells

An earlier study reported that BMP4 regulates hematopoietic stem cells niche (Goldman et al., 2009) and was responsible for HSC maintenance. In K562-MSC co-culture system, phospho SMAD1/8 levels were higher in AD-K562 cells compared to SUS-K562 cells and remained unaffected by IM treatment. To further understand the involvement of BMP/SMAD signaling in cell-cell interaction and chemoresistance, K562 cells were lentivirally transduced with BMP2, BMP4 and its antagonist GDF3 (Figure 4.43). Although BMP2, BMP4 and GDF3 expression did not affect the cell proliferation of K562 cells (Figure 4.44 A), however, BMP2 and BMP4 transduced K562 cells had higher percentage of K562 cells that attached to the MSC layer compared to the control or GDF3 transduced cells (Figure 4.44 B).

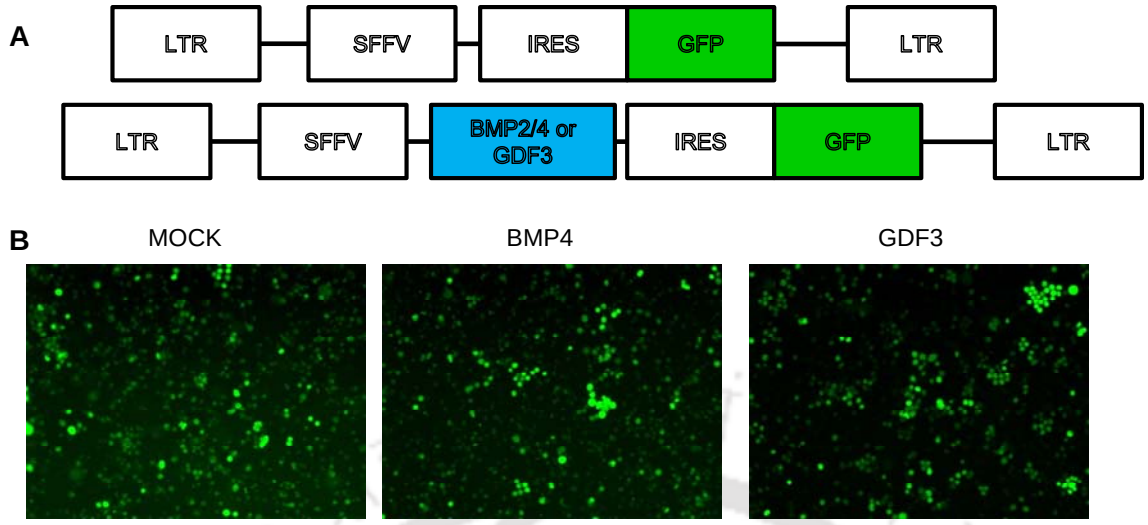

Figure 4.43:BMP2, BMP4 and GDF3 exogenous expression. *(A) Figure representing the lentiviral constructs cloned and used for exogenous expression of BMP2, BMP4 and GDF3. The genes were under SFFV promoter with a reporter GFP separated from the gene through IRES. (B) Representative microscopic figures showing MOCK, BMP4 and GDF3 transduced cells expressing the reporter gene GFP.*

However, treatment of K562-MSC co-culture with BMP signaling inhibitor LDN 193189 significantly reduced K562 adhesion to MSC in a dose dependent manner (Figure 4.44 C).Various concentrations of LDN 193189 was tested and as reported by others (Raymond et al., 2014), a final concentration of 3µM was found to be optimal for treatment of K562 cells to inhibit their adherence to the stromal cells (Supplementary Figure 7.5).

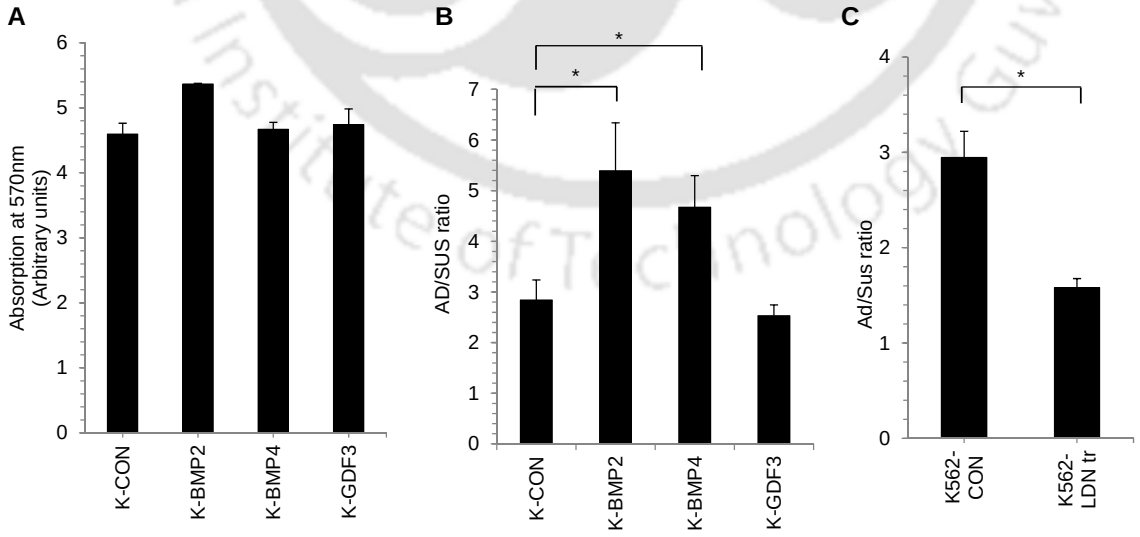

Figure 4.44: Effect of BMP pathway in cell adhesion.*(A) MOCK vector, BMP2, BMP4 and GDF3 transduced K562 cells were subjected to MTT assay to check their cell proliferation. No change in cell proliferation was observed with overexpression of BMP2, BMP4, GDF3 compared to the MOCK*

*transduced K562 cells (K-CON). (B) Equal number of CON, BMP2, BMP4, and GDF3 transduced K562 cells were added to the stromal layer and allowed to interact for 24 hours. The stroma adherent and suspension fractions were separated and counted. K562 cells transduced with BMP2, BMP4 showed increased stroma adherence compared to the control or GDF3 transduced cells. (C) K562 cells were co-cultured with stromal cells for 24 hours in presence of BMP inhibitor LDN 193189 (3μM), which reduced stroma adherence of K562 cells. Values are Mean±SE, n=3; * p<0.05.*

BMPRI inhibitor LDN 193189 treatment increased IM induced cell death in K562 cells cultured without stromal cells (Figure 4.45 A). However at optimal concentration of 3μM LDN 193189 had an additive effect on apoptosis induced by IM in AD-K562 cells. When the cells were treated with LDN 193189 (3μM) together with IM, there was a significantly higher percentage of apoptosis in AD-K562cells compared to treatment with IM alone (Figure 4.45 C). Similarly, treatment of K562 with ERK1/2 inhibitor U0126 significantly increased cell death percentage in AD-K562 cells (Figure 4.45 C) and combination of LDN 193189 and U0126in the presence of IM increased the cell death in AD-K562 cells further. Also, combination of LDN 193189 together with ROCK inhibitor Y27632 further increased the chemosensitivity of AD-K562 cells to IM treatment (Figure 4.45 C). Higher percentage of IM induced cell death was observed in AD-K562 cells when they were treated with a combination of LDN 193189, CYD and Y27632 (Figure 4.45 D). Thus, a combinatorial inhibitor treatment effectively chemosensitizedAD-K562 cells to IM treatment which were largely unaffected by IM treatment alone.

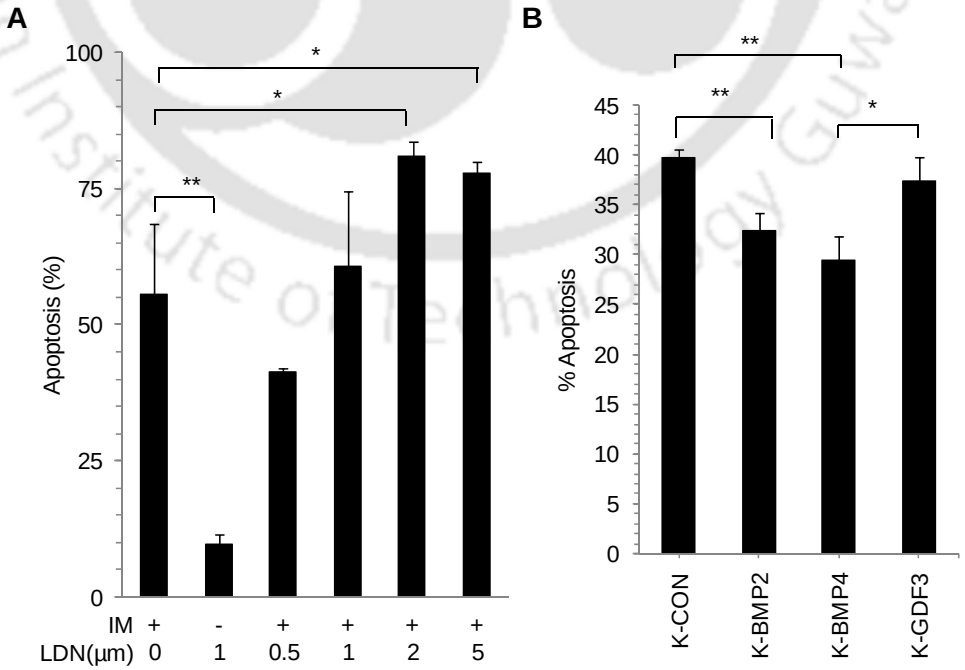

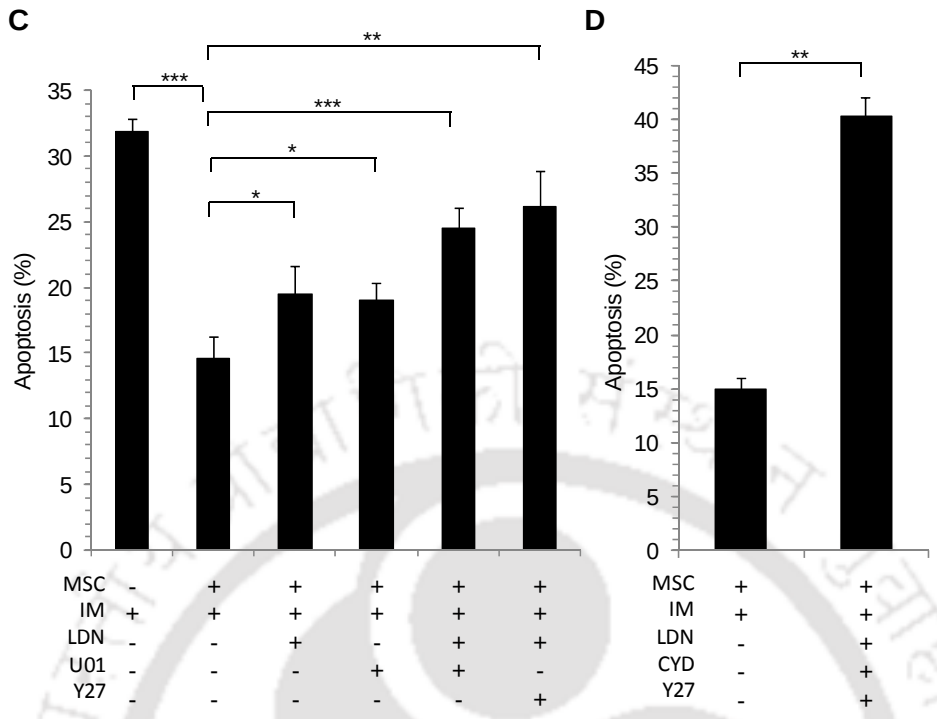

Figure 4.45: Combinatorial treatment of AD-K562 cells.*(A) K562 cells in suspension or in co-culture with stromal cells and were treated with or without IM in the presence of different concentration of BMPRI inhibitor LDN 193189 for 48 hours and apoptosis percentage was analyzed by An-V/PI staining through flow cytometry. LDN 193189 treatment enhanced IM induced apoptosis in suspension K562 cells.(B) K562 cells transduced with MOCK, BMP2,BMP4 and GDF3 overexpression vectors were treated with IM and their apoptosis was analysed. There was a significant reduction in apoptosis in cells expressing exogenous BMP2 and BMP4 proteins. (C) Stroma adherent K562 (AD-K562) cells were treated with combinations of BMPRI inhibitor (LDN) 3µM, ERK inhibitor (U01) 10µM, ROCK inhibitor (Y27) 20µM in presence of IM (10µM) for 48 hours and apoptosis percentage was analyzed by flow cytometry. (D) AD-K562 cells were treated with a combination of LDN (3µM), CYD (0.3µg/ml) and Y27 (20µM)and apoptosis was analyzed through An-V/PI staining which showed higher apoptosis percentage compared to treatment with IM alone. Values are mean±SE, n=3 independent experiments; * p<0.05, ** p<0.005, *** p<0.0005.*

Thus, the chemoprotection of CML cells were mediated by direct interaction of the leukemic cells with the stromal cells in their microenvironment and several signaling pathways were aberrantly regulated in the stroma adherent CML cells. The chemosensitivity of adherent CML cells to IM induced cell death could be increased by inhibiting ERK and BMP signaling pathways.

4.4 Derivation of niche mediated chemo-resistant CML cell line

Generally, chemo-resistant cell lines are derived through the treatment of the cells with a low concentration of the chemotherapeutic drug for a long period of time (Puissant et al., 2012; Traer et al., 2014). However, in the patient, under physiological conditions, such mode of drug resistance development does not exist. As reported by several studies and seen in cases of many patients, chemo-resistance to drugs develop due to mutation and activation of signaling pathways through intracellular or extracellular inducers.

Analysis of patient samples showed that similar to the control BM cells, BM cells from patients diagnosed for CML or relapsed CML formed cobble-stone forming areas in the stromal co-culture (Figure 4.46). To understand the development of chemoresistance in CML, a co-culture method with the CML BM derived stromal cells was developed *in vitro* to derive chemoresistant K562 cells. To derive chemoresistant cells in manner similar to the physiological conditions in the patient, the K562 cells were first co-cultured with stromal cells in a long-term culture in the presence of IM at physiologically relevant concentration of 10μM. This culture method resulted in the derivation of IM resistant K562 cells which survive and proliferate in IM (10μM) dosage similar to that used for patient treatment (Figure 4.47), whereas the non-resistant K562 cells underwent 95-100% cell death. The method of chemoresistant K562 derivation and its signaling profile is explained in this section.

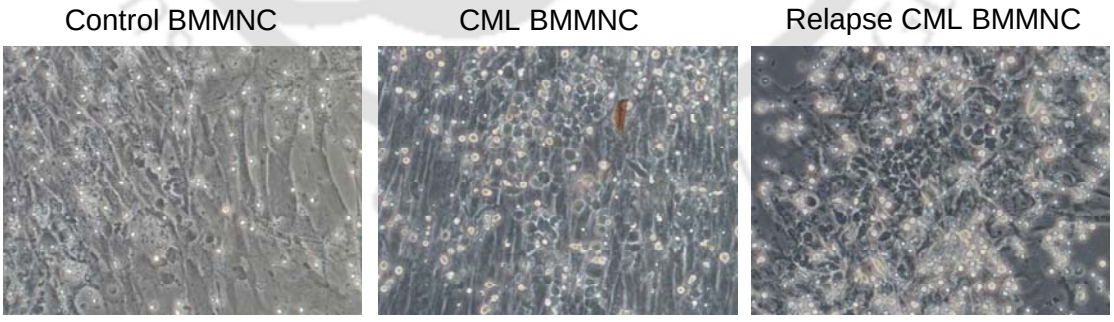

Figure 4.46: Cobble-stone area forming assay. *Cobble-stone forming assay was performed for bone marrow mononuclear cells obtained from Control (Control BMMNC), CML diagnosis patients (CML BMMNC) and CML patients who had relapsed after treatment (Relapse CML BMMNC). The BMMNC were plated onto stromal layer isolated from unrelated CML bone marrow. After 1 week, the cobble stone area forming cells were observed under phase contrast microscope. Representative microscopic images were shown.*

4.4.1 Continuous IM treatment of K562 cells adherent to the stromal layer

Initially, K562 cells were added to MSC layer for 5-7 days to establish the co-culture system. The suspension cells were removed from the co-culture and the adherent K562 cells were left undisturbed. IM was added to the co-culture system every 72 hours with fresh media and AD-K562 cell number was monitored at regular intervals (Figure 4.47).

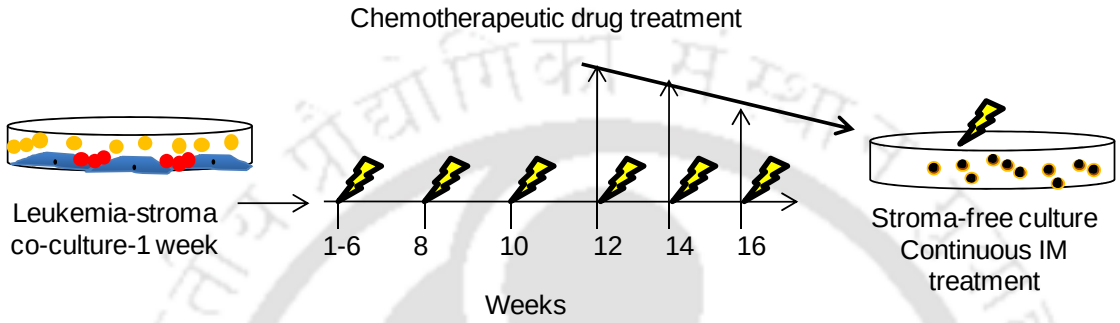

Figure 4.47: Derivation of chemoresistant K562 cells. *Pictorial representation of experimental set-up to derive chemoresistant K562 cell line using stromal layer and continuous treatment with IM.*

During long-term IM treatment, as expected, there was a significant decline in the number ofAD-K562 cells (Figure 4.48 A). However, after 2 weeks of IM treatment, the AD-K562 cell numbers started to increase in the presence of IM. After 4 weeks of co-culture and IM treatment, the number of AD-K562 cells was significantly higher or similar to the initial untreated controls suggesting proliferation and chemoresistance development in AD-K562 cells (Figure 4.48 A).

Microscopic analysis revealed several clones of chemoresistant AD-K562 cells proliferating rapidly while still being attached to the MSC layer. They formed 3D microspheres on top of the stromal cells (Figure 4.48 B) which could be easily detached by trypsinization without affecting the MSC layer. The cells were termed stroma dependent chemoresistant K562 cells (SD-CR-K562).

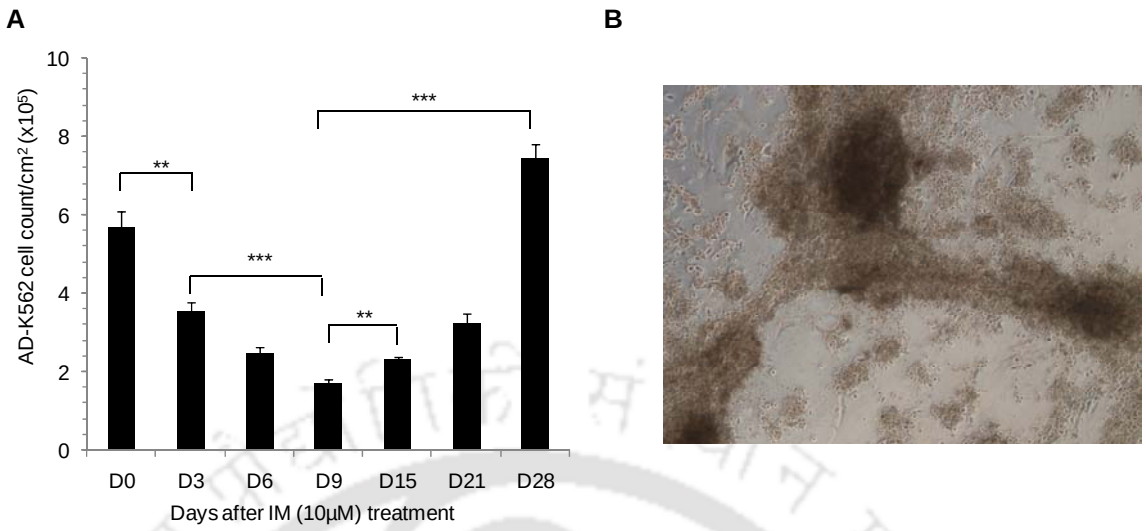

Figure 4.48: Derivation of chemoresistant K562 cells using stromal co-culture method. *(A) K562 cells were added to the stromal layer and IM was added to the cells every 3 days. The suspension cells were removed and the adherent cells (AD-K562) were collected at indicated time points and counted. Values are mean±SD, n=3 independent experiments; ** p<0.005, *** p<0.0005. (B) Representative microscopic image showing the co-cultured K562 cells growing as a 3D microsphere on the MSC layer in the presence of IM.*

We already established with our earlier experiments that stroma interaction provided chemo-protective environment to K562 cells. Acquired chemoresistance in patients, however, results in stroma free proliferation of CML cells in the presence of chemo-drug. To test whether the AD-K562 that were proliferating in the stromal co-culture with IM have acquired cell autonomous chemoresistance, long-term IM treated AD-K562 cells were transferred to suspension culture without the MSC layer. The cells were treated with IM for continuously and apoptosis percentage was analyzed at regular intervals and compared with the control cells. There was a significant increase in apoptosis in IM treated control cells, which increased further on prolonged IM treatment and attained maximum percentage of apoptotic cells after 120 hrs of treatment (Figure 4.49). Surprisingly, SD-CR-K562 when transferred to stroma free suspension culture showed significantly minimal apoptosis even at the initial time point of 48 hrs of IM treatment and apoptosis percentage did not increase even after treatment for 120 hrs (Figure 4.49) confirming the emergence of chemo-resistant K562 cells (CR-K562).

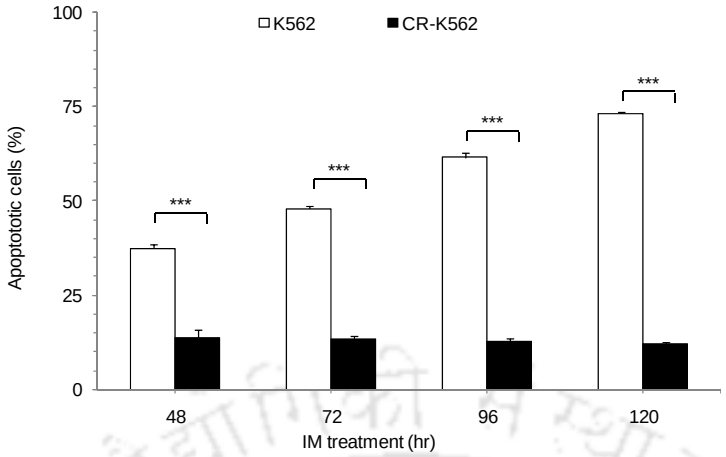

Figure 4.49: Survival of stroma independent CR-K562 in the presence of IM. *The chemoresistant (CR-K562) derived through stromal co-culture were transferred to a suspension culture in the absence of stromal cells. The cells were treated with IM (10µM) and cells were collected at indicated time points and apoptosis percentage was analyzed by An-V/PI staining through flow cytometry and compared with control cells (K562) grown in suspension. Values are mean±SD, n=3 independent experiments; ** p<0.005, *** p<0.0005.*

These CR-K562 cells thus derived could be continuously maintained in the suspension culture in the presence of physiological concentrations of IM. However, in our earlier observation we found that, most of AD-K562 cells were maintained in G0 cell cycle stage and this was proposed by others as one of the mechanisms of drug resistance (Trumpp et al., 2010).

To determine whether the CR-K562 cells maintained themselves in G0 stage for chemoresistance, as BCR-ABL is required for proliferation but not survival, the cell cycle profile of CR-K562 cells was compared with control K562 cells. There was no difference in the cell cycle profile of both the cell types and comparable percentage of cells in G1, S or G2/M phase of the cell cycle was seen in both control and CR-K562 cells, indicating that cell cycle profile alteration was not the reason for chemoresistance in CR-K562 cells (Figure 4.50).

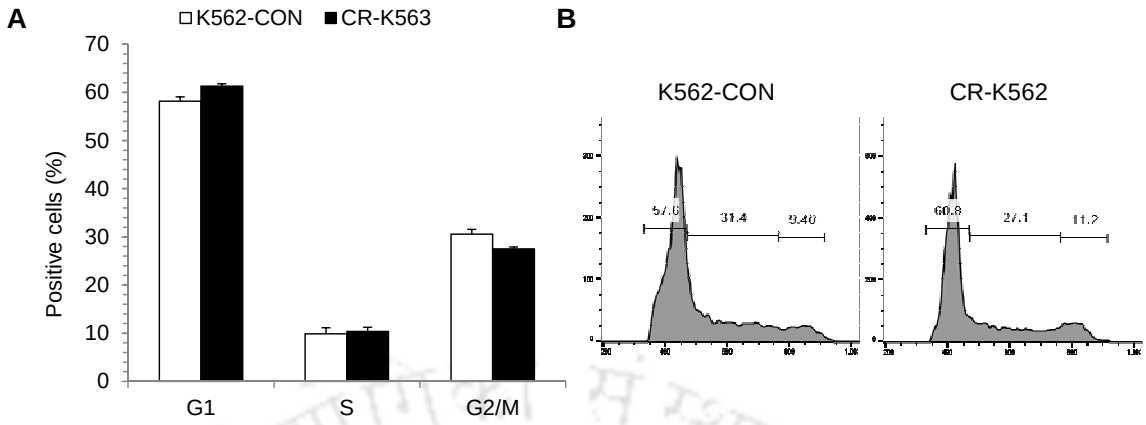

Figure 4.50: Cell cycle prolife of CR-K562 cells.*(A)Cell cycle profile of K562 control cells (K562-CON) grown in suspension culture without IM and chemoresistant cells (CR-K562) grown in presence of continuous dose of IM was analyzed by propidium iodide (PI) staining. The graph shows the percentage of different cell cycle stages in K562-CON and CR-K562 cells. Values are mean±SD, n=3. (B) Representative flow cytometric plots showing cell cycle profile in K562-CON and CR-K562 cells.*

4.4.2 Intracellular IM concentration in chemoresistant K562 cells

There are several reports that cancer cells actively extrude the chemotherapeutic drug through drug pumps as one of the mechanisms of chemoresistance and for survival during therapy (An et al., 2010). To functionally identify whether the CR-K562 cells that are proliferating in the presence of IM have increased drug efflux ability, the intracellular IM concentration was measured in the control and CR-K562 cells. Surprisingly, the CR-K562 cells had significantly higher intracellular IM concentration compared to the control IM treated cells (Figure 4.51), however CR-K562 cells did not undergo apoptosis during IM treatment.

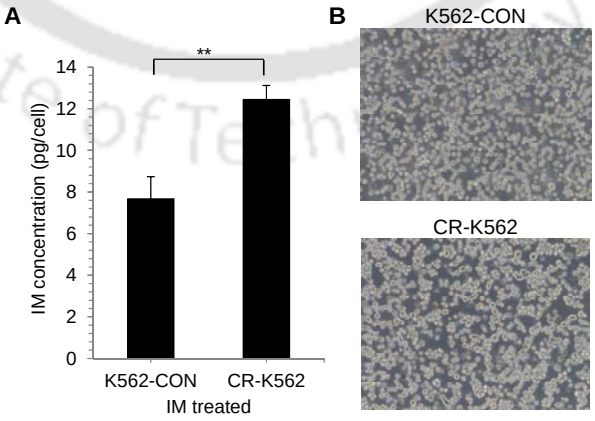

Figure 4.51: Intracellular IM concentration.*(A) Graph showing the intracellular IM concentration of control K562 cells (K562-CON) and chemoresistant K562 cells (CR-K562) cultured with IM for 3 hours.*

Values are mean±SD, n=6. (B) Microscopic picture showing the morphology of K562-CON and CR-K562 cells.

The expression levels of ROS scavenging genes such as CAT, MnSOD which affect the cell survival were determined in control and CR-K562 cells. Interestingly, CAT, MnSOD levels were significantly lower in CR-K562 (Figure 4.52). Similarly, CD47 mRNA expression levels were significantly lower in CR-K562 compared to control K562 levels negating the role of ROS scavenging enzymes in chemoresistance development in K562 cells.

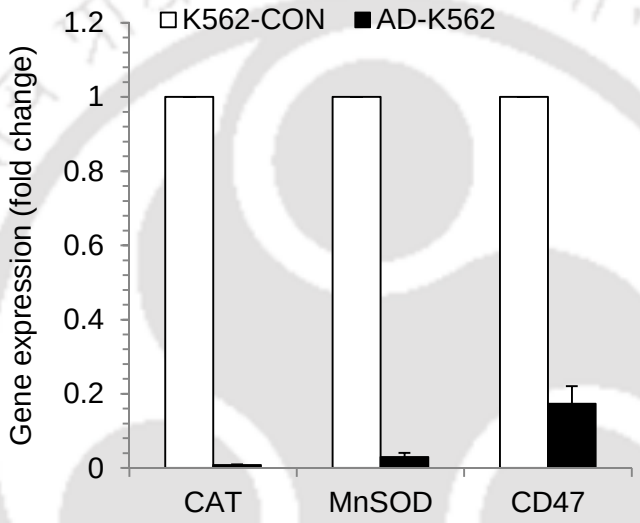

Figure 4.52: *RNA was isolated from control and CR K562 cells and reverse transcribed to produce cDNA. The expression levels of CAT, MnSOD and CD47 were determined by real-time PCR. Values are mean±SE, n=3.*

4.4.3 Phospho ERK, SMAD and STAT3 levels in chemoresistant K562 cells

To identify the signaling pathways that might be aberrantly regulated in CR-K562 cells, the phospho levels of ERK1/2 MAPK, SMAD1/8, STAT3 and STAT5 were determined in control K562 cells, IM treated control and CR-K562 cells. When control K562 were treated with IM for 48 hrs, the phospho levels of ERK1/2 MAPK, SMAD1/8, STAT3 and STAT5 were significantly downregulated (Figure 4.53). However, CR-K562 cells even though continuously cultured in the presence of IM, had phospho ERK1/2 MAPK and SMAD1/8 levels similar to the control K562 cells which were not treated with IM (Figure 4.53). Similar to IM treated K562, the phospho STAT3 and STAT5 levels in CR-K562

were downregulated (Figure 4.53) indicating the inhibition of BCR-ABL mediated STAT3, STAT5 phosphorylation by IM treatment.

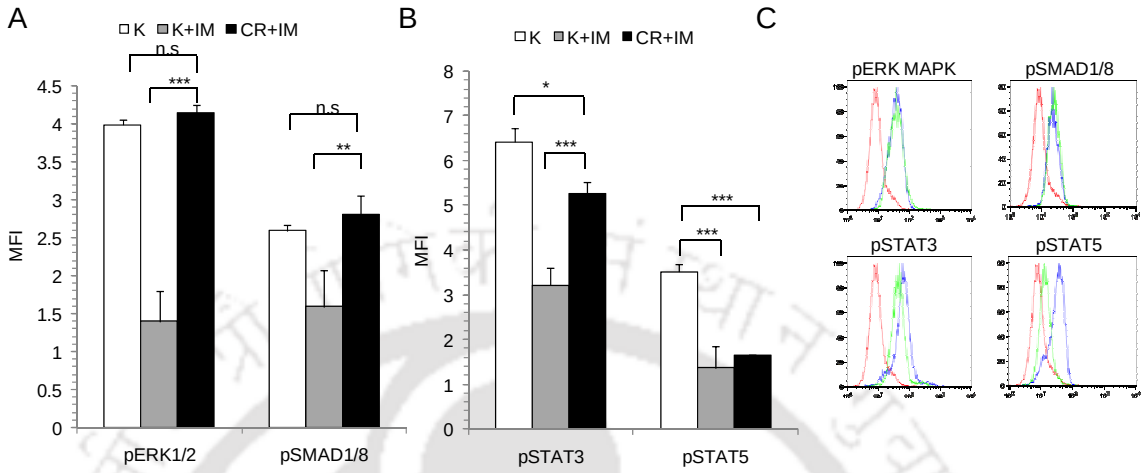

Figure 4.53: Active pathways in chemoresistant K562 CML cells. *(A) The phospho proteins levels of signaling molecules ERK1/2 MAPK, SMAD1/8, STAT3 and STAT5 were analyzed in control K562 cells (K562-CON), K562 cells treated with IM for 48 hours (K562+IM) and chemoresistant K562 cells (CR-K562+IM) cultured in the presence of IM by intracellular staining with phospho specific antibodies. MFI of the stained sample was normalized to MFI of respective isotype control.(B) Representative flow cytometric histogram showing staining for isotype control (redline), K562+IM (green line) and CR-K562+IM (blue line) for different phospho specific antibodies. Values are mean±SD, n=3-6 independent experiments; * p<0.05** p<0.005, *** p<0.0005; n.s-not significant.*

4.4.4 ERK and BMPRI inhibition in chemosensitization of chemoresistant K562 cells

Next we sought to identify a potential treatment strategy to induce cell death in SD-CR-K562 cells which persisted as stroma adherent cells in long-term co-culture, as well as CR-K562 cells which could be maintained in suspension culture in presence of IM. After 5 weeks of co-culture with stroma in presence of IM, SD-CR-K562 were treated with CYD (0.3µg/ml), U0126 (10µM) or LDN 193189 (3µM) alone or in combination with each other, in presence of IM for 2 weeks. Inhibitors were added every 3 days along with IM in fresh media. After 2 weeks the number of remaining adherent K562 cells were counted to check the effect of these inhibitors in clearing off of the persistent CML cells from co-culture system. Interestingly, CYD treatment along with IM significantly reduced the number of SD-CR-K562 cells after 2 weeks. Decrease in cell number was more significant seen when cells were treated with LDN 193189 and U0126 along with IM (Figure 4.54A). Cells in suspension were found to be mostly apoptotic and adherent

cells were mostly viable (95-98%). Similarly in case of C.R.-K562 cells, increase in percentage of apoptosis, similar to that observed in IM treated control K562, was detected when they were treated with IM in combination with LDN 193189 (3µM) and U0126 (10µM) (Figure 4.54B). These results suggest that ERK MPAK, BMP/Smad and actin cytoskeleton inhibitors could be effective in inducing apoptosis in persistent leukemic cells as well as induce apoptosis in chemoresistant CML cells.

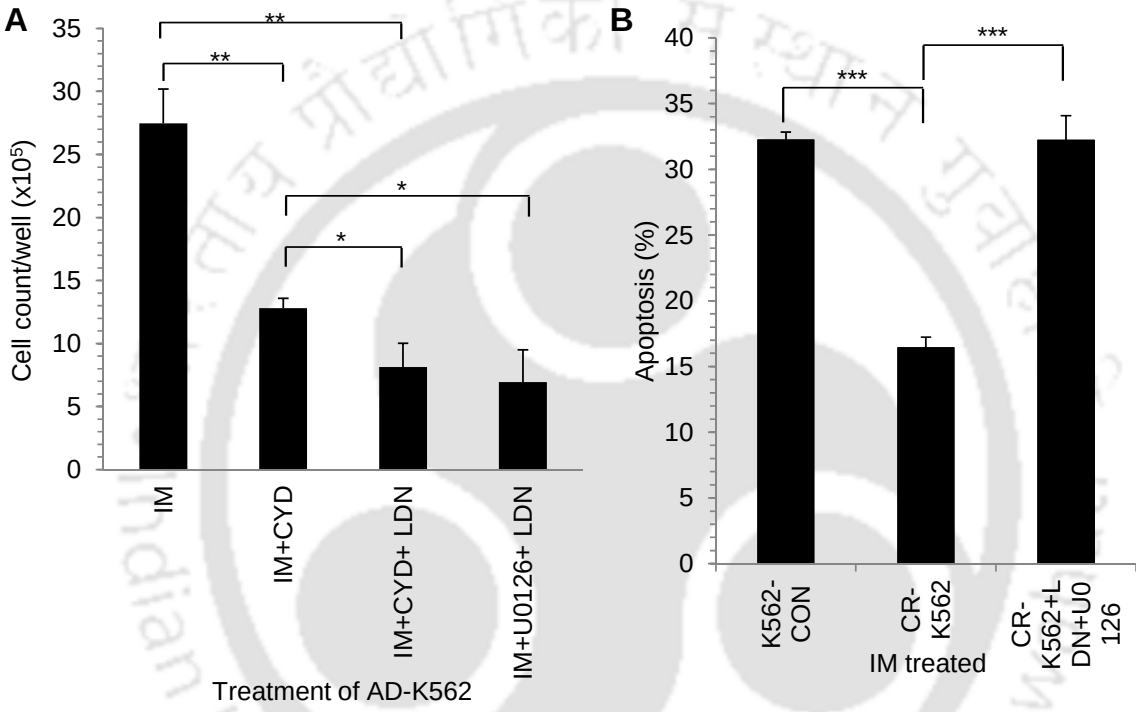

Figure 4.54: Inducing apoptosis in CR-K562.*(A) The long term AD-K562 cells were treated with CYD (0.3µg/ml), LDN (3µM) and U0126 (10µM) for 2 weeks in addition to IM and the viable cell count per well of a 12 well plate, was done by trypan blue exclusion staining for SD-CR-K562 cells. (B) Apoptosis in control (K562-CON), chemoresistant K562 cells (CR-K562) were determined by treating control cells with IM and CR-K562 cells with IM in combination with LDN (3µM) and U0126 (10µM) for 48 hours. Values are mean±SD, n=3; * p<0.05, ** p<0.005, *** p<0.0005.*

Thus, stroma cells offer chemoprotection to adherent CML cells, but in the presence of prolonged IM treatment, stromal cells support the development of chemoresistant cell clones which gained the ability to proliferate in a stroma independent manner in the presence of IM. A combinatorial approach that inhibits BMP and ERK1/2 MAPK pathway is a suitable method to induce apoptosis in these chemoresistant CML cells.

5.0 Discussion

Leukemia is a disorder of the blood cells which results in abnormal production of non-functional cells resulting in BM failure. Even though genetic aberrations such as mutations and translocations initiate the transformation of healthy cells into cancer cells, microenvironment plays an important role in cancer initiation and progression. CML treatment was revolutionized with the advent of TKIs which specifically target the ATP binding site of constitutively active BCR-ABL kinase, which is characteristic of CML cells. However, like other cancers, development of chemoresistance and relapse is a major problem during CML treatment. Apart from mutations in the *BCR-ABL* oncogene, presence of residual CML cells in the BM after chemotherapeutic treatment is a major cause for chemoresistance development in CML patients. Better understanding of the mechanisms of chemoresistance development is required for more efficient targeting of the residual leukemic cells. Therefore in the present study, we investigated the importance of reciprocal interaction between CML cells and stromal cells in chemoresistance development. Furthermore, important signaling pathways that might trigger stroma mediated chemoresistance development were also studied.

5.1 Effect of leukemic cells on the stromal cells

BM stromal cells support and regulate normal and leukemic stem cells by providing signaling cues for maintenance, proliferation, survival, migration, homing and differentiation (Levesque et al., 2010; Lo Celso and Scadden, 2011). BM microenvironment cells have been extensively studied for their role in normal hematopoiesis. Modifications in the stromal cells were reported to disrupt HSC self-renewal, homing and engraftment (Morrison and Scadden, 2014). Leukemic cells were proposed to hijack the normal BM microenvironment and render it more supportive for leukemic cells and less suitable for normal hematopoiesis (Krause and Scadden, 2015).

BM stroma was implicated in leukemia initiation where dysfunctional osteoprogenitor cells or osteoblasts in the mouse BM resulted in deregulation of normal hematopoiesis, leading to MDS which gave further rise to AML (Kode et al., 2014; Kode et al., 2016; Raaijmakers et al., 2010). MSC isolated form hematological malignancies have been

reported to carry functional differences compared to MSC derived healthy individuals (Campioni et al., 2009; Huang et al., 2015). Mutations have also been reported in MSC isolated from patients with hematologic malignancies. MSC from MDS and AML were reported to carry cytogenetic abnormalities which were distinct from those seen in leukemic cells (Blau et al., 2011).MSC derived from CML patients lacked *BCR-ABL* fusion gene (Wohrer et al., 2007). We identified in our study that MSC proliferated at a higher rate when cultured with leukemic cells derived conditioned media suggesting that leukemic cells alter the MSC characteristics which might benefit the proliferation of leukemic cells.

Surface marker expression profile of MSC was reported to be an indicator of their functional characteristics. $CD90^{High}$ MSC isolated from mouse adipose tissue had higher differentiation and reprogramming capability (Kawamoto et al., 2013). MSC isolated from patients with hematologic malignancies expressed low CD90, which was co-related with their reduced immuno-modulatory ability (Campioni et al., 2009). In our study on CML, MSC isolated from CML patients showed reduced CD90 expression which was further confirmed by addition of leukemic cells conditioned media or leukemic cells to the MSC culture. A significant decrease in CD90 cell surface expression as well as transcript levels were seen in MSC cultured with leukemic cells derived conditioned media or in direct co-culture with the leukemic cells. With several reports suggesting the role of CD90 in cancer progression (Kumar et al., 2016), CD90 might be an important molecule to study in detail to understand its importance in leukemia progression and chemoresistance.

In addition to gene expression changes, MSC from hematologic malignancies have been shown to have functional abnormalities such high adipogenic differentiation which was observed in MSC from ALL patients (Lopez et al., 2014). Similarly, in our study we found that although CML-MSC could differentiate into adipocytes and osteocytes, they had significantly decreased osteogenic differentiation potential compared to the control MSC. This was further confirmed by gene expression analysis, where MSC were co-cultured with leukemic cell line K562 and their expression levels of adipogenic gene ADIPOQ and osteogenic gene BSP were determined. There was a significant

downregulation of ADIPOQ and BSP in co-cultured MSC compared to control MSC, which corroborates with their decreased osteogenic differentiation analyzed by functional assays in CML-MSC. As discussed earlier (Kode et al., 2014; Raaijmakers et al., 2010), reduction in osteoblast number in the BM or dysfunctional osteoprogenitor cells are less supportive of normal hematopoiesis. A leukemia induced reduction in differential potential of MSC may result in BM microenvironment which is hostile for normal HSC but conducive to the leukemic cells. Co-cultured MSC also showed reduced expression of death receptors CD95 and tumor necrosis factor receptor 1 (CD120A) but increased transcript levels of TNF-α. These changes observed in MSC might limit autocrine effect of TNF-α on MSC themselves.

5.2 Aberrant signaling pathways in stromal cells during leukemia

Stromal cells in the BM are a major source of cytokines and growth factors. Under normal conditions, these secreted factors maintain regulate HSC self-renewal, differentiation and proliferation. Secreted factors also play an essential role in HSC self-renewal, differentiation and migration. An aberrant expression of cytokines was reported in multiple myeloma and in some cases of lymphoma (Arnulf et al., 2007; Wallace et al., 2001). High levels of pro-survival cytokines were identified in the bone marrow aspirates of cancer patients (Civini et al., 2013; Hodge et al., 2012; Semesiuk et al., 2013). Schmidt et al identified a high expression of angiogenic cytokines such as VEGF, PIGF, IL-6 in the BM of CML mouse model (Schmidt et al., 2011). These cytokines were proposed to play an important role in the progression of leukemia in mice. Similarly, our study found significantly higher levels of *IL-6* mRNA expression in MSC isolated from CML as well as AML patients. Addition of exogenous IL-6 was reported to inhibit adipogenesis whereas no effect was reported in MSC differentiation into osteocytes (Pricola et al., 2009). Although increase in *IL-6* mRNA levels during osteogenesis was found in our study, no significant correlation was observed between the *IL-6* mRNA levels and osteogenic differentiation potential of MSC. High levels of IL-6 along with transforming growth factor-α (TGF-α) were detected in the plasma of CML patients which failed to achieve an early molecular response (Nievergall et al., 2014). Similar results were reported for *BCR-ABL* mouse models where high levels of TNF-α and IL-6 were found in

the BM plasma providing a preferential growth advantage to LSC and resulting in selective growth inhibition of LT-HSC (Zhang et al., 2012a). In the present study, MSC which were co-cultured with K562 CML cells showed increased transcript levels of *TNF-α* and *IL-6*. MSC subjected to co-culture also produced significantly higher levels of secreted IL-6. Schmidt et al reported role of NFκB activation in secretion of inflammatory cytokines by MSC, which was dependent on VLA-4/VCAM-1 interaction (Schmidt et al., 2011). Similarly in our study, an increased phosphorylation of NFκB was identified in MSC co-cultured with CML cells. Thus, the increase in IL-6 levels found in co-cultured MSC might have been due to NFκB activation via cell-cell interaction. However, even though MSC isolated from CML patients are separated from the CML cells and cultured alone, the *IL-6* expression levels remained significantly higher than the control cells, suggesting sustained aberrations in gene expression in MSC isolated from leukemic BM. Our study found that increased IL-6 secretion by MSC after co-culture with CML cells, was brought down to the basal levels by addition of NFκB inhibitor BAY 11-7082 confirming the role of NFκB signaling in CML induced IL-6 secretion by MSC.

Since the present study showed that CML MSC had modified function and gene expression profile, which was further confirmed by co-culture studies, the study utilized CML derived MSC to understand chemoprotection and chemoresistance in CML cells. The conditioned media from CML cells were sufficient to offer chemoprotection from IM induced cell death. When cultured in the presence of MSC derived CM, the CML cells had increased STAT3 phosphorylation. STAT3 signaling offers survival advantage (Nair et al., 2012) and increased phospho STAT3 seen in our study suggests that MSC secreted factors offer a survival advantage to the CML cells. Although high IL-6 levels were seen in CM of CML-MSC, inhibiting IL-6 receptors (secreted and cell surface bound) through the monoclonal antibody tocilizumab even at high concentrations did not provide an additive apoptotic effect to IM. Saini et al reported that the pro-survival effects offered by IL-6 did not depend on IL-6 receptor expression but rather on iNOS pathway (Saini et al., 2014) which might explain the lack of apoptotic effect that was observed when IL-6 receptor was inhibited in CML cells in our study. Additionally, inhibiting NFκB pathway

in MSC using BAY 11-7082 before collecting the conditioned media also did not produce any significant changes in the chemoprotection offered by the stroma derived CM. However, others have shown that STAT3 inhibitor sensitized CML cells to IM induced apoptosis in presence of stromal cell line HS-5 derived CM (Bewry et al., 2008). ERK1/2 activation was also reported to be responsible for FGF2 induced chemoprotection in CML cells (Traer et al., 2014). However we did not see these effects in our study. This might be because of the fact that unlike Bewry et al, we used CML BM derived MSC instead of stromal cell lines and CML-MSC derived CM was used instead of individual growth factors used by Traer et al. However, the mechanism of CM mediated chemoprotection needs to studied in more detail to find out the complex signaling pathways which might be compensatory as well.

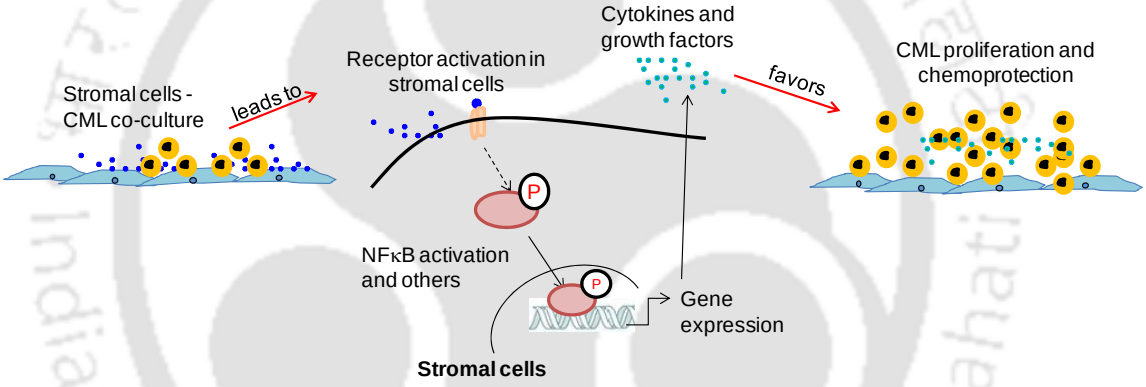

Figure 5.1: *Interaction between leukemic cells and stromal cells resulting in abberatn expression of cytokines and growth factors by the stromal cells that helps in CML proliferation and chemoprotection.*

Thus, interaction of leukemic cells with the stromal cells modifies the stromal cells by activating NFκB and other cytokine producing pathways in stromal cells. These aberrantly produced cytokines and growth factors by the stromal cells might aid in CML cell proliferation and chemoprotection (Figure 5.1).

5.3 Cell-cell interaction for chemoprotection

Stromal cells interact with HSC and LSC via direct cell contact which is an important characteristic of the endosteal niche, where LT-HSC and LSC have been reported to reside in contact with the osteoblasts (Trumpp et al., 2010). This direct interaction between the stromal and the leukemic cells has been hypothesized as a major contributor

in the persistence of LSC in CML patients following TKI treatment (Zhang et al., 2013). In agreement with this hypothesis, in our study, we found that cell-cell contact between CML cells and stromal cells chemoprotected CML cells during IM treatment. We separated the suspension and adherent CML cells during co-culture to study the apoptosis percentage in each fraction. There was no difference in apoptosis percentage between the cells cultured alone or cells in suspension during co-culture. This was also confirmed with the primary samples obtained from CP-CML patients. Although, we found that the CM alone from stromal cells were able to chemo protect, we did not see chemoprotection of CML cells in suspension during co-culture. This suggests that chemoprotective effect of cytokines might be exerted more on the neighboring adherent CML cells. A comparison of chemokine profile of CM derived from MSC, cultured with CML cells in transwell system or direct co-culture system might provide some interesting cues to the lack of chemoprotection in suspension cells. As stated earlier, MSC which were in contact with CML cells showed altered gene expression profile and cell surface receptor expression, which partially prove that MSC underwent changes during co-culture which in turn affected their secreted factors.

However, during co-culture of CML cells with stromal cells, CML cells exist as both suspension and stroma adherent fractions. Hence, it might be possible that the drug availability to the stroma adherent CML cells was less compared to the suspension cells. To check this in detail, the SUS-K562 cells were removed from co-culture before IM treatment. Nevertheless, low apoptosis was observed in AD-K562 cells on IM treatment. In another experiment, AD-K562 cells were transferred to a new stromal layer after IM treatment. Again, in all the conditions tested, when K562 cells were adherent to the stromal cells, there was significantly lower IM induced apoptosis. It is expected that when adherent cells undergo apoptosis, they come out into suspension. In order to analyze the complete apoptosis percentage in adherent cells, suspension cells were discarded before IM treatment and post IM treatment both stroma adherent and suspension cells were collected together and analyzed for apoptosis percentage. The result was further confirmed by detection of active caspase-3 in both adherent and suspension fractions. Thus, our results strongly suggest that cell-cell interaction is absolutely essential for the CML cells to evade drug induced apoptosis.

Although cell-cell interaction was found to be required for chemoprotection, the adherent cells when transferred to a fresh stromal layer again converted into adherent and suspension fractions with similar ratio as seen in the first plating. Our control experiments also negated the role of IM in enhancing adhesion of CML cells to the stromal layer. It was found through our study that the stroma adherent CML cells were not chemoresistant cells, because when the adherent cells were cultured in stroma free culture they became susceptible to apoptosis induction by IM, which was comparable to control cells. This also provides a strategy that if the sroma adherent cells could be brought into suspension at the start of the IM therapy, then majority of the leukemic cells could be eliminated. However, if the leukemic cells remain adherent to stromal cells through the chemo drug treatment in the patients, it might give rise to chemoresistant leukemic cells.

5.4 Characteristics of stroma adherent CML cells

Since adhesion to stromal layer was found to be critical for chemoprotection, we further studied CML cell adhesion to the stromal cells. We studied the cell cycle profile of stroma adherent CML cells and compared it with suspension CML cells. Since TKIs induce cell death in BCR-ABL+ cells by blocking their proliferation, TKIs are not equally effective on non-cycling or quiescent leukemic cells. As reported by others as well (Ramasamy et al., 2007), stroma adherent CML cells were found to be more quiescent compared to suspension CML cells. Leukemic cells have higher levels of intrinsic reactive oxygen species (ROS) and BCR-ABL expression was reported to increase ROS levels in hematopoietic cells (Sattler et al., 2000). Zhang et al reported that stromal cells protected CLL cells from ROS induced cell death by enhancing synthesis of glutathione in primary CLL cells cultured *in vitro* (Zhang et al., 2012b). ROS levels were also reported to regulate HSC maintenance and differentiation (Ludin et al., 2014) and LT-HSC were reported to reside in low oxygenic endosteal niche in the BM which limits ROS levels in LT-HSC and maintain them in undifferentiated state (Jang and Sharkis, 2007). LSC in AML were also characterized by low levels of ROS (Lagadinou et al.). Hence, we analyzed the effect of stromal cells on ROS levels in K562 CML cells. K562 cells had high levels of ROS in suspension culture. However, ROS levels in K562 cells

which were adherent to the stromal cells were significantly lower compared to the suspension cells. These results suggest that the stromal cells might reduce the metabolic stress in the leukemic cells and keep them in a non-cycling quiescent state which protects leukemic cells from drug induced cell death.

Co-culture with stromal cells also altered the cell surface phenotype of K562 cells and of all the markers that were tested, CD49E cell surface expression was downregulated in adherent K562 cells. Kramer et al reported an increase in CD49E expression in *BCR-ABL* transfected murine hematopoietic cells which was associated with higher adhesion to fibronectin and increased proliferation (Kramer et al., 1999). Since the stroma adherent K562 cells were more quiescent than the non-adherent or cells cultured without stromal layer, CD49E downregulation might represent a reduced proliferation or quiescent stem cell like state in CML cells.

Reynaud et al reported that *BCR-ABL* induces IL-6 expression in CML cells and IL-6 secreted by CML cells acts in a paracrine manner to induce CML-MPP cells towards myeloid differentiation (Reynaud et al., 2011). However, in our experiments, we found a significant reduction in *IL-6* transcript levels in K562 during stroma co-culture which further decreased in the adherent K562 cells. Nevertheless, the co-cultured stromal cells had higher *IL-6* transcript and secreted levels which suggest that the increase in IL-6 secretion by stroma might act in a paracrine manner to impact CML cells and CML cells themselves might have reduced their IL-6 secretion through a feedback mechanism when co-cultured with stromal cells. However, the anti-apoptotic gene cIAP2 was upregulated in adherent K562 cells when treated with IM, showing a possible mechanism through which these cells might resist apoptosis during IM treatment.

CXCL-12 acts as a chemo-attractant for HSC and LSC and regulates their homing in the BM. Stromal cells secrete high levels of CXCL-12 in the BM niche. Induction of higher plasma level of CXCL-12 has been employed as an effective method for HSC mobilization from BM to the plasma cells (Hattori et al., 2001). Combination of CXCR-4 anatgonists and IM was proposed as more effective therapy against CML (Beider et al., 2014; Vianello et al., 2010). Jin et al. reported that IM treatment increases surface expression of CXCR4 on CML cells. Increase in CXCR4 expression was accompanied

by increase in migration of CML cell towards stromal layer in a transwell assay (Jin et al., 2008). Adhesion of CD34+ CML cells to stromal cells was also reported to increase in presence of IM (Zhang et al., 2013). However, others have shown that addition of CXCL-12 or CXCR4 antagonist AMD3100 did not have any significant effect on K562 cell adhesion to stromal cells (Zepeda-Moreno et al., 2012). Hence we studied the effect of IM on adhesion of CML cells to the stromal layer. Although IM treatment did not induce the adhesion of CML cells to the stromal cells, we found a significantly high percentage of CD34+ positive population in stromal adherent fraction compared to the suspension cells. In addition, the stroma adherent CML cells also had high percentage of N-Cad positive cells suggesting that leukemic stem cells preferentially adhere to the stromal cells to maintain their self-renewal potential and undifferentiated state.

However, addition of CXCR4 inhibitor AMD 3100 to the cells decreased CML cell adhesion to the stromal cells at high concentrations. Addition of AMD3100 to the co-culture system did not increase IM induced cell death in stroma adherent K562 cells. Our results are contradictory to those reported by Vianello et al, where they added IM and AMD3100 to CML cells in co-culture with MSC and found increased apoptosis (Vianello et al., 2010). Conversely, in our experiments, we removed suspension cells from the co-culture system prior to the treatment with IM and AMD3100 to enable us to analyze effect of CXCR-4 inhibition in the adherent fraction which were the chemoprotected cells during the disease.

Since direct cell-cell interaction seemed to be a major regulator of chemoprotection, we intended to study factors involved in adhesion of CML cells to the stroma. Actin is involved in adhesion of different cell types to extracellular surface and is also involved in integrin related signal transduction (Sonowal et al., 2013). In the present study, disrupting actin polymerization by CYD treatment resulted in significant reduction of K562 cell adhesion to the stromal layer in a dose dependent manner. Pre-treatment of either K562 cells or MSC with CYD resulted in reduced stromal adhesion of K562 cells. Addition of CYD to the already established adherent K562 cells resulted in their detachment from the stromal layer, which then can be effectively killed by IM treatment. Trendowski et al reported that addition of CYD and CYB showed synergistic effect with doxorubicin on

chemoresistant murine leukemia cells (Trendowski et al., 2015). At high concentration of 1µg/ml, CYD alone was sufficient to induce apoptosis of K562 cells whereas at lower concentration of 0.3µg/ml, there was no effect on cell death. Interestingly, when combined with IM, CYD at non-toxic concentration of 0.3µg/ml resulted in increased apoptosis of adherent K562 cells. Actin is regulated in cells by Rho GTPase through ROCK (Amano et al., 2010; Sit and Manser, 2011) and addition of ROCK inhibitor Y27632, similar to CYD reduced adhesion of K562 to stromal cells. Dominant negative RHOA expression also significantly reduced K562 adhesion to stromal cells confirming the role of actin cytoskeleton in cell-cell interaction of CML cells with the stromal cells. As proposed by others, that mobilization of persistent LSC using alternative methods might render them more susceptible to chemotherapeutic agents (Buss et al., 2011; Trumpp et al., 2010), actin cytoskeleton inhibitors at low concentration might be combined with the treatment regime to obtain better outcomes.

5.5 Active signaling pathways in stroma adherent leukemic cells

Constitutively active BCR-ABL tyrosine kinase in the CML cells activates several signaling pathways (refer Introduction section). TKIs function to inhibit BCR-ABL tyrosine kinase activity thereby abrogating its downstream signaling pathways including ERK1/2 MAPK and STAT5 to induce apoptosis in CML cells. Phospho flow cytometric analysis showed that several signaling pathways involving ERK1/2 MAPK, P38 MAPK, NFκB, SMAD1/8, STAT3 and STAT5 were active in K562 cells which were cultured in co-culture system or stroma free culture. However, adherent K562 cells had higher phosphoryated levels of ERK1/2 MAPK and SMAD1/8 signaling molecules showing higher activity of these signaling pathways in adherent CML cells. During IM treatment, however, there was a downregulation in pERK1/2, pSTAT3 and pSTAT5 levels in cells in suspension whereas in adherent K562 cells only pSTAT5 levels were downregulated. Interestingly, pERK1/2 levels were upregulated during IM treatment in adherent K562 cells suggesting the involvement of ERK1/2 MAPK pathway in chemoprotection of adherent CML cells.

Several studies have used small molecule inhibitors to chemosensitize leukemic cells. Jacamo et al reported that NFκB activation in ALL cells induced by the stromal cells via

VLA-4/ VCAM-1 interaction played an important role in chemoresistance against standard chemotherapeutic agents (Jacamo et al., 2014). Similarly, inhibition of Etoposide induced NFκB activation by treatment with NFκB inhibitor BAY 11-7082, rendered K562 cells more sensitive to Etoposide induced apoptosis (Morotti et al., 2006). On the other hand, Schmidt et al reported that CML cells activated NFκB pathway in stromal cells via VLA-4/VCAM-1 interaction, which resulted in higher secretion of proliferative cytokines by the stromal cells (Schmidt et al., 2011). Based on these reports we expected that NFκB inhibition in our experimental set up might be effective in abrogating chemoprotective effect of the stromal cells. However, addition of BAY 11-7082 did not have any additive effect on IM induced apoptosis of control or stroma adherent K562 cells. Furthermore, BAY 11-7082 treatment did not inhibit the adhesion of K562 cells to the stromal layer. This seeming contradiction might be because, NFκB signaling might chemoprotect against standard chemotherapeutic drugs in ALL cells but not TKI induced apoptosis in CML cells which is independent of NFκB signaling. Moreover, unlike Etoposide, IM treatment did not result in NFκB activation in CML cells.

A potential role of ERK1/2 MAPK pathway in chemoresistance of CML was highlighted by other studies as well. Increased pERK1/2 levels were reported in CD34+ CML cells upon IM treatment (Chu et al., 2004). Similarly, induction of FGF2 mediated chemoresistance in K562 cells against IM was also associated with high levels of pERK1/2 (Traer et al., 2014). Furthermore, PlGF secreted by stromal cells activated ERK1/2 signaling in CML cells, which lead to CML disease progression (Schmidt et al., 2011). Besides, BCR-ABL fusion protein is also responsible for activation of ERK1/2 MAPK (Sattler et al., 2002). As mentioned earlier, in our study, IM treatment downregulated phospho ERK1/2 levels in control cells whereas in stroma adherent K562 cells, there was a significant increase in pERK1/2 levels. ERK inhibition by treating the cells with U0126 significantly increased the sensitivity of AD-K562 cells to IM treatment. This coincides with the assertion by other studies that ERK1/2 signaling pathway might be a key mediator in CML chemoresistance to IM and inhibition of ERK signaling might have an important effect in preventing disease progression in CML.

Another signaling pathway that was active in CML cells and was found to be of importance in chemoresistance was BMP/SMAD signaling. Goldman et al reported that BMP signaling was important in embryonic hematopoiesis and for HSC maintenance in adult BM (Goldman et al., 2009). Higher levels of BMP2 and BMP4 in CML BM microenvironment were reported to be responsible for maintenance and expansion of LSC and myeloid progenitors (Laperrousaz et al., 2013). BMP-SMAD signaling are BCR-ABL independent as pSMAD1/8 levels were unaffected by IM treatment in CML cells. BMP signaling inhibitor LDN193189 was used to inhibit BMP-SMAD signaling in the CML cells. LDN193189 treatment reduced adhesion of K562 cells to the stromal layer in a dose dependent manner. To further confirm the role of BMP signaling in CML cell adhesion to the stromal cells, K562 cells were transduced with *BMP4* and *BMP2* genes. BMP2 and BMP4 transduced K562 cells showed significantly higher adhesion to the stromal layer. BMP inhibitor LDN193189 treatment increased the susceptibility of control K562 cells to IM induced cell death. Interestingly, addition of LDN193189 to AD-K562 cells made them significantly more susceptible to IM treatment confirming the important role of BMP-SMAD signaling in stroma mediated chemoresistance.

Thus, our study has shown that actin cytoskeleton, RhoA, ERK1/2 MAPK and BMP-SMAD signaling were involved in chemoprotection of CML cells through interaction with stromal cells. We propose that a combinatorial approach might be a more effective strategy in eradicating chemoresistant CML cells that persist long after IM treatment. To test this in our study, we used different combinations of inhibitors in addition to IM to induce cell death in AD-K562 cells. We found that several combinations of inhibitors such as actin inhibition with BMP inhibition (CYD+LDN193189), ERK inhibition with BMP inhibition (U0126+LDN193189) and ROCK inhibition with BMP inhibition (Y27632/LDN193189) in the presence of IM had maximum effect in inducing cell death in the stroma adherent K562 cells. Although single pathway inhibitors had an additive effect on apoptosis induction by IM treatment, we found that combinatorial approach was more effective.

5.6 Development of chemoresistant CML cells

Several of our experiments have clearly shown the involvement of BCR-ABL independent signaling pathways in chemoprotection of stroma adherent CML cells. It is of great importance to understand if they lead to development of chemoresistance. In addition, the mechanism through which chemoresistance is initiated and attained in CML cells will enable us to inhibit the chemoresistance development in the first place. For this, we developed a system to generate chemoresistant CML cells that might closely resemble the scenario that might happen in the patient. Generally, the chemoresistant cells were generated by exposing the cancer cells to 100 fold lower concentration of the chemotherapeutic drug for a longer period and subsequently increasing the dosage in a step-wise manner (Puissant et al., 2012) or by sustained exposure to low dosage of IM in presence of growth factors (Traer et al., 2014). However, in case of CML patients, they are exposed to a constant therapeutic dosage of IM at regular intervals. So, in our study, a co-culture system was established consisting of stromal cells and K562 cells for a week and IM (10μM) treatment was given every 3 days. The suspension cells obtained in log-term cultures were found to have 90% apoptotic cells. During this period of long term treatment, as expected, several adherent K562 cells underwent apoptosis. However after continuous IM treatment for 3-4 weeks, the remaining few adherent K562 cells started clonally proliferating in the presence of IM which appeared as 3D spheroid structures. Regular analysis of the suspension cells revealed that the non-adherent cells were indeed apoptotic whereas the adherent K562 cells kept proliferating. These adherent chemoresistant K562 cells could be transferred to a new stromal layer without affecting their proliferation in presence of IM as stroma adherent cells. Due to the effect of continuous IM addition, the AD-K562 cell proliferation was also kept in check and AD-K562 cell number remained constant after 5 weeks, mimicking minimal residual disease. This culture could be maintained up to 20 weeks on the same or fresh stromal layer.

On the other hand, earlier experiments with AD-K562 cells showed that actin cytoskeleton, ERK and BMP inhibition had maximum effect in inducing apoptosis of AD-K562 cells. Therefore we sought to find out whether treating the stroma-K562 co-culture system with these pathway inhibitors might abrogate the development of

chemoresistant cells. Surprisingly, when CYD or a combination of U0126 and LDN193189 were added together with IM to the long-term AD-K562 cells, significant reduction was observed in number long term AD-K562 cells which were maintained in presence of IM.

Most interestingly, when these long-term AD-K562 cells, which were proliferating amidst IM treatment, were transferred to a stromal free culture in the presence of IM, continued to proliferate with minimal apoptotic ratio showing signs of acquired chemoresistance. These chemoresistant K562 cells had similar cell cycle profile compared to IM sensitive K562 cells. Surprisingly, the intracellular IM concentration in chemoresistant K562 cells was significantly higher than IM treated K562 control cells, suggesting that the K562 cells had developed BCR-ABL independent chemoresistance. As a possible treatment strategy, these chemoresistant K562 cells were treated with ERK and BMP inhibitors in combination with IM, which significantly increased their apoptosis percentage, which can be taken as a treatment option to inhibit the development of chemoresistance and also to treat chemoresistant CML cells.

5.7 Conclusions and future directions

Thus our study, clearly demonstrates that a reciprocal relationship exists between the leukemic cells and stromal compartment in CML. CML cells modified the stromal cells to secrete increased levels of IL-6 which is mediated by leukemic cells induced NFκB activation in the stromal cells. In addition, the CML associated stroma cells also underwent functional, phenotypic and gene expression changes. A deeper investigation of the leukemia associated stromal cells is required, to identify the targetable altered signaling pathways in the stromal cells to prevent the rise of chemoresistant cells in CML.

Stroma derived secreted factors were sufficient to provide a short-term chemoresistance to the CML cells from the apoptotic effect of IM treatment. Importantly, cell-cell interactions between the CML cells and stromal cells were essential to induce oncogene-independent signaling pathways that contributed to chemoresistance in the stroma adherent CML cells. There adherent chemoresistant cells further developed stroma

independent chemoresistance which can be abrogated by treatment with BMP and ERK inhibitors. BMP and ERK pathway inhibition was sufficient to induce apoptosis in chemoresistant CML cells that did not undergo apoptosis even after accumulating high levels of intracellular IM.

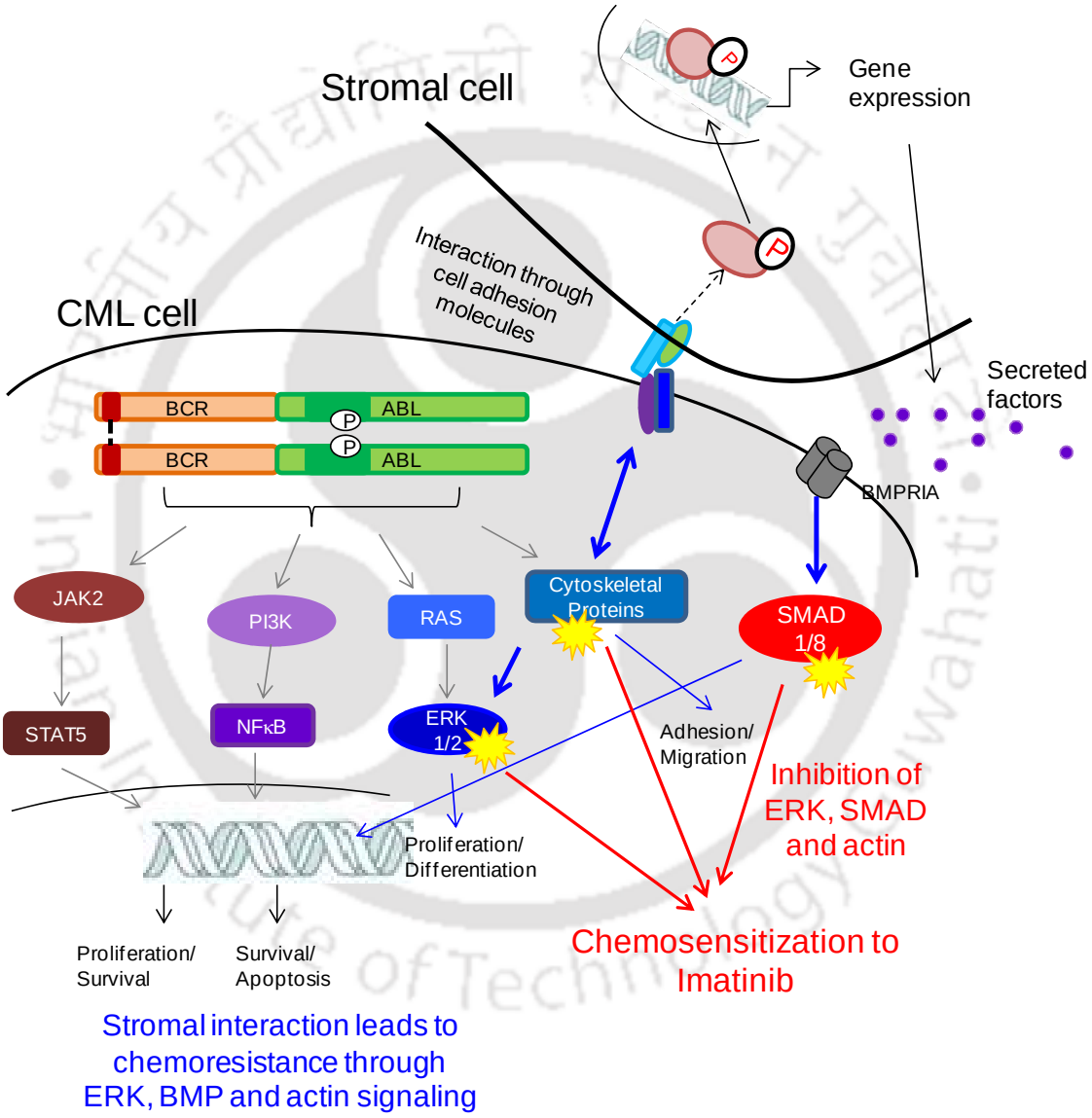

Figure 5.2: Model representing the development of stroma mediated chemoresistance and signaling molecules that could be targeted for therapy.

Future studies could include, testing the mechanism in an *in vivo* model to better develop the therapeutic combinations that will help the CML patients. In addition, *in vivo* model systems will also help us to understand the effect of the treatment on normal HSC and reconstitution of normal hematopoiesis and disease free survival.

6.0 REFERENCES

1. Amano, M., Nakayama, M., and Kaibuchi, K. (2010). Rho-Kinase/ROCK: A Key Regulator of the Cytoskeleton and Cell Polarity. Cytoskeleton 67, 545-554.
2. An, X., Tiwari, A.K., Sun, Y., Ding, P.R., Ashby, C.R., and Chen, Z.S. (2010). BCR-ABL tyrosine kinase inhibitors in the treatment of Philadelphia chromosome positive chronic myeloid leukemia: A review. Leukemia Research 34, 1255-1268.
3. Arnulf, B., Lecourt, S., Soulier, J., Ternaux, B., Lacassagne, M.N., Crinquette, A., Dessoly, J., Sciaini, A.K., Benbunan, M., Chomienne, C., et al. (2007). Phenotypic and functional characterization of bone marrow mesenchymal stem cells derived from patients with multiple myeloma. Leukemia 21, 158-163.
4. Baccarani, M., Cortes, J., Pane, F., Niederwieser, D., Saglio, G., Apperley, J., Cervantes, F., Deininger, M., Gratwohl, A., Guilhot, F., et al. (2009). Chronic Myeloid Leukemia: An Update of Concepts and Management Recommendations of European LeukemiaNet. Journal of Clinical Oncology 27, 6041-6051.
5. Barila, D., and Superti-Furga, G. (1998). An intramolecular SH3-domain interaction regulates c-Abl activity. Nat Genet 18, 280-282.
6. Baskaran, R., Chiang, G.G., Mysliwiec, T., Kruh, G.D., and Wang, J.Y. (1997). Tyrosine phosphorylation of RNA polymerase II carboxyl-terminal domain by the Abl-related gene product. J Biol Chem 272, 18905-18909.
7. Beider, K., Darash-Yahana, M., Blaier, O., Koren-Michowitz, M., Abraham, M., Wald, H., Wald, O., Galun, E., Eizenberg, O., Peled, A., et al. (2014). Combination of Imatinib with CXCR4 Antagonist BKT140 Overcomes the Protective Effect of Stroma and Targets CML In Vitro and In Vivo. Molecular Cancer Therapeutics 13, 1155-1169.
8. Bernardo, M.E., and Fibbe, W.E. (2013). Mesenchymal Stromal Cells: Sensors and Switchers of Inflammation. Cell Stem Cell 13, 392-402.
9. Bewry, N.N., Nair, R.R., Emmons, M.F., Boulware, D., Pinilla-Ibarz, J., and Hazlehurst, L.A. (2008). Stat3 contributes to resistance toward BCR-ABL inhibitors in a bone marrow microenvironment model of drug resistance. Molecular Cancer Therapeutics 7, 3169-3175.
10. Bhardwaj, G., Murdoch, B., Wu, D., Baker, D.P., Williams, K.P., Chadwick, K., Ling, L.E., Karanu, F.N., and Bhatia, M. (2001). Sonic hedgehog induces the proliferation of primitive human hematopoietic cells via BMP regulation. Nature Immunology 2, 172-180.
11. Bitencourt, R., Zalcberg, I., and Louro, I.D. (2011). Imatinib resistance: a review of alternative inhibitors in chronic myeloid leukemia. Rev Bras Hematol Hemoter 33, 470-475.

12. Blau, O., Baldus, C.D., Hofmann, W.K., Thiel, G., Nolte, F., Burmeister, T., Turkmen, S., Benlasfer, O., Schumann, E., Sindram, A., et al. (2011). Mesenchymal stromal cells of myelodysplastic syndrome and acute myeloid leukemia patients have distinct genetic abnormalities compared with leukemic blasts. Blood 118, 5583-5592.
13. Bonnet, D., and Dick, J.E. (1997). Human acute myeloid leukemia is organized as a hierarchy that originates from a primitive hematopoietic cell. Nature Medicine 3, 730-737.
14. Bourgne, C., Bamdad, M., Janel, A., Libert, F., Gagnieu, M.C., Rapatel, C., Pigeon, P., Pereira, S., Hermet, E., Guerci, A., et al. (2012). Measurement of imatinib uptake by flow cytometry. Cytometry Part A 81A, 996-1004.
15. Buss, E.C., Kalinkovich, S., Schajnovitz, A., Kollet, O., Dar, A., Tesio, M., Fruehauf, S., Hotfilder, M., Shultz, L.D., Ho, A.D., et al. (2011). Mobilization mechanisms of human primary precursor-B-ALL cells in an in vivo model system by the CXCR4-antagonist AMD3100 and by catecholamines. Onkologie 34, 244-244.
16. Calvi, L.M., Adams, G.B., Weibrecht, K.W., Weber, J.M., Olson, D.P., Knight, M.C., Martin, R.P., Schipani, E., Divieti, P., Bringhurst, F.R., et al. (2003). Osteoblastic cells regulate the haematopoietic stem cell niche. Nature 425, 841-846.
17. Campioni, D., Rizzo, R., Stignani, M., Melchiorri, L., Ferrari, L., Moretti, S., Russo, A., Bagnara, G.P., Bonsi, L., Alviano, F., et al. (2009). A Decreased Positivity for CD90 on Human Mesenchymal Stromal Cells (MSCs) Is Associated with a Loss of Immunosuppressive Activity by MSCs. Cytometry Part B-Clinical Cytometry 76B, 225-230.
18. Caplan, A.I., and Bruder, S.P. (2001). Mesenchymal stem cells: building blocks for molecular medicine in the 21st century. Trends in Molecular Medicine 7, 259-264.
19. Carlesso, N., Frank, D.A., and Griffin, J.D. (1995). Tyrosyl phosphorylation and DNA binding activity of STAT proteins in hematopoietic cells transformed by p210 BCR/ABL. Blood 86, 1042-1042.
20. Carlesso, N., Frank, D.A., and Griffin, J.D. (1996). Tyrosyl phosphorylation and DNA binding activity of signal transducers and activators of transcription (STAT) proteins in hematopoietic cell lines transformed by Bcr/Abl. Journal of Experimental Medicine 183, 811-820.
21. Chai, S.K., Nichols, G.L., and Rothman, P. (1997). Constitutive activation of JAKs and STATs in BCR-Abl-expressing cell lines and peripheral blood cells derived from leukemic patients. Journal of Immunology 159, 4720-4728.
22. Challen, G.A., Boles, N.C., Chambers, S.M., and Goodell, M.A. (2010). Distinct Hematopoietic Stem Cell Subtypes Are Differentially Regulated by TGF-beta 1. Cell Stem Cell 6, 265-278.
23. Chu, S., Holtz, M., Gupta, M., and Bhatia, R. (2004). BCR/ABL kinase inhibition by imatinib mesylate enhances MAP kinase activity in chronic myelogenous leukemia CD34(+) cells. Blood 103, 3167-3174.

24. Civini, S., Jin, P., Ren, J.Q., Sabatino, M., Castiello, L., Jin, J.J., Wang, H., Zhao, Y.L., Marincola, F., and Stroncek, D. (2013). Leukemia cells induce changes in human bone marrow stromal cells. Journal of Translational Medicine 11.
25. Daley, G.Q., Vanetten, R.A., and Baltimore, D. (1990). Induction of Chronic Myelogenous Leukemia in Mice by the P210bcr/Abl Gene of the Philadelphia-Chromosome. Science 247, 824-830.
26. Damiano, J.S., Hazlehurst, L.A., and Dalton, W.S. (2001). Cell adhesion-mediated drug resistance (CAM-DR) protects the K562 chronic myelogenous leukemia cell line from apoptosis induced by BCR/ABL inhibition, cytotoxic drugs, and gamma-irradiation. Leukemia 15, 1232-1239.
27. Deininger, M.W., Goldman, J.M., and Melo, J.V. (2000). The molecular biology of chronic myeloid leukemia. Blood 96, 3343-3356.
28. Diekmann, D., Brill, S., Garrett, M.D., Totty, N., Hsuan, J., Monfries, C., Hall, C., Lim, L., and Hall, A. (1991). Bcr Encodes a Gtpase-Activating Protein for P21rac. Nature 351, 400-402.
29. Dillmann, F., Veldwijk, M.R., Laufs, S., Sperandio, M., Calandra, G., Wenz, F., Zeller, W.J., and Fruehauf, S. (2009). Plerixafor inhibits chemotaxis toward SDF-1 and CXCR4-mediated stroma contact in a dose-dependent manner resulting in increased susceptibility of BCR-ABL(+) cell to Imatinib and Nilotinib. Leukemia & Lymphoma 50, 1676-1686.
30. Ding, L., Saunders, T.L., Enikolopov, G., and Morrison, S.J. (2012). Endothelial and perivascular cells maintain haematopoietic stem cells. Nature 481, 457-U465.
31. Druker, B.J. (2008). Translation of the Philadelphia chromosome into therapy for CML. Blood 112, 4808-4817.
32. Druker, B.J., Guilhot, F., O'Brien, S.G., Gathmann, I., Kantarjian, H., Gattermann, N., Deininger, M.W.N., Silver, R.T., Goldman, J.M., Stone, R.M., et al. (2006). Five-year follow-up of patients receiving imatinib for chronic myeloid leukemia. New England Journal of Medicine 355, 2408-2417.
33. Druker, B.J., Tamura, S., Buchdunger, E., Ohno, S., Segal, G.M., Fanning, S., Zimmermann, J., and Lydon, N.B. (1996). Effects of a selective inhibitor of the Abl tyrosine kinase on the growth of Bcr-Abl positive cells. Nat Med 2, 561-566.
34. Duhrsen, U., and Hossfeld, D.K. (1996). Stromal abnormalities in neoplastic bone marrow diseases. Annals of Hematology 73, 53-70.
35. Duncan, A.W., Rattis, F.M., DiMascio, L.N., Congdon, K.L., Pazianos, G., Zhao, C., Yoon, K., Cook, J.M., Willert, K., Gaiano, N., et al. (2005). Integration of Notch and Wnt signaling in hematopoietic stem cell maintenance. Nature Immunology 6, 314-322.
36. Duyster, J., Baskaran, R., and Wang, J.Y. (1995). Src homology 2 domain as a specificity determinant in the c-Abl-mediated tyrosine phosphorylation of the RNA

polymerase II carboxyl-terminal repeated domain. Proc Natl Acad Sci U S A 92, 1555-1559.

37. Eiring, A.M., Khorashad, J.S., Anderson, D.J., Yu, F., Redwine, H.M., Mason, C.C., Reynolds, K.R., Clair, P.M., Gantz, K.C., Zhang, T.Y., et al. (2015). beta-Catenin is required for intrinsic but not extrinsic BCR-ABL1 kinase-independent resistance to tyrosine kinase inhibitors in chronic myeloid leukemia. Leukemia 29, 2328-2337.
38. Etet, P.F.S., Vecchio, L., and Kamdje, A.H.N. (2012). Signaling pathways in chronic myeloid leukemia and leukemic stem cell maintenance: Key role of stromal microenvironment. Cellular Signalling 24, 1883-1888.
39. Fabbro, D. (2012). Bcr-Abl Signaling a New Status in Cml. Nature Chemical Biology 8, 228-229.
40. Fang, Z.H., Dong, C.L., Chen, Z., Zhou, B., Liu, N., Lan, H.F., Liang, L., Liao, W.B., Zhang, L., and Han, Z.C. (2009). Transcriptional regulation of survivin by c-Myc in BCR/ABL-transformed cells: implications in anti-leukaemic strategy. Journal of Cellular and Molecular Medicine 13, 2039-2052.
41. Fleming, H.E., Janzen, V., Lo Celso, C., Guo, J., Leahy, K.M., Kronenberg, H.M., and Scadden, D.T. (2008). Wnt signaling in the niche enforces hematopoietic stem cell quiescence and is necessary to preserve self-renewal in vivo. Cell Stem Cell 2, 274-283.
42. Fliedner, T.M., Graessle, D., Paulsen, C., and Reimers, K. (2002). Structure and function of bone marrow hemopoiesis: Mechanisms of response to ionizing radiation exposure. Cancer Biotherapy and Radiopharmaceuticals 17, 405-426.
43. Frank, D.A., and Varticovski, L. (1996). BCR/abl leads to the constitutive activation of Stat proteins, and shares an epitope with tyrosine phosphorylated Stats. Leukemia 10, 1724-1730.
44. Friedenstein, A.J., Chailakhyan, R.K., and Gerasimov, U.V. (1987). Bone marrow osteogenic stem cells: in vitro cultivation and transplantation in diffusion chambers. Cell Tissue Kinet 20, 263-272.
45. Gambacorti-Passerini, C.B., Gunby, R.H., Piazza, R., Galietta, A., Rostagno, R., and Scapozza, L. (2003). Molecular mechanisms of resistance to imatinib in Philadelphia-chromosome-positive leukaemias. Lancet Oncol 4, 75-85.
46. Geay, J.F., Buet, D., Zhang, Y., Foudi, A., Jarrier, P., Berthebaud, M., Turhan, A.G., Vainchenker, W., and Louache, F. (2005). p210BCR-ABL inhibits SDF-1 chemotactic response via alteration of CXCR4 signaling and down-regulation of CXCR4 expression. Cancer Res 65, 2676-2683.
47. Gesbert, F., and Griffin, J.D. (2000). Bcr/Abl activates transcription of the Bcl-X gene through STAT5. Blood 96, 2269-2276.
48. Giacca, M., and Zacchigna, S. (2012). VEGF gene therapy: therapeutic angiogenesis in the clinic and beyond. Gene Ther 19, 622-629.

49. Gilliland, D.G., and Griffin, J.D. (2002). The roles of FLT3 in hematopoiesis and leukemia. Blood 100, 1532-1542.
50. Goldman, D.C., Bailey, A.S., Pfaffle, D.L., Al Masri, A., Christian, J.L., and Fleming, W.H. (2009). BMP4 regulates the hematopoietic stem cell niche. Blood 114, 4393-4401.
51. Gorre, M.E., Mohammed, M., Ellwood, K., Hsu, N., Paquette, R., Rao, P.N., and Sawyers, C.L. (2001). Clinical resistance to STI-571 cancer therapy caused by BCR-ABL gene mutation or amplification. Science 293, 876-880.
52. Gotoh, A., Miyazawa, K., Ohyashiki, K., Tauchi, T., Boswell, H.S., Broxmeyer, H.E., and Toyama, K. (1995). Tyrosine Phosphorylation and Activation of Focal Adhesion Kinase (P125(Fak)) by Bcr-Abl Oncoprotein. Experimental Hematology 23, 1153-1159.
53. Greenbaum, A., Hsu, Y.M.S., Day, R.B., Schuettpelz, L.G., Christopher, M.J., Borgerding, J.N., Nagasawa, T., and Link, D.C. (2013). CXCL12 in early mesenchymal progenitors is. required for haematopoietic stem-cell maintenance. Nature 495, 227-230.
54. Groffen, J., Stephenson, J.R., Heisterkamp, N., Deklein, A., Bartram, C.R., and Grosveld, G. (1984). Philadelphia Chromosomal Breakpoints Are Clustered within a Limited Region, Bcr, on Chromosome-22. Cell 36, 93-99.
55. Hantschel, O., Warsch, W., Eckelhart, E., Kaupe, I., Grebien, F., Wagner, K.U., Superti-Furga, G., and Sexl, V. (2012). BCR-ABL uncouples canonical JAK2-STAT5 signaling in chronic myeloid leukemia. Nature Chemical Biology 8, 285-293.
56. Hass, R., Kasper, C., Bohm, S., and Jacobs, R. (2011). Different populations and sources of human mesenchymal stem cells (MSC): A comparison of adult and neonatal tissue-derived MSC. Cell Communication and Signaling 9.
57. Hattori, K., Heissig, B., Tashiro, K., Honjo, T., Tateno, M., Shieh, J.H., Hackett, N.R., Quitoriano, M.S., Crystal, R.G., Rafii, S., et al. (2001). Plasma elevation of stromal cell-derived factor-1 induces mobilization of mature and immature hematopoietic progenitor and stem cells. Blood 97, 3354-3360.
58. Haug, J.S., He, X.C., Grindley, J.C., Wunderlich, J.P., Gaudenz, K., Ross, J.T., Paulson, A., Wagner, K.P., Xie, Y.C., Zhu, R.H., et al. (2008). N-cadherin expression level distinguishes reserved versus primed states of hematopoietic stem cells. Cell Stem Cell 2, 367-379.
59. Heisterkamp, N., Stephenson, J.R., Groffen, J., Hansen, P.F., de Klein, A., Bartram, C.R., and Grosveld, G. (1983). Localization of the c-ab1 oncogene adjacent to a translocation break point in chronic myelocytic leukaemia. Nature 306, 239-242.
60. Hellqvist, E., Holm, F., Mason, C.N., Runza, V., Weigand, S., Sadarangani, A., and Jamieson, C.H.M. (2013). CD44 Monoclonal Antibody-Enhanced Clearance Of Chronic Myeloid Leukemia Stem Cells From The Malignant Niche. Blood 122.

61. Hirano, T., Taga, T., Matsuda, T., Hibi, M., Suematsu, S., Tang, B., Murakami, M., and Kishimoto, T. (1990). Interleukin-6 and Its Receptor in the Immune-Response and Hematopoiesis. International Journal of Cell Cloning 8, 155-167.
62. Hodge, L.S., Ziesmer, S.C., Yang, Z.Z., Secreto, F.J., Gertz, M.A., Novak, A.J., and Ansell, S.M. (2012). IL-21 in the bone marrow microenvironment contributes to IgM secretion and proliferation of malignant cells in Waldenstrom macroglobulinemia. Blood 120, 3774-3782.
63. Huang, J.C., Basu, S.K., Zhao, X., Chien, S., Fang, M., Oehler, V.G., Appelbaum, F.R., and Becker, P.S. (2015). Mesenchymal stromal cells derived from acute myeloid leukemia bone marrow exhibit aberrant cytogenetics and cytokine elaboration. Blood Cancer Journal 5.
64. Hunter, T. (2007). Treatment for chronic myelogenous leukemia: the long road to imatinib. Journal of Clinical Investigation 117, 2036-2043.
65. Ilaria, R.L., and VanEtten, R.A. (1996). P210 and P190(BCR/ABL) induce the tyrosine phosphorylation and DNA binding activity of multiple specific STAT family members. Journal of Biological Chemistry 271, 31704-31710.
66. Jacamo, R., Chen, Y., Wang, Z.Q., Ma, W.C., Zhang, M., Spaeth, E.L., Wang, Y., Battula, V.L., Mak, P.Y., Schallmoser, K., et al. (2014). Reciprocal leukemia-stroma VCAM-1/VLA-4-dependent activation of NF-kappa B mediates chemoresistance. Blood 123, 2691-2702.
67. Jaganathan, B.G., Anjos-Afonso, F., Kumar, A., and Bonnet, D. (2013). Active RHOA favors retention of human hematopoietic stem/progenitor cells in their niche. Journal of Biomedical Science 20.
68. Jaganathan, B.G., Ruester, B., Dressel, L., Stein, S., Grez, M., Seifried, E., and Henschler, R. (2007). Rho inhibition induces migration of mesenchymal stromal cells. Stem Cells 25, 1966-1974.
69. Jang, Y.Y., and Sharkis, S.J. (2007). A low level of reactive oxygen species selects for primitive hematopoietic stem cells that may reside in the low-oxygenic niche. Blood 110, 3056-3063.
70. Jiang, X.Y., Lopez, A., Holyoake, T., Eaves, A., and Eaves, C. (1999). Autocrine production and action of IL-3 and granulocyte colony-stimulating factor in chronic myeloid leukemia. Proceedings of the National Academy of Sciences of the United States of America 96, 12804-12809.
71. Jin, L., Tabe, Y., Konoplev, S., Xu, Y., Leysath, C.E., Lu, H., Kimura, S., Ohsaka, A., Rios, M.B., Calvert, L., et al. (2008). CXCR4 up-regulation by imatinib induces chronic myelogenous leukemia (CML) cell migration to bone marrow stroma and promotes survival of quiescent CML cells. Mol Cancer Ther 7, 48-58.
72. Kantarjian, H.M., Giles, F., Quintas-Cardama, A., and Cortes, J. (2007). Important therapeutic targets in chronic myelogenous leukemia. Clin Cancer Res 13, 1089-1097.

73. Kawamoto, K., Konno, M., Nagano, H., Nishikawa, S., Tomimaru, Y., Akita, H., Hama, N., Wada, H., Kobayashi, S., Eguchi, H., et al. (2013). CD90-(Thy-1-) High Selection Enhances Reprogramming Capacity of Murine Adipose-Derived Mesenchymal Stem Cells. Disease Markers, 573-579.
74. Khurana, S., Melacarne, A., Yadak, R., Schouteden, S., Notelaers, T., Pistoni, M., Maes, C., and Verfaillie, C.M. (2014). SMAD Signaling Regulates CXCL12 Expression in the Bone Marrow Niche, Affecting Homing and Mobilization of Hematopoietic Progenitors. Stem Cells 32, 3012-3022.
75. Kode, A., Manavalan, J.S., Mosialou, I., Bhagat, G., Rathinam, C.V., Luo, N., Khiabanian, H., Lee, A., Murty, V.V., Friedman, R., et al. (2014). Leukaemogenesis induced by an activating beta-catenin mutation in osteoblasts. Nature 506, 240-+.
76. Kode, A., Mosialou, I., Manavalan, S.J., Rathinam, C.V., Friedman, R.A., Teruya-Feldstein, J., Bhagat, G., Berman, E., and Kousteni, S. (2016). FoxO1-dependent induction of acute myeloid leukemia by osteoblasts in mice. Leukemia 30, 1-13.
77. Kolibaba, K.S., Bhat, A., Heaney, C., Oda, T., and Druker, B.J. (1999). CRKL binding to BCR-ABL and BCR-ABL transformation. Leukemia & Lymphoma 33, 119-126.
78. Kollet, O., Dar, A., Shivtiel, S., Kalinkovich, A., Lapid, K., Sztainberg, Y., Tesio, M., Samstein, R.M., Goichberg, P., Spiegel, A., et al. (2006). Osteoclasts degrade endosteal components and promote mobilization of hematopoietic progenitor cells. Nature Medicine 12, 657-664.
79. Konopka, J.B., Watanabe, S.M., and Witte, O.N. (1984). An Alteration of the Human C-Abl Protein in K562 Leukemia-Cells Unmasks Associated Tyrosine Kinase-Activity. Cell 37, 1035-1042.
80. Kramer, A., Horner, S., Willer, A., Fruehauf, S., Hochhaus, A., Hallek, M., and Hehlmann, R. (1999a). Adhesion to fibronectin stimulates proliferation of wild-type and bcr/abl-transfected murine hematopoietic cells. Proc Natl Acad Sci U S A 96, 2087-2092.
81. Kramer, A., Horner, S., Willer, A., Fruehauf, S., Hochhaus, A., Hallek, M., and Hehlmann, R. (1999b). Adhesion to fibronectin stimulates proliferation of wild-type and bcr/abl-transfected murine hematopoietic cells. Proceedings of the National Academy of Sciences of the United States of America 96, 2087-2092.
82. Krause, D.S., Lazarides, K., Lewis, J.B., von Andrian, U.H., and Van Etten, R.A. (2014). Selectins and their ligands are required for homing and engraftment of BCR-ABL1(+) leukemic stem cells in the bone marrow niche. Blood 123, 1361-1371.
83. Krause, D.S., Lazarides, K., von Andrian, U.H., and Van Etten, R.A. (2006). Requirement for CD44 in homing and engraftment of BCR-ABL-expressing leukemic stem cells. Nature Medicine 12, 1175-1180.
84. Krause, D.S., and Scadden, D.T. (2015). A hostel for the hostile: the bone marrow niche in hematologic neoplasms. Haematologica 100, 1376-1387.

85. Kumar, A., Bhanja, A., Bhattacharyya, J., and Jaganathan, B.G. (2016). Multiple roles of CD90 in cancer. Tumour Biol.
86. Kurzrock, R., Kantarjian, H.M., Druker, B.J., and Talpaz, M. (2003). Philadelphia chromosome-positive leukemias: From basic mechanisms to molecular therapeutics. Annals of Internal Medicine 138, 819-830.
87. Lagadinou, E.D., Sach, A., Callahan, K., Rossi, R.M., Neering, S.J., Minhajuddin, M., Ashton, J.M., Pei, S., Grose, V., O'Dwyer, K.M., et al. (2013). BCL-2 inhibition targets oxidative phosphorylation and selectively eradicates quiescent human leukemia stem cells. Cell Stem Cell 12, 329-341.
88. Laperrousaz, B., Jeanpierre, S., Sagorny, K., Voeltzel, T., Ramas, S., Kaniewski, B., Ffrench, M., Salesse, S., Nicolini, F.E., and Maguer-Satta, V. (2013). Primitive CML cell expansion relies on abnormal levels of BMPs provided by the niche and on BMPRIb overexpression. Blood 122, 3767-3777.
89. Lapidot, T., Sirard, C., Vormoor, J., Murdoch, B., Hoang, T., Caceres cortes, J., Minden, M., Paterson, B., Caligiuri, M.A., and Dick, J.E. (1994). A Cell Initiating Human Acute Myeloid-Leukemia after Transplantation into Scid Mice. Nature 367, 645-648.
90. Larsson, J., and Karlsson, S. (2005). The role of Smad signaling in hematopoiesis. Oncogene 24, 5676-5692.
91. Laurent, E., Talpaz, M., Kantarjian, H., and Kurzrock, R. (2001). The BCR gene and philadelphia chromosome-positive leukemogenesis. Cancer Res 61, 2343-2355.
92. Lee, J.W., Fang, X., Krasnodembskaya, A., Howard, J.P., and Matthay, M.A. (2011). Concise review: Mesenchymal stem cells for acute lung injury: role of paracrine soluble factors. Stem Cells 29, 913-919.
93. Levesque, J.P., Helwani, F.M., and Winkler, I.G. (2010). The endosteal 'osteoblastic' niche and its role in hematopoietic stem cell homing and mobilization. Leukemia 24, 1979-1992.
94. Lo Celso, C., and Scadden, D.T. (2011). The haematopoietic stem cell niche at a glance. Journal of Cell Science 124, 3529-3535.
95. Lopez, A.V., Garcia, M.N.V., Melen, G.J., Martinez, A.E., Moreno, I.C., Garcia-Castro, J., Orellana, M.R., and Gonzalez, A.G.Z. (2014). Mesenchymal Stromal Cells Derived from the Bone Marrow of Acute Lymphoblastic Leukemia Patients Show Altered BMP4 Production: Correlations with the Course of Disease. Plos One 9.
96. Ludin, A., Gur-Cohen, S., Golan, K., Kaufmann, K.B., Itkin, T., Medaglia, C., Lu, X.J., Ledergor, G., Kollet, O., and Lapidot, T. (2014). Reactive Oxygen Species Regulate Hematopoietic Stem Cell Self-Renewal, Migration and Development, As Well As Their Bone Marrow Microenvironment. Antioxidants & Redox Signaling 21, 1605-1619.
97. Luis, T.C., Weerkamp, F., Naber, B.A.E., Baert, M.R.M., de Haas, E.F.E., Nikolic, T., Heuvelmans, S., De Krijger, R.R., van Dongen, J.J.M., and Staal, F.J.T. (2009).

Wnt3a deficiency irreversibly impairs hematopoietic stem cell self-renewal and leads to defects in progenitor cell differentiation. Blood 113, 546-554.

98. Lukasova, E., Kozubek, S., Kozubek, M., Kjeronska, J., Ryznar, L., Horakova, J., Krahulcova, E., and Horneck, G. (1997). Localisation and distance between ABL and BCR genes in interphase nuclei of bone marrow cells of control donors and patients with chronic myeloid leukaemia. Human Genetics 100, 525-535.
99. Lydon, N. (2009). Attacking cancer at its foundation. Nature Medicine 15, 1153-1157.
100. Ma, S., Xie, N., Li, W., Yuan, B., Shi, Y., and Wang, Y. (2013). Immunobiology of mesenchymal stem cells. Cell Death Differ 21, 216-225.
101. Mancini, S.J.C., Mantei, N., Dumortier, A., Suter, U., MacDonald, H.R., and Radtke, F. (2005). Jagged1-dependent Notch signaling is dispensable for hematopoietic stem cell self-renewal and differentiation. Blood 105, 2340-2342.
102. Mansour, A., Abou-Ezzi, G., Sitnicka, E., Jacobsen, S.E.W., Wakkach, A., and Blin-Wakkach, C. (2012). Osteoclasts promote the formation of hematopoietic stem cell niches in the bone marrow. Journal of Experimental Medicine 209, 537-549.
103. Maru, Y. (2012). Molecular biology of chronic myeloid leukemia. Cancer Science 103, 1601-1610.
104. Mayer, B.J., Hirai, H., and Sakai, R. (1995). Evidence that SH2 domains promote processive phosphorylation by protein-tyrosine kinases. Curr Biol 5, 296-305.
105. Mayer, I.A., Verma, A., Grumbach, I.M., Uddin, S., Lekmine, F., Ravandi, F., Majchrzak, B., Fujita, S., Fish, E.N., and Platanias, L.C. (2001). The p38 MAPK pathway mediates the growth inhibitory effects of interferon-alpha in BCR-ABL-expressing cells. Journal of Biological Chemistry 276, 28570-28577.
106. Mcwhirter, J.R., Galasso, D.L., and Wang, J.Y.J. (1993). A Coiled-Coil Oligomerization Domain of Bcr Is Essential for the Transforming Function of Bcr-Abl Oncoproteins. Molecular and Cellular Biology 13, 7587-7595.
107. Mendez-Ferrer, S., Lucas, D., Battista, M., and Frenette, P.S. (2008). Haematopoietic stem cell release is regulated by circadian oscillations. Nature 452, 442-U444.
108. Mendez-Ferrer, S., Michurina, T.V., Ferraro, F., Mazloom, A.R., MacArthur, B.D., Lira, S.A., Scadden, D.T., Ma'ayan, A., Enikolopov, G.N., and Frenette, P.S. (2010). Mesenchymal and haematopoietic stem cells form a unique bone marrow niche. Nature 466, 829-U859.
109. Mishima, S., Nagai, A., Abdullah, S., Matsuda, C., Taketani, T., Kumakura, S., Shibata, H., Ishikura, H., Kim, S.U., and Masuda, J. (2010). Effective ex vivo expansion of hematopoietic stem cells using osteoblast-differentiated mesenchymal stem cells is CXCL12 dependent. European Journal of Haematology 84, 538-546.
110. Morotti, A., Cilloni, D., Pautasso, M., Messa, F., Arruga, F., Defilippi, I., Carturan, S., Catalano, R., Rosso, V., Chiarenza, A., et al. (2006). NF-kB inhibition

as a strategy to enhance etoposide-induced apoptosis in K562 cell line. American Journal of Hematology 81, 938-945.

111. Morrison, S.J., and Scadden, D.T. (2014). The bone marrow niche for haematopoietic stem cells. Nature 505, 327-334.

112. Muller, A.J., Pendergast, A.M., Havlik, M.H., Puil, L., Pawson, T., and Witte, O.N. (1992). A Limited Set of Sh2 Domains Binds Bcr through a High-Affinity Phosphotyrosine-Independent Interaction. Molecular and Cellular Biology 12, 5087-5093.

113. Nagar, B., Hantschel, O., Young, M.A., Scheffzek, K., Veach, D., Bornmann, W., Clarkson, B., Superti-Furga, G., and Kuriyan, J. (2003). Structural basis for the autoinhibition of c-Abl tyrosine kinase. Cell 112, 859-871.

114. Nair, R.R., Tolentino, J.H., and Hazlehurst, L.A. (2012). Role of STAT3 in Transformation and Drug Resistance in CML. Front Oncol 2, 30.

115. Nakamura, Y., Arai, F., Iwasaki, H., Hosokawa, K., Kobayashi, I., Gomei, Y., Matsumoto, Y., Yoshihara, H., and Suda, T. (2010). Isolation and characterization of endosteal niche cell populations that regulate hematopoietic stem cells. Blood 116, 1422-1432.

116. Neshat, M.S., Raitano, A.B., Wang, H.G., Reed, J.C., and Sawyers, C.L. (2000). The survival function of the Bcr-Abl oncogene is mediated by Bad-dependent and -independent pathways: Roles for phosphatidylinositol 3-kinase and Raf. Molecular and Cellular Biology 20, 1179-1186.

117. Neves, H., Ramos, C., da Silva, M.G., Parreira, A., and Parreira, L. (1999). The nuclear topography of ABL, BCR, PML, and RAR alpha genes: Evidence for gene proximity in specific phases of the cell cycle and stages of hematopoietic differentiation. Blood 93, 1197-1207.

118. Nievergall, E., Reynolds, J., Kok, C.H., Watkins, D., Biondo, M., Busfield, S.J., Vairo, G., Yeung, D.T., Lopez, A., Hiwase, D.K., et al. (2014). High Plasma Levels of TGF-alpha and IL-6 at Diagnosis Predict Early Molecular Response Failure and Transformation in CML. Blood 124.

119. Nilsson, S.K., Johnston, H.M., Whitty, G.A., Williams, B., Webb, R.J., Denhardt, D.T., Bertoncello, I., Bendall, L.J., Simmons, P.J., and Haylock, D.N. (2005). Osteopontin, a key component of the hematopoietic stem cell niche and regulator of primitive hematopoietic progenitor cells. Blood 106, 1232-1239.

120. Notari, M., Neviani, P., Santhanam, R., Blaser, B.W., Chang, J.S., Galietta, A., Willis, A.E., Roy, D.C., Caligiuri, M.A., Marcucci, G., et al. (2006). A MAPK/HNRPK pathway controls BCR/ABL oncogenic potential by regulating MYC mRNA translation. Blood 107, 2507-2516.

121. Nowell, P.C., and Hungerford, D.A. (1960). Chromosome studies on normal and leukemic human leukocytes. J Natl Cancer Inst 25, 85-109.

122. O'Brien, S.G., Guilhot, F., Larson, R.A., Gathmann, I., Baccarani, M., Cervantes, F., Cornelissen, J.J., Fischer, T., Hochhaus, A., Hughes, T., et al. (2003). Imatinib compared with interferon and low-dose cytarabine for newly diagnosed chronic-phase chronic myeloid leukemia. New England Journal of Medicine 348, 994-1004.

123. Passegue, E., Jamieson, C.H.M., Ailles, L.E., and Weissman, I.L. (2003). Normal and leukemic hematopoiesis: Are leukemias a stem cell disorder or a reacquisition of stem cell characteristics? Proceedings of the National Academy of Sciences of the United States of America 100, 11842-11849.

124. Pendergast, A.M. (2002). The Abl family kinases: mechanisms of regulation and signaling. Adv Cancer Res 85, 51-100.

125. Pendergast, A.M., Muller, A.J., Havlik, M.H., Maru, Y., and Witte, O.N. (1991). Bcr Sequences Essential for Transformation by the Bcr-Abl Oncogene Bind to the Abl-Sh2 Regulatory Domain in a Non-Phosphotyrosine-Dependent Manner. Cell 66, 161-171.

126. Pendergast, A.M., Quilliam, L.A., Cripe, L.D., Bassing, C.H., Dai, Z.H., Li, N.X., Batzer, A., Rabun, K.M., Der, C.J., Schlessinger, J., et al. (1993). Bcr-Abl-Induced Oncogenesis Is Mediated by Direct Interaction with the Sh2 Domain of the Grb-2 Adapter Protein. Cell 75, 175-185.

127. Pricola, K.L., Kuhn, N.Z., Haleem-Smith, H., Song, Y.J., and Tuan, R.S. (2009). Interleukin-6 Maintains Bone Marrow-Derived Mesenchymal Stem Cell Stemness by an ERK1/2-Dependent Mechanism. Journal of Cellular Biochemistry 108, 577-588.

128. Puil, L., Liu, J.X., Gish, G., Mbamalu, G., Bowtell, D., Pelicci, P.G., Arlinghaus, R., and Pawson, T. (1994). Bcr-Abl Oncoproteins Bind Directly to Activators of the Ras Signaling Pathway. Embo Journal 13, 764-773.

129. Puissant, A., Dufies, M., Fenouille, N., Ben Sahra, I., Jacquel, A., Robert, G., Cluzeau, T., Deckert, M., Tichet, M., Cheli, Y., et al. (2012). Imatinib triggers mesenchymal-like conversion of CML cells associated with increased aggressiveness. Journal of Molecular Cell Biology 4, 207-220.

130. Quintas-Cardama, A., and Cortes, J. (2009). Molecular biology of bcr-abl1-positive chronic myeloid leukemia. Blood 113, 1619-1630.

131. Raaijmakers, M.H.G.P., Mukherjee, S., Guo, S.Q., Zhang, S.Y., Kobayashi, T., Schoonmaker, J.A., Ebert, B.L., Al-Shahrour, F., Hasserjian, R.P., Scadden, E.O., et al. (2010). Bone progenitor dysfunction induces myelodysplasia and secondary leukaemia. Nature 464, 852-U858.

132. Raitano, A.B., Halpern, J.R., Hambuch, T.M., and Sawyers, C.L. (1995). The Bcr-Abl Leukemia Oncogene Activates Jun Kinase and Requires Jun for Transformation. Proceedings of the National Academy of Sciences of the United States of America 92, 11746-11750.

133. Ramasamy, R., Lam, E.W.F., Soeiro, I., Tisato, V., Bonnet, D., and Dazzi, F. (2007). Mesenchymal stem cells inhibit proliferation and apoptosis of tumor cells: impact on in vivo tumor growth. Leukemia 21, 304-310.
134. Ramirez, P., Rettig, M.P., Uy, G.L., Deych, E., Holt, M.S., Ritchey, J.K., and DiPersio, J.F. (2009). BIO5192, a small molecule inhibitor of VLA-4, mobilizes hematopoietic stem and progenitor cells. Blood 114, 1340-1343.
135. Rappold, I., Watt, S.M., Kusadasi, N., Rose-John, S., Hatzfeld, J., and Ploemacher, R.E. (1999). Gp130-signaling synergizes with FL and TPO for the long-term expansion of cord blood progenitors. Leukemia 13, 2036-2048.
136. Rappold, I., Watt, S.M., Rose-John, S., and Ploemacher, R.E. (1998). Gp130 signalling synergizes with FL and TPO for the longterm expansion of human hematopoietic progenitors. Blood 92, 724a-724a.
137. Raymond, A., Liu, B., Liang, H., Wei, C.M., Guindani, M., Lu, Y., Liang, S.D., John, L.S.S., Molldrem, J., and Nagarajan, L. (2014). A role for BMP-induced homeobox gene MIXL1 in acute myelogenous leukemia and identification of type I BMP receptor as a potential target for therapy. Oncotarget 5, 12675-12693.
138. Ren, G.W., Zhang, L.Y., Zhao, X., Xu, G.W., Zhang, Y.Y., Roberts, A.I., Zhao, R.C., and Shi, Y.F. (2008). Mesenchymal stem cell-mediated immunosuppression occurs via concerted action of chemokines and nitric oxide. Cell Stem Cell 2, 141-150.
139. Ren, G.W., Zhao, X., Wang, Y., Zhang, X., Chen, X.D., Xu, C.L., Yuan, Z.R., Roberts, A.I., Zhang, L.Y., Zheng, B., et al. (2012). CCR2-Dependent Recruitment of Macrophages by Tumor-Educated Mesenchymal Stromal Cells Promotes Tumor Development and Is Mimicked by TNF alpha. Cell Stem Cell 11, 812-824.
140. Ren, G.W., Zhao, X., Zhang, L.Y., Zhang, J.M., L'Huillier, A., Ling, W.F., Roberts, A.I., Le, A.D., Shi, S.T., Shao, C.S., et al. (2010). Inflammatory Cytokine-Induced Intercellular Adhesion Molecule-1 and Vascular Cell Adhesion Molecule-1 in Mesenchymal Stem Cells Are Critical for Immunosuppression. Journal of Immunology 184, 2321-2328.
141. Ren, R., Ye, Z.S., and Baltimore, D. (1994). Abl protein-tyrosine kinase selects the Crk adapter as a substrate using SH3-binding sites. Genes Dev 8, 783-795.
142. Rettig, M.P., Ansstas, G., and DiPersio, J.F. (2012). Mobilization of hematopoietic stem and progenitor cells using inhibitors of CXCR4 and VLA-4. Leukemia 26, 34-53.
143. Reya, T., Duncan, A.W., Ailles, L., Domen, J., Scherer, D.C., Willert, K., Hintz, L., Nusse, R., and Weissman, I.L. (2003). A role for Wnt signalling in self-renewal of haematopoietic stem cells. Nature 423, 409-414.
144. Reynaud, D., Pietras, E., Barry-Holson, K., Mir, A., Binnewies, M., Jeanne, M., Sala-Torra, O., Radich, J.P., and Passegue, E. (2011). IL-6 Controls Leukemic

Multipotent Progenitor Cell Fate and Contributes to Chronic Myelogenous Leukemia Development. Cancer Cell 20, 661-673.

145. Rowley, J.D. (1973). Letter: A new consistent chromosomal abnormality in chronic myelogenous leukaemia identified by quinacrine fluorescence and Giemsa staining. Nature 243, 290-293.

146. Sacchetti, B., Funari, A., Michienzi, S., Di Cesare, S., Piersanti, S., Saggio, I., Tagliafico, E., Ferrari, S., Robey, P.G., Riminucci, M., et al. (2007). Self-renewing osteoprogenitors in bone marrow sinusoids can organize a hematopoietic microenvironment. Cell 131, 324-336.

147. Saini, A.S., Shenoy, G.N., Rath, S., Bal, V., and George, A. (2014). Inducible nitric oxide synthase is a major intermediate in signaling pathways for the survival of plasma cells. Nature Immunology 15, 275-282.

148. Salesse, S., and Verfaillie, C.M. (2002). BCR/ABL: from molecular mechanisms of leukemia induction to treatment of chronic myelogenous leukemia. Oncogene 21, 8547-8559.

149. Salgia, R., Li, J.L., Lo, S.H., Brunkhorst, B., Kansas, G.S., Sobhany, E.S., Sun, Y.P., Pisick, E., Hallek, M., Ernst, T., et al. (1995a). Molecular-Cloning of Human Paxillin, a Focal Adhesion Protein Phosphorylated by P210(Bcr/Abl). Journal of Biological Chemistry 270, 5039-5047.

150. Salgia, R., Uemura, N., Okuda, K., Li, J.L., Pisick, E., Sattler, M., Dejong, R., Druker, B., Heisterkamp, N., Chen, L.B., et al. (1995b). Crkl Links P210(Bcr/Abl) with Paxillin in Chronic Myelogenous Leukemia-Cells. Journal of Biological Chemistry 270, 29145-29150.

151. Sattler, M., Mohi, M.G., Pride, Y.B., Quinnan, L.R., Malouf, N.A., Podar, K., Gesbert, F., Iwasaki, H., Li, S.G., Van Etten, R.A., et al. (2002). Critical role for Gab2 in transformation by BCR/ABL. Cancer Cell 1, 479-492.

152. Sattler, M., Verma, S., Shrikhande, G., Byrne, C.H., Pride, Y.B., Winkler, T., Greenfield, E.A., Salgia, R., and Griffin, J.D. (2000). The BCR/ABL tyrosine kinase induces production of reactive oxygen species in hematopoietic cells. Journal of Biological Chemistry 275, 24273-24278.

153. Sawyers, C.L. (1999). Chronic myeloid leukemia. N Engl J Med 340, 1330-1340.

154. Schaniel, C., Sirabella, D., Qiu, J.J., Niu, X.H., Lemischka, I.R., and Moore, K.A. (2011). Wnt-inhibitory factor 1 dysregulation of the bone marrow niche exhausts hematopoietic stem cells. Blood 118, 2420-2429.

155. Schmidt, T., Kharabi Masouleh, B., Loges, S., Cauwenberghs, S., Fraisl, P., Maes, C., Jonckx, B., De Keersmaecker, K., Kleppe, M., Tjwa, M., et al. (2011). Loss or inhibition of stromal-derived PlGF prolongs survival of mice with imatinib-resistant Bcr-Abl1(+) leukemia. Cancer Cell 19, 740-753.

156. Semesiuk, N.I., Zhylchuk, A., Bezdenezhnykh, N., Lykhova, A., Vorontsova, A.L., Zhylchuk, V.E., and Kudryavets, Y.I. (2013). Disseminated tumor cells and

enhanced level of some cytokines in bone marrow and peripheral blood of breast cancer patients as predictive factors of tumor progression. Exp Oncol 35, 295-302.

157. Sen, M., Joyce, S., Panahandeh, M., Li, C.Y., Thomas, S.M., Maxwell, J., Wang, L., Gooding, W.E., Johnson, D.E., and Grandis, J.R. (2012). Targeting Stat3 Abrogates EGFR Inhibitor Resistance in Cancer. Clinical Cancer Research 18, 4986-4996.

158. Shi, L.A., and Hu, L.H. (2011). The normal flora may contribute to the quantitative preponderance of myeloid cells under physiological conditions. Medical Hypotheses 76, 141-143.

159. Shuai, K., Halpern, J., tenHoeve, J., Rao, X.P., and Sawyers, C.L. (1996). Constitutive activation of STAT5 by the BCR-ABL oncogene in chronic myelogenous leukemia. Oncogene 13, 247-254.

160. Siegel, G., Schafer, R., and Dazzi, F. (2009). The Immunosuppressive Properties of Mesenchymal Stem Cells. Transplantation 87, S45-S49.

161. Sit, S.T., and Manser, E. (2011). Rho GTPases and their role in organizing the actin cytoskeleton. Journal of Cell Science 124, 679-683.

162. Skorski, T., Kanakaraj, P., Nieborowskaskorska, M., Ratajczak, M.Z., Wen, S.C., Zon, G., Gewirtz, A.M., Perussia, B., and Calabretta, B. (1995). Phosphatidylinositol-3 Kinase-Activity Is Regulated by Bcr/Abl and Is Required for the Growth of Philadelphia-Chromosome-Positive Cells. Blood 86, 726-736.

163. Sonowal, H., Kumar, A., Bhattacharyya, J., Gogoi, P.K., and Jaganathan, B.G. (2013). Inhibition of actin polymerization decreases osteogeneic differentiation of mesenchymal stem cells through p38 MAPK pathway. Journal of Biomedical Science 20.

164. Sugiyama, T., Kohara, H., Noda, M., and Nagasawa, T. (2006). Maintenance of the hematopoietic stem cell pool by CXCL12-CXCR4 chemokine signaling in bone marrow stromal cell niches. Immunity 25, 977-988.

165. Tabe, Y., and Konopleva, M. (2014). Advances in understanding the leukaemia microenvironment. British Journal of Haematology 164, 767-778.

166. Tang, X.W., Downes, C.P., Whetton, A.D., and Owen-Lynch, P.J. (2000). Role of phosphatidylinositol 3-kinase and specific protein kinase B isoforms in the suppression of apoptosis mediated by the Abelson protein-tyrosine kinase. Journal of Biological Chemistry 275, 13142-13148.

167. Tawara, K., Oxford, J.T., and Jorcyk, C.L. (2011). Clinical significance of interleukin (IL)-6 in cancer metastasis to bone: potential of anti-IL-6 therapies. Cancer Manag Res 3, 177-189.

168. Traer, E., Javidi-Sharifi, N., Agarwal, A., Dunlap, J., English, I., Martinez, J., Tyner, J.W., Wong, M., and Druker, B.J. (2014). Ponatinib overcomes FGF2-mediated resistance in CML patients without kinase domain mutations. Blood 123, 1516-1524.

169. Trendowski, M., Mitchell, J.M., Corsette, C.M., Acquafondata, C., and Fondy, T.P. (2015). Chemotherapy with cytochalasin congeners in vitro and in vivo against murine models. Investigational New Drugs 33, 290-299.
170. Trumpp, A., Essers, M., and Wilson, A. (2010). Awakening dormant haematopoietic stem cells. Nature Reviews Immunology 10, 201-209.
171. Uemura, N., Salgia, R., Ewaniuk, D.S., Little, M.T., and Griffin, J.D. (1999). Involvement of the adapter protein CRKL in integrin-mediated adhesion. Oncogene 18, 3343-3353.
172. Van Etten, R.A., Jackson, P.K., Baltimore, D., Sanders, M.C., Matsudaira, P.T., and Janmey, P.A. (1994). The COOH terminus of the c-Abl tyrosine kinase contains distinct F- and G-actin binding domains with bundling activity. J Cell Biol 124, 325-340.
173. Vardiman, J.W., Harris, N.L., and Brunning, R.D. (2002). The World Health Organization (WHO) classification of the myeloid neoplasms. Blood 100, 2292-2302.
174. Varnum-Finney, B., Brashem-Stein, C., Flowers, D., Xu, L.W., Bakkour, S., Pear, W., and Bernstein, I.D. (2000a). Notch signaling enhances the self-renewal of primitive hematopoietic precursor cells. Blood 96, 64a-64a.
175. Varnum-Finney, B., Xu, L.W., Brashem-Stein, C., Nourigat, C., Flowers, D., Bakkour, S., Pear, W.S., and Bernstein, I.D. (2000b). Pluripotent, cytokine-dependent, hematopoietic stem cells are immortalized by constitutive Notch1 signaling. Nature Medicine 6, 1278-1281.
176. Vianello, F., Villanova, F., Tisato, V., Lymperi, S., Ho, K.K., Gomes, A.R., Marin, D., Bonnet, D., Apperley, J., Lam, E.W.F., et al. (2010). Bone marrow mesenchymal stromal cells non-selectively protect chronic myeloid leukemia cells from imatinib-induced apoptosis via the CXCR4/CXCL12 axis. Haematologica-the Hematology Journal 95, 1081-1089.
177. Wallace, S.R., Oken, M.M., Lunetta, K.L., Panoskaitsis-Mortari, A., and Masellis, A.M. (2001). Abnormalities of bone marrow mesenchymal cells in multiple myeloma patients. Cancer 91, 1219-1230.
178. Weisberg, E., Azab, A.K., Manley, P.W., Kung, A.L., Christie, A.L., Bronson, R., Ghobrial, I.M., and Griffin, J.D. (2012). Inhibition of CXCR4 in CML cells disrupts their interaction with the bone marrow microenvironment and sensitizes them to nilotinib. Leukemia 26, 985-990.
179. Weisberg, E., Manley, P.W., Cowan-Jacob, S.W., Hochhaus, A., and Griffin, J.D. (2007). Second generation inhibitors of BCR-ABL for the treatment of imatinib-resistant chronic myeloid leukaemia. Nat Rev Cancer 7, 345-356.
180. Weisberg, E., Wright, R.D., McMillin, D.W., Mitsiades, C., Ray, A., Barrett, R., Adamia, S., Stone, R., Galinsky, I., Kung, A.L., et al. (2008). Stromal-mediated protection of tyrosine kinase inhibitor-treated BCR-ABL-expressing leukemia cells. Molecular Cancer Therapeutics 7, 1121-1129.

181. Wetzler, M., Talpaz, M., Van Etten, R.A., Hirsh-Ginsberg, C., Beran, M., and Kurzrock, R. (1993). Subcellular localization of Bcr, Abl, and Bcr-Abl proteins in normal and leukemic cells and correlation of expression with myeloid differentiation. J Clin Invest 92, 1925-1939.

182. Winkler, I.G., Sims, N.A., Pettit, A.R., Barbier, V., Nowlan, B., Helwani, F., Poulton, I.J., van Rooijen, N., Alexander, K.A., Raggatt, L.J., et al. (2010). Bone marrow macrophages maintain hematopoietic stem cell (HSC) niches and their depletion mobilizes HSCs. Blood 116, 4815-4828.

183. Wohrer, S., Rabitsch, W., Shehata, M., Kondo, R., Esterbauer, H., Streubel, B., Sillaber, C., Raderer, M., Jaeger, U., Zielinski, C., et al. (2007). Mesenchymal stem cells in patients with chronic myelogenous leukaemia or bi-phenotypic ph plus acute leukaemia are not related to the leukaemic clone. Anticancer Research 27, 3837-3841.

184. Wu, M.F., Kwon, H.Y., Rattis, F., Blum, J., Zhao, C., Ashkenazi, R., Jackson, T.L., Gaiano, N., Oliver, T., and Reya, T. (2007). Imaging hematopoietic precursor division in real time. Cell Stem Cell 1, 541-554.

185. Xie, S.H., Wang, Y., Liu, J.X., Sun, T., Wilson, M.B., Smithgall, T.E., and Arlinghaus, R.B. (2001). Involvement of Jak2 tyrosine phosphorylation in Bcr-Abl transformation. Oncogene 20, 6188-6195.

186. Zeng, Z., Samudio, I.J., Munsell, M., An, J., Huang, Z., Estey, E., Andreeff, M., and Konopleva, M. (2006). Inhibition of CXCR4 with the novel RCP168 peptide overcomes stroma-mediated chemoresistance in chronic and acute leukemias. Mol Cancer Ther 5, 3113-3121.

187. Zepeda-Moreno, A., Saffrich, R., Walenda, T., Hoang, V.T., Wuchter, P., Sanchez-Enriquez, S., Corona-Rivera, A., Wagner, W., and Ho, A.D. (2012). Modeling SDF-1-induced mobilization in leukemia cell lines. Experimental Hematology 40, 666-674.

188. Zhang, B., Ho, Y.W., Huang, Q., Maeda, T., Lin, A., Lee, S.U., Hair, A., Holyoake, T.L., Huettner, C., and Bhatia, R. (2012a). Altered Microenvironmental Regulation of Leukemic and Normal Stem Cells in Chronic Myelogenous Leukemia. Cancer Cell 21, 577-592.

189. Zhang, B., Li, M., McDonald, T., Holyoake, T.L., Moon, R.T., Campana, D., Shultz, L., and Bhatia, R. (2013). Microenvironmental protection of CML stem and progenitor cells from tyrosine kinase inhibitors through N-cadherin and Wnt-beta-catenin signaling. Blood 121, 1824-1838.

190. Zhang, J.W., and Li, L.H. (2005). BMP signaling and stem cell regulation. Developmental Biology 284, 1-11.

191. Zhang, J.W., Niu, C., Ye, L., Huang, H.Y., He, X., Tong, W.G., Ross, J., Haug, J., Johnson, T., Feng, J.Q., et al. (2003). Identification of the haematopoietic stem cell niche and control of the niche size. Nature 425, 836-841.

192. Zhang, W., Trachootham, D., Liu, J.Y., Chen, G., Pelicano, H., Garcia-Prieto, C., Lu, W.Q., Burger, J.A., Croce, C.M., Plunkett, W., et al. (2012b). Stromal control of cystine metabolism promotes cancer cell survival in chronic lymphocytic leukaemia. Nature Cell Biology 14, 276-+.

193. Zhang, X.W., Subrahmanyam, R., Wong, R., Gross, A.W., and Ren, R.B. (2001). The NH2-terminal coiled-coil domain and tyrosine 177 play important roles in induction of a myeloproliferative disease in mice by Bcr-Abl. Molecular and Cellular Biology 21, 840-853.

7.0 SUPPLEMENTARY INFORMATION

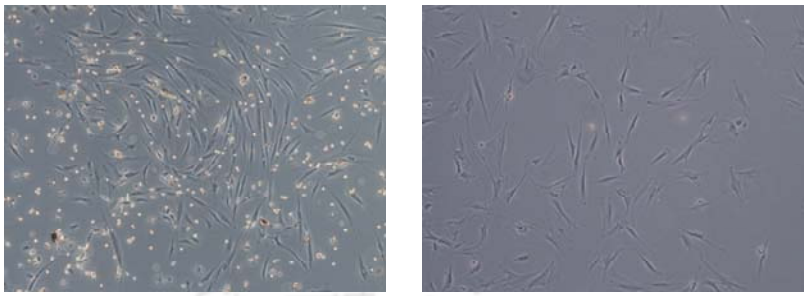

Figure 7.1:Morphology of MSC*. MSC derived from bone marrow of CML patients showed spindle shaped cells which proliferated as adherent cells.*

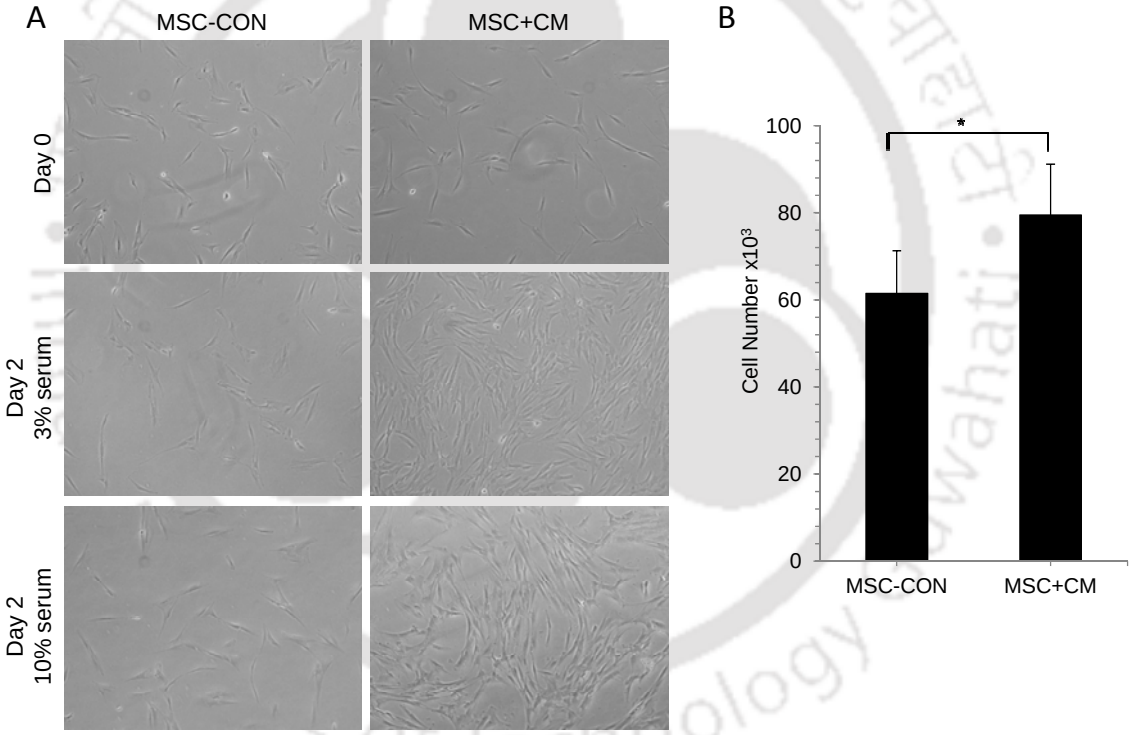

Figure 7.2: Effect of CML cells paracrine factors on MSC proliferation. *Conditioned media (CM) containing the paracrine factors were collected from K562 CML cells in serum free media and added to MSC in the presence of 3% or 10% serum. (A) Representative phase-contrast microscopic images of cells cultured in control or CML-CM. (B) The cell proliferation was assessed by cell counting with trypan blue after 72 hours. A significant increase in cell proliferation was observed in MSC cultured with CML cells conditioned media. Values are mean+SD, n=3.*

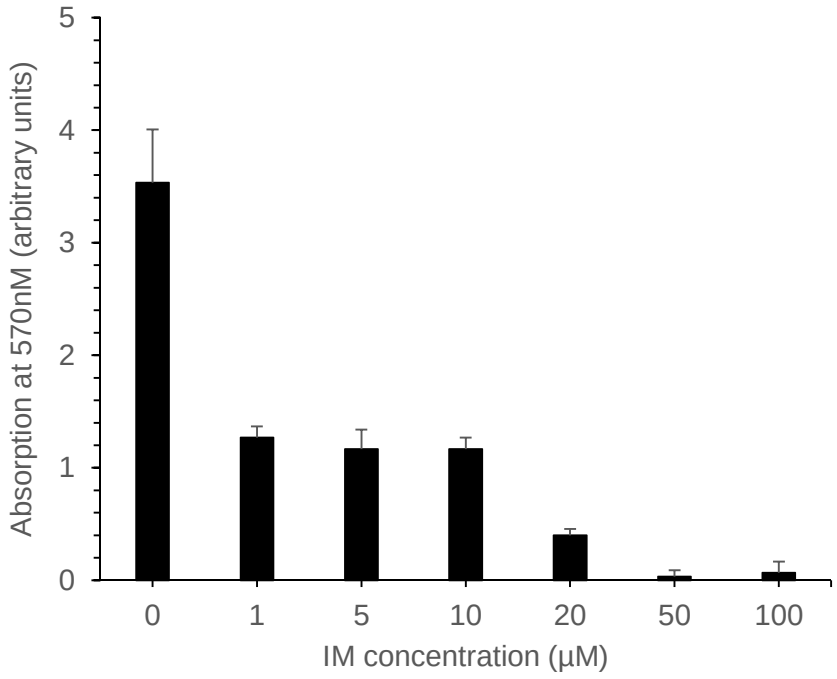

Figure 7.3: K562 CML cells were treated with different concentrations of Imatinib mesylate (IM) *for 48 hours and MTT was performed to assess the cell viability. A significant reduction in cell viability was identified at higher concentrations whereas it was similar at 1, 5 or 10µM. Values are mean+SD, n=3.*

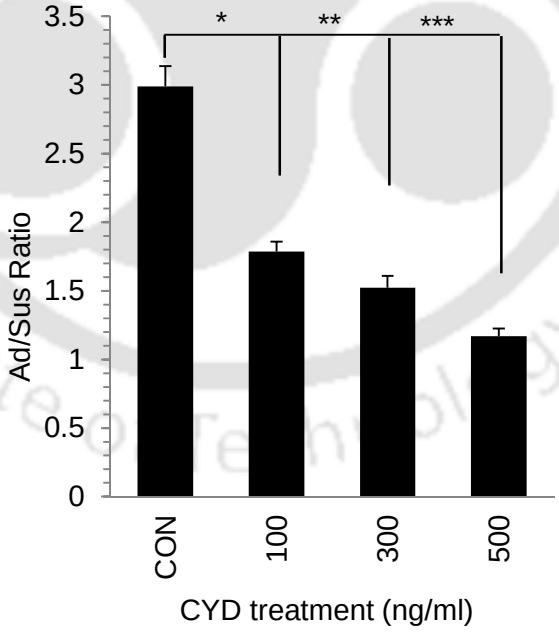

Figure 7.4: Effect of CYD on K562 adhesion to stromal layer. *The adhesion of K562 cells decreased at all the concentrations of CYD (100, 300, 500ng/ml) tested. The cells were incubated for 48 hours with the stromal cells before the analysis.*

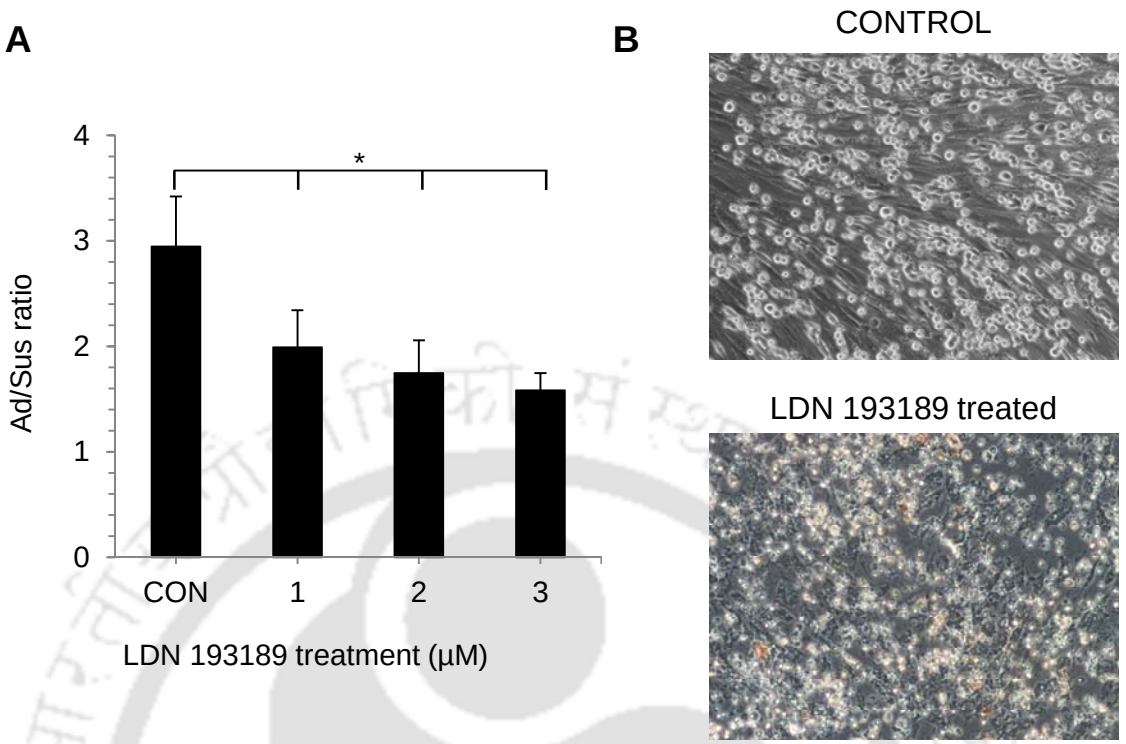

Figure 7.5: BMPRI inhibition on K562 adhesion to stroma. *(A)K562 cells were co-cultured with stromal cells for 48 hours and treated with BMP inhibitor LDN 193189 at various concentrations, which reduced stroma adherence of K562 cells. (B) Representative microscopic image showing control and BMP inhibitor (BI) treated K562 cells during interaction with the stromal cells. Values are mean+SD, n=3 independent experiments.*

ACKNOWLEDGEMENTS

First of all, I thank the LORD God for His love, grace and strength for the successful completion of my thesis work. Through the course of my PhD, I learnt about the value of trusting in the promises of God.

I thank my supervisor Dr. Bithiah Grace Jaganathan for her constant guidance during the entire course of my PhD work and for encouragement to try different strategies and methods to understand and solve the research problems. I also thank her for the insightful discussions for framing the experiments and trusting me to finish them successfully. Thanks also for providing all the necessary resources to complete my thesis work.

I gratefully acknowledge my doctoral committee members Prof. A. Srinivasan, Prof. Venkata Dasu, Prof. Pranab Goswami and Dr. Anil Limaye for their constant encouragement and insightful suggestions to make my thesis work better. My special thanks again to Prof. Srinivasan for always being interested in my research work and progress and all the positive remarks and kindness which were very encouraging.

My special thanks go to our collaborators Prof. Jina Bhattacharyya, Dr. Damodar Das, Dr. Smita Das and Dr. Sewali Deka for all their support in providing clinical samples and information. I especially thank Prof. Jina Bhattacharyya for her constant guidance and sharing her expertise on the clinical aspects of the study. She was a source of motivation to search and identify therapeutically relevant conclusions through my research work.

I acknowledge and thank Dr. Dennis Ridenour and Dr. Paul Kulesa for providing Cycle Trak plasmid used for cell cycle studies. I thank Dr. Dominique Bonnet for providing some of the FACS antibodies used in the initial part of the study.

I thank the former Academic Dean Prof. Sukumar Nandi and former HoD Prof. Arun Goyal for allowing me to take written comprehensive exam so that I could start my research work immediately after joining PhD.

I thank the HoDs of BSBE department, Prof. Goyal, Prof. Dasu, Prof. Pakshirajan for providing the necessary infrastructure and department staffs Mr. Nurul, Mr. Niranjan and Mr. Raghuveer for always being helpful during the course of my PhD work.

I thank my lab members for their constant help in preparing routine reagents, buffers and for help with the plasmid isolation work. Thanks to Somaiah for help with plasmid isolation and sample collection. Thanks to Vinoh Swu, Amit Sharma, Balwant Singh and Anuj Kumar for providing good work environment.

I thank Vishal Anand and Jithin for always being ready to discuss several important issues.

My heartfelt thanks belong to both my dear sons for making this life joyful at all times; my family and extended family for their constant prayers, encouragement and support throughout my research work. My special thanks also belong to my Pastor for his constant support and prayer at all times.